ÇUKUROVA UNIVERSITY
INSTITUTE OF NATURAL AND APPLIED SCIENCES

PhD THESIS

Ulduz MAMMADOVA OZEL

MONITORING OF CONWAY-MAXWELL-POISSON PROFILES UNDER MULTICOLLINEARITY

DEPARTMENT OF STATISTICS

ADANA – 2022

ABSTRACT

PhD THESIS

MONITORING OF CONWAY-MAXWELL-POISSON PROFILES UNDER MULTICOLLINEARITY

Ulduz MAMMADOVA OZEL

ÇUKUROVA UNIVERSITY
INSTITUTE OF NATURAL AND APPLIED SCIENCES
DEPARTMENT OF STATISTICS

Supervisor : Prof. Dr. Mahmude Revan ÖZKALE
Year: 2022. Pages: 153
Jury : Prof. Dr. Mahmude Revan ÖZKALE
: Prof. Dr. Sadullah SAKALLOĞLU
: Prof. Dr. Rızvan EROL
: Prof. Dr. Sevil ŞENTÜRK
: Assoc. Dr. Eralp DOĞU

As a result of the application of evolving technologies in the industry, the data generated in the manufacturing process necessitates the development of new methods for process control which can address several problems simultaneously. In this thesis, we aim to identify shifts in the count profiles while reducing the negative impact of the multicollinearity caused by correlated predictors.

We propose PCR, ridge, Liu, and *r-k* deviance-based Shewhart, CUSUM, and EWMA control charts for detecting out-of-control observations where the process data is modelled through the Conway-Maxwell-Poisson profile. The Conway-Maxwell-Poisson distribution facilitates the analysis of the count process data that exhibit varying levels of dispersion, whilst adjusted PCR, ridge, Liu, and *r-k* class estimation methods overcome the multicollinearity. Extensive simulation studies and real-life data analysis are carried out to illustrate the effectiveness of the proposed residual-based control charts.

Key Words: Conway-Maxwell-Poisson distribution, control charts, multicollinearity, profile monitoring

ÖZ

DOKTORA TEZİ

ÇOKLU İÇ İLİŞKİ ALTINDA CONWAY-MAXWELL-POİSSON PROFİLLERİNİN DENETİMİ

Ulduz MAMMADOVA OZEL

ÇUKUROVA ÜNİVERSİTESİ
FEN BİLİMLERİ ENSTİTÜSÜ
İSTATİSTİK

Danışman : Prof. Dr. Mahmude Revan ÖZKALE
Yıl: 2022. Sayfa: 153

Jüri : Prof. Dr. Mahmude Revan ÖZKALE
: Prof. Dr. Sadullah SAKALLOĞLU
: Prof. Dr. Rızvan EROL
: Prof. Dr. Sevil ŞENTÜRK
: Doç. Dr. Eralp DOĞU

Gelişen teknolojilerin endüstride uygulanması sonucunda, üretim sürecinde ortaya çıkan veriler, süreç kontrolü için aynı anda birçok sorunu ele alan yöntemlerin geliştirilmesini zorunlu kılmaktadır. Bu çalışmada, ilişkili açıklayıcı değişkenlerin neden olduğu çoklu bağlantının olumsuz etkisini azaltırken, sayım profillerindeki kontrol dışı durumları tespit etmeyi amaçlıyoruz.

Bu tez çalışmasında süreç verilerini Conway-Maxwell-Poisson profili yardımı ile modellemeyi ve kontrol dışı gözlemleri belirlemek için PCR, ridge, Liu ve *r-k* sınıf tahmin edicileri kullanılarak elden edilen rezidülere dayalı Shewhart, CUSUM ve EWMA kontrol grafiklerini kullanmayı öneriyoruz. Conway-Maxwell-Poisson profili farklı düzeylerdeki yayılıma sahip olan sayım verilerinin analizini kolaylaştırırken, yeniden düzenlenmiş PCR, ridge, Liu ve *r-k* sınıf tahmin edicileri çoklu iç ilişki sorununun üstesinden gelir. Önerilen rezidüye dayalı kontrol grafiklerinin etkinliği farklı performans ölçümleri kullanılarak kapsamlı simulasyon çalışmaları ve gerçek veri kümeleri yardımı ile gösterilmiştir.

Anahtar Kelimeler: Conway-Maxwell-Poisson dağılımı, kontrol grafikleri, çoklu iç ilişki, profil denetimi

EXTENDED ABSTRACT

Quality control is the mixture of inspecting, analyzing, and application of preventive measures to ensure that a manufactured product maintains the required uniformity and quality. However, occasional random disruptions negatively impact the manufacturing process which requires addressing an issue and making necessary adjustments promptly. The main goal of statistical process control is to identify variabilities in the process due to these disruptions. Utilizing a control chart is one way to accomplish that.

Control charts were introduced as an effective graphical tool for identifying irregularities by visualizing the process data in the early 1920s. The predefined limits of the control chart set boundaries of two separate areas known as control and out-of-control. Thus, the researcher can identify the unwanted variabilities in the process since every monitored observation that falls outside the control area reflects the potential issues in the workflow.

The researchers' interest in the control chart technique led to the development of improved control charts and a thorough examination of them within different frameworks. Profile monitoring also made use of control charts, specifically residual-based control charts. The residual-based control charts are extensions of the traditional control charts to monitor estimated responses from the current stage that are assumed to be impacted by prior stages of the process. The monitoring process with residual control charts is possible by establishing a relationship between response and predictors and obtaining residuals. Later, changes in the process can be identified by considering these residuals as monitored observations.

The extension of the method is also used to monitor generalized linear profiles. The generalized linear profiles are beneficial for defining a wide range of pro-

cess profiles with response variables from the exponential distribution family, such as Poisson, binom, gamma, etc.

In this thesis, we examine monitoring methods for the COM-Poisson profile in the case of interrelated predictors. Conway-Maxwell-Poisson (COM-Poisson) distribution is also a member of the exponential distribution family. This distribution is the two-parameter generalization of the Poisson distribution and facilitates the analysis of count data that exhibit varying levels of dispersion. Dispersion in count data emerges as a result of differences in the mean and variance of the count data. It is possible to determine if data is underdispersed or overdispersed based on the value of the dispersion parameter of the COM-Poisson data.

The concept of interrelated predictors, on the other hand, is known in the literature as multicollinearity. It contradicts the core assumptions of the regression analysis and adds significant challenges throughout the data analysis by undermining the statistical significance of the predictor variable and causing computational problems. Therefore, the initial step in monitoring the profile data is to examine the predictor matrix for the presence of examination that can be achieved by visually inspecting the correlation matrix and using various metrics such as condition number and variance inflation factor. Once the presence of multicollinearity is confirmed, parameters need to be estimated. However, since traditional parameter estimation methods like ordinary least squares and maximum likelihood estimation require the calculation of the inverse of the covariance matrix, alternative estimation methods are studied. Some of these approaches are principal component-based, and others are biased estimation methods.

In this thesis, we adjusted four estimation methods for fitting the COM-Poisson profile to overcome the issue of multicollinearity in generalized linear profiles. We then defined iterative principal components regression (PCR), ridge, Liu,

and *r-k* deviance residuals derived from the fitted model with the corresponding estimation. These residuals utilized to establish new adjusted PCR, ridge, Liu, and *r-k* deviance-based Shewhart, cumulative sum (CUSUM), and exponentially weighted moving average (EWMA) control charts. Shewhart chart is a practical tool to detect process variations in sizes from medium to large. In contrast, CUSUM and EWMA charts are known to be responsive to small-sized shifts since both charts utilize current and past information from the observations that make the control chart effective in detecting small shifts.

The proposed methods are evaluated and compared to existing methods through simulated artificial and real-life data examinations. The simulations are carried out in two stages for a fixed number of observations and correlation levels, various combinations of predictor numbers, dispersion levels, shift types, and shift sizes. They cover the comparative analysis of the proposed control charts to respective residual-based control charts. The relative superiority of the proposed control charts was also evaluated along with the effect of the tuning parameter selection for biased estimation methods. The performance of the control charts was interpreted in terms of the average run length and standard deviation of the run length.

The performance of ridge deviance-based control charts and the impact of tuning parameters on the overall performance of the proposed control charts are demonstrated using the ”laminated plastic plywood” data set where the response is the number of defects in manufactured laminated wooden plates. Likewise, the effectiveness of the proposed principal component-based approach is investigated through a ”semiconductor manufacturing” data set. The response variable in the ”semiconductor manufacturing” data set is the number of test passes which manufactured product subjects at the end of the production line, and predictor variables are the recorded values from several sensors. The ”bike-sharing application” data set includes the

weather information and the number of the count of casual users' bike shares for a particular day taken from the bike-sharing application system. This data set is used to assess the performance of Liu deviance-based control charts and results compared to the deviance and ridge deviance-based control charts. Each data set is subjected to diagnostic analysis to ensure the presence of multicollinearity and determine the best-fitted distribution of the response.

Simulation results show that the layout of the control chart statistics of the proposed Shewhart, CUSUM, and EWMA control charts are similar to that of residual-based control charts while using the ridge and Liu estimation methods, even though the values of the residuals differ. The structural changes become apparent when principal component-based approaches for parameter estimation are utilized.

The findings indicate that for large sample sizes, proposed ridge deviance-based control charts perform better than deviance-based control charts. Liu's deviance-based Shewhart, CUSUM, and EWMA charts are generally well at detecting shifts than deviance-based control charts. Furthermore, considering the results for the performance evaluation of ridge and Liu deviance-based control charts, it is possible to conclude that control chart methods based on a biased estimation approach are affected by the value of the tuning parameter. The simulations for principal component-based approaches showed that the *r-k* deviance-based control charts are superior to those based on the deviance and ridge deviance residuals, whereas the PCR deviance-based control charts come in as a close second.

In general, proposed control charts mostly outperform deviance residual-based control charts in the case of multicollinearity. The outcomes of real-life "laminated plastic plywood", "bike-sharing application", and "semiconductor manufacturing" data analysis confirm the findings of simulated studies.

ACKNOWLEDGEMENTS

First and foremost, I would like to express my sincere gratitude to my supervisor Dr. M. Revan ÖZKALE, for her academic support, encouragement, and immersing patience during my PhD. She is an inspiration. I am thankful to her for being a great mentor throughout.

I appreciate the timely and invaluable guidance provided by my committee members, Dr. Sadullah SAKALLIOĞLU and Dr. Rızvan EROL.

A very special thank you to all the colleagues who have helped along the way and to my lovely husband, my beautiful sister, and my wonderful friends whose support was very appreciated.

Finally, I would especially like to express my profound gratitude to my family for providing me with continuous love and support during this period. Thank you for everything.

CONTENTS **PAGE**

ABSTRACT I

ÖZ II

EXTENDED ABSTRACT III

ACKNOWLEDGEMENTS VII

CONTENTS VIII

LIST OF TABLES XII

LIST OF FIGURES XVIII

LIST OF ABBREVIATIONS XX

1 INTRODUCTION 1

1.1. Aims and scope 10

1.2. Organization of the thesis 10

2 GENERALIZED LINEAR MODELS 13

2.1. GLMs with count response: COM-Poisson model 14

2.2. Parameter estimation 16

2.2.1. Uncorrelated predictors 16

2.2.2. Correlated predictors 17

2.2.2.1. *PCR estimator* 17

2.2.2.2. *Ridge estimator* 19

2.2.2.3. *Liu estimator* 20

2.2.2.4. *r-k class estimator* 21

2.3. Tuning parameters for biased estimators 22

2.3.1. Tuning parameter for the ridge and *r-k* class estimators 22

2.3.2. Tuning parameter for the Liu estimator 24

2.4. Iterative estimation algorithms 26

2.5. Multicollinearity diagnostics 29
2.6. Deviance residuals 31
3 MONITORING COM-POISSON PROFILES 35
3.1. Control charts as a process monitoring tool 35
3.2. Performance of the control charts 36
3.3. Residual-based control charts for COM-Poisson profiles 37
3.3.1. Residual-based Shewhart chart 38
3.3.2. Residual-based CUSUM and EWMA charts 39
4 SIMULATION STUDY 45
4.1. Design of the simulation study 45
4.2. Performance of ridge deviance-based control charts 47
4.2.1. Ridge deviance-based control charts for monitoring COM-Poisson profile 50
4.2.2. Effect of ridge tuning parameter on profile monitoring 52
4.3. Performance of PCR and *r-k* deviance-based control charts 66
4.3.1. Residual-based Shewhart chart 68
4.3.1.1. *Stage 1 analysis* 68
4.3.1.2. *Stage 2 analysis* 68
4.3.2. Residual-based CUSUM and EWMA charts 72
4.3.2.1. *Stage 1 analysis* 72
4.3.2.2. *Stage 2 analysis* 73
4.4. Performance of Liu deviance-based control charts 79
4.4.1. *Stage 1 analysis* 79
4.4.2. *Stage 2 analysis* 80
5 REAL DATA ANALYSIS 85
5.1. *"LPP"* data set analysis 85

5.1.1. Data processing 86
5.1.2. Monitoring process 88
5.2. *"SECOM"* data set analysis 91
5.2.1. Analysis with residual-based Shewhart chart 93
5.2.1.1. *Data reconstruction* 93
5.2.1.2. *Data processing* 94
5.2.1.3. *Monitoring process* 96
5.2.2. Analysis with residual-based CUSUM and EWMA charts 99
5.2.2.1. *Data reconstruction* 99
5.2.2.2. *Data processing* 100
5.2.2.3. *Monitoring process* 101
5.3. *"BikeShare"* data set analysis 106
5.3.1. Data processing 109
5.3.2. Monitoring process 111
6 CONCLUSIONS 117
APPENDICES 139
A. Performance of PCR and *r-k* deviance-based control charts 139
B. Performance of Liu deviance-based control charts 148

LIST OF TABLES **PAGE**

Table 3.1. Control chart statistics of the deviance, ridge deviance, and Liu deviance-based CUSUM and EWMA charts. 40

Table 3.2. Control limits of the deviance, ridge deviance, and Liu deviance-based CUSUM and EWMA charts. 41

Table 4.1. Stage 1 analysis results for simulated COM-Poisson profile data. 51

Table 4.2. Stage 2 analysis results for simulated COM-Poisson profile data. 51

Table 4.3. Stage 1 analysis results regarding ridge tuning parameter selection, $\rho^2 = 0.90$. 54

Table 4.4. Stage 1 analysis results regarding ridge tuning parameter selection, $\rho^2 = 0.99$. 55

Table 4.5. Stage 2 analysis of ridge deviance-based control charts with different tuning parameters in case of additive shift, $\rho^2 = 0.90$. 56

Table 4.6. Stage 2 analysis of ridge deviance-based control charts with different tuning parameters in case of multiplicative shift in intercept, $\rho^2 = 0.90$. 57

Table 4.7. Stage 2 analysis of ridge deviance-based control charts with different tuning parameters in case of multiplicative shift in regression coefficients intercept included, $\rho^2 = 0.90$. 58

Table 4.8. Stage 2 analysis of ridge deviance-based control charts with different tuning parameters in case of multiplicative shift in regression coefficients intercept excluded, $\rho^2 = 0.90$. 59

Table 4.9. Stage 2 analysis of ridge deviance-based control charts with different tuning parameters in case of additive shift, $\rho^2 = 0.99$. 60

Table 4.10. Stage 2 analysis of ridge deviance-based control charts with different tuning parameters in case of multiplicative shift in intercept, $\rho^2 = 0.99$. 61
Table 4.11. Stage 2 analysis of ridge deviance-based control charts with different tuning parameters in case of multiplicative shift in regression coefficients intercept excluded, $\rho^2 = 0.99$. 62
Table 4.12. Stage 2 analysis of ridge deviance-based control charts with different tuning parameters in case of multiplicative shift in regression coefficients intercept included, $\rho^2 = 0.99$. 63
Table 4.13. Performance of ridge deviance-based control charts with different tuning parameters under various shift for no intercept model. 67
Table 4.14. Stage 1 analysis results for residual-based Shewhart charts. 69
Table 4.15. Stage 1 analysis results for residual-based control charts with respective ARL_0 values..... 81
Table 5.1. Descriptive statistics for *LPP* data set..... 86
Table 5.2. Comparison of deviance residuals calculated from the models with ML and ridge estimators. 87
Table 5.3. Change in the mean of the process data..... 90
Table 5.4. Control chart constants for in-control Poisson profile..... 90
Table 5.5. Performance analysis of residual-based control charts for monitoring Poisson profile in terms of ARL_1. 91
Table 5.6. Diagnostic analysis of best-fitted distribution for response variable of *SECOM* data set for application of the residual-based Shewhart charts..... 95

Table 5.7. Comparison of deviance residuals calculated from the models with ML, ridge, PCR, and *r-k* class estimators. 96
Table 5.8. Control chart constant and control limits calculated using the corresponding l, $ARL_0 \approx 370$. 98
Table 5.9. Diagnostic analysis of best-fitted distribution for response variable of *SECOM* data set for application of the residual-based CUSUM and EWMA charts. 100
Table 5.10. Comparison of deviance residuals calculated from the models with ML, ridge, PCR, and *r-k* class estimators. 101
Table 5.11. Control limits and number of out-of-control observations identified by respective CUSUM chart. 103
Table 5.12. Control limit constants and number of out-of-control observations identified by respective EWMA chart. 103
Table 5.13. CUSUM chart limits, in-control mean, and standard deviation of the historical set. 104
Table 5.14. EWMA chart limit constants, in-control mean, and standard deviation of the historical set. 104
Table 5.15. Performance analysis of CUSUM and EWMA charts with *SECOM* data set, ARL_1. 105
Table 5.16. The difference in the mean of the residuals from the in-control control set and historical set. 105
Table 5.17. Diagnostic analysis of best-fitted distribution for the response of the *BikeShare* data set. 109
Table 5.18. ML, ridge, and Liu estimation results for COM-Poisson model of the *BikeShare* data set. 110

Table 5.19. Control limits for residual-based Shewhart, CUSUM, and EWMA charts..... 113
Table 5.20. Performance analysis of control charts with *BikeShare* data set, ARL_1..... 115
Table A.1. Performance analysis results of the PCR and *r-k* deviance-based Shewhart chart in case of additive shift, $\rho^2 = 0.95$..... 138
Table A.2. Performance analysis results of the PCR and *r-k* deviance-based Shewhart chart in case of additive shift, $\rho^2 = 0.99$..... 139
Table A.3. Performance analysis results of the PCR and *r-k* deviance-based Shewhart chart in case of multiplicative shift, $\rho^2 = 0.95$. 140
Table A.4. Performance analysis results of the PCR and *r-k* deviance-based Shewhart chart in case of multiplicative shift, $\rho^2 = 0.99$. 141
Table A.5. Stage 1 analysis results for residual-based CUSUM and EWMA charts with respective ARL_0 values, in-control mean and in-control standard deviations. 142
Table A.6. Performance analysis results in terms of ARL_1 of PCR and *r-k* deviance-based CUSUM and EWMA charts in case of additive shift..... 143
Table A.7. Performance analysis results in terms of ARL_1 of PCR and *r-k* deviance-based CUSUM and EWMA charts in case of multiplicative shift. 144
Table A.8. Performance analysis results in terms of *SDRL* of PCR and *r-k* deviance-based CUSUM and EWMA charts in case of additive shift. 145

Table A.9. Performance analysis results in terms of *SDRL* of PCR and *r-k* deviance-based CUSUM and EWMA charts in case of multiplicative shift. 146
Table B.10. Performance analysis results of Liu deviance-based Shewhart chart in terms of ARL_1. 147
Table B.11. Performance analysis results of Liu deviance-based Shewhart chart in terms of *SDRL*. 148
Table B.12. Performance analysis results of Liu deviance-based CUSUM chart in terms of ARL_1. 149
Table B.13. Performance analysis results of Liu deviance-based CUSUM chart in terms of *SDRL*. 150
Table B.14. Performance analysis results of Liu deviance-based EWMA chart in terms of ARL_1. 151
Table B.15. Performance analysis results of Liu deviance-based EWMA chart in terms of *SDRL*. 152

LIST OF FIGURES **PAGE**

Figure 4.1. Simulation flowchart for comparative analysis of Shewhart charts. 48

Figure 4.2. Simulation flowchart for comparative analysis of CUSUM and EWMA charts. 49

Figure 4.3. Performance analysis of deviance and ridge deviance-based control charts during monitoring COM-Poisson profile, $\rho^2 = 0.90$. 52

Figure 5.1. Analysis of *LPP* data set. 86

Figure 5.2. Monitoring of the Poisson profile with residual-based Shewhart charts. 88

Figure 5.3. Monitoring of the Poisson profile with residual-based CUSUM charts. 89

Figure 5.4. Monitoring of the Poisson profile with residual-based EWMA charts. 89

Figure 5.5. Analyzing *SECOM* data set. 93

Figure 5.6. Graph of residual differences against the observation numbers. 97

Figure 5.7. Control charts established based on the control set. 99

Figure 5.8. Analysis of control set with CUSUM charts. 106

Figure 5.9. Analysis of control set with EWMA charts with $\lambda = 0.05$. 107

Figure 5.10. Analysis of control set with EWMA charts with $\lambda = 0.1$. 107

Figure 5.11. Analysis of control set with EWMA charts with $\lambda = 0.2$. 108

Figure 5.12. Difference between residuals obtained from the *BikeShare* data set model. 111

Figure 5.13. Analyzing *BikeShare* data set. 112

Figure 5.14. Monitoring historical set with Shewhart chart. 113
Figure 5.15. Monitoring historical set with CUSUM chart. 114
Figure 5.16. Monitoring historical set with EWMA chart. 114

LIST OF ABBREVIATIONS

AIC	: Akaike information criterion
ARL	: Average run length
BIC	: Bayesian information criterion
COM-Poisson	: Conway-Maxwell-Poisson
CN	: Condition number
CUSUM	: Cumulative sum
DTF	: Date time frame
EWMA	: Exponentially weighted moving average
GLM	: Generalized linear model
GLP	: Generalized linear profile
IRLS	: Iteratively reweighted least squares
LCL	: Lower control limit
ML	: Maximum likelihood
MSE	: Mean squared error
OLS	: Ordinary least squares
PCR	: Principal components regression
PTV	: Percentage of total variation
RL	: Run length
SDRL	: Standard deviation of run length
SPC	: Statistical process control
SVD	: Singular value decomposition
UCL	: Upper control limit
VIF	: Variance inflation factor

1. INTRODUCTION

Industrial processes generate data that can be analyzed to optimize the process by detecting anomalies as early as possible, avoiding significant production disruptions, material loss, and reducing the number of faulty products.

Statistical process control (SPC) studies various methods to identify irregularities in the process and the control charts are the most basic and extensively used tool in SPC. A simple control chart has its upper and lower limit. The area between those control limits is the control area. The process is considered under control when all the monitored observations are within control limits. One or more observations outside the control area indicate that the process is out-of-control. Based on the type of quality characteristics, control charts are categorized as variable and attribute control charts. Variable control charts monitor the process with a quality characteristic that can be measured and expressed as a number on a continuous scale of measurement. On the other hand, attribute control charts monitor the data that is not measured on a quantitative scale. Our research falls into the first category, hence the attribute control charts are not covered here. The well known Shewhart, cumulative sum (CUSUM), and exponentially weighted moving average (EWMA) control charts provide adequate information regarding the status of the process. While Shewhart control charts utilize the data itself for monitoring, new set of control chart statistics should be calculated by considering the impact of previous ones for CUSUM and EWMA control charts.

The advantages due to the simplicity of the control charts paved the way for the emergence of new methods. A method introduced by Mandel (1969) involves a combination of a traditional control chart and regression model. The proposed regression control chart monitors the estimated response, which is linearly dependent

on predictors. Later Zhang (1984) extended the regression control chart and presented a cause-selecting control chart. Zhang (1984) reviewed the whole production process as sub-processes and each sub-process as response that was affected by previous ones. This approach also made easy to find the cause of the irregularities. In the study, the authors laid a foundation of the residual-based control charts. Wade and Woodall (1993) examined the link between the cause-selecting control chart and the T^2 control chart. They expanded on the concept and proposed utilizing prediction limits with cause-selecting charts to increase the performance. Hawkins (1991) proposed to monitor the process by using scaled residuals of the regression of each variable on all others. Shu et al. (2004) investigated the run length performance of Shewhart and EWMA charts based on the regression residuals. The authors also pointed out the importance of the sample size and recommended acquiring a data set with a large enough sample to guarantee that estimated parameters are close to the actual parameters.

The residual control charts are widely used in the monitoring of autocorrelated processes (see Runger et al., 1995; Loredo et al., 2002; Jiang, 2004; Karaoglan and Bayhan, 2014), in pharmaceutical studies (Mihalovits and Kemény, 2020), even for academic performance analysis (Rashid et al., 2013).

Researchers also studied the residual-based control charts for the monitoring process with non-normal (Poisson, binomial, gamma, etc.) response variables. In these approaches, control charts mainly utilize residuals derived from generalized linear models (GLMs). Skinner et al. (2003) inspired by the concept and proposed a procedure which was based on the likelihood ratio statistic, i.e., the deviance residual obtained from Poisson regression. Jearkpaporn et al. (2003) used a residual control chart for monitoring gamma-distributed multiple variables under the assumption that the shape parameter was unchanged. Zeng and Zhou (2007) reviewed regression-

based control charts and studied variable selection for the multistage processes with the normal and non-normal response. Asgari et al. (2014) proposed a method for monitoring the two-stage processes with a Poisson variable and where deviance residuals used to construct EWMA chart. Kinat et al. (2020) considered response with inverse Gaussian distribution and compared deviance and Pearson residual-based Shewhart charts. Mahmood et al. (2022) investigated the process with Poisson response where standardized residuals derived from the Poisson model were used to construct memory type control charts similar to EWMA charts.

The advantage of the residual-based control charts for analyzing regression-like processes allows for their easy transition to profile monitoring. In SPC, profile monitoring is the field that investigates monitoring methods where quality characteristics can be expressed by the relationship between response and one or more predictors similar to the regression models. Profiles can be categorized as univariate (only one predictor variable) and multivariate (more than one predictor variable) profiles depending on the number of predictors involved. Also, as in regression models, there are several types of profiles based on the relation type, such as linear, non-linear, generalized linear, and other types of profiles. Generalized linear profiles (GLPs) cover the profiles such as Poisson, binom, gamma, and so on.

Profile monitoring methods have been the subject of research for some time. In a study by Mestek et al. (1994), the authors introduced a linear profile monitoring concept by examining the stability of calibration curves with T^2 control charts. Stover and Brill (1998) considered multilevel ion chromatography linear calibrations to determine instrument response stability. Kang and Albin (2000) proposed two T^2 chart-based along with the two different residual-based (residual-based EWMA chart and residual-based range chart) approaches to monitor linear profiles. The main difference between these two strategies is that T^2 uses parameterized data for mon-

itoring intercept and slope, while the residual-based strategy uses each data point. Kim et al. (2003) used a similar approach but recommended coding the predictor matrix such that the average will be 0 and replaced the range chart with a one-sided EWMA chart. Mahmoud and Woodall (2004) suggested testing the stability of the variation with the global F test and applying of Shewhart-type chart for monitoring intercept and slope in combination with the coding technique proposed by Kim et al. (2003). The superiority of the method is illustrated through the simulation study. Mahmoud and Woodall (2004) proposed progressive and double progressive mean charting for Poisson profiles. The authors used standardized residuals from the Poisson model as monitored observations. Later, Gupta et al. (2006) compared combined control charts of Kim et al. (2003) to the monitoring scheme proposed by Croarkin and Varner (1982). An integrated EWMA chart with a likelihood ratio test was proposed by Zhang et al. (2009) for simultaneous monitoring of the intercept, slope, and standard deviation of the linear profile. Saghaei et al. (2010) studied monitoring methods for the simple linear profiles by using CUSUM chart. Yeh et al. (2009) examined several control charting mechanisms using logistic regression when the response variable of interest is binary. Two of the best methods proposed by Yeh et al. (2009) was investigated by Amiri et al. (2011) for monitoring Poisson profiles under step shifts and drifts. Shang et al. (2011) expanded on the concept of profile monitoring by proposing an EWMA chart that monitors not only the functional connection that formed the profile but also the mean of the predictors. Soleymanian et al. (2013) developed a T^2-based, likelihood ratio-based, and F method and modified the order of application in monitoring binary response profiles. A similar approach was presented by Amiri et al. (2015) for GLPs in the example of profile with count response. Qi et al. (2016) on the other hand, introduced a monitoring method based on the weighted likelihood ratio test. The efficiency of the double EWMA chart under

Bayesian methodology was showed by Abbas et al. (2017). Derakhshani et al. (2020) compared T^2, multivariate EWMA, likelihood ratio test method, and r-chart, which was constructed based on the standardized raw residuals for Poisson profiles. Maleki et al. (2018) conducted extensive research on the topic and reviewed studies in profile monitoring spanning a decade. Fan et al. (2013, 2017), Cano et al. (2015), Guevara and Vargas (2015, 2016), Steiner et al. (2016) mainly concentrated on monitoring methods for nonlinear profiles.

In this thesis, to model the relationship between predictors and count response, we particularly focus on the Conway-Maxwell-Poisson (COM-Poisson) profiles which is a special case of GLPs.

Even though COM-Poisson distribution simplifies the analysis of count data with under- and overdispersion. Under certain conditions it converges to the Poisson, Bernoulli, and geometric distributions. The COM-Poisson distribution, a two-parameter distribution as a generalization of the Poisson distribution is introduced to the literature by Conway and Maxwell (1962). Later, Boatwright et al. (2003), Shmueli et al. (2005) extensively studied COM-Poisson distribution. Conjugate analysis of the distribution is performed by Boatwright et al. (2006) and Gupta et al. (2014) developed the likelihood ratio and score test for testing equidispersion. Sellers et al. (2016) formulated the bivariate form of the COM-Poisson distribution and presented parameter estimation along with the hypothesis tests. Lord et al. (2008), Guikema and Goffelt (2008), and Sellers and Shmueli (2010) examined the distribution within the framework of GLM. Lord et al. (2008) benefited from the advantages of COM-Poisson distribution and developed COM-Poisson GLM for modelling motor vehicle crash data set. Guikema and Goffelt (2008) mentioned that despite its flexibility, COM-Poisson distribution has some limitations and suggested reformulating the distribution for modelling count data. Sellers and Shmueli (2010) discussed esti-

mation, extraction, diagnosis, and interpretation of the COM-Poisson model. Francis et al. (2012) addressed the characterization of the parameter estimation accuracy of the maximum likelihood (ML) implementation and the estimate of the prediction accuracy of the COM-Poisson model by using simulated data sets.

In recent years univariate data are become almost nonexistent. But, as the number of predictors increases, new problems emerge. One of them is the interrelated predictors. The correlation between predictors contrasts with the fundamental assumptions of the regression analysis. This phenomenon is known as multicollinearity in the literature and poses significant challenges throughout the analysis.

Introduced by Frisch (1934), the problem of multicollinearity in regression models is revisited and reviewed later by Farrar and Glauber (1967), Haitovsky (1969), Gunst and Webster (1975), and Paul (2006). Cheng and Iglarsh (1976) state that the multicollinearity undermines the statistical significance of the predictor variable and causes computational problems since traditional parameter estimation methods (ordinary least squares and ML) require the calculation of the inverse of the covariance matrix. In the GLM framework, the consequences of multicollinearity were investigated by Mackinnon and Puterman (1989), Weissfeld and Sereika (1991), and Lesaffre and Marx (1993).

In general, numerous methods were developed to address the problem and orthogonalization of the predictor matrix to obtain a smaller set of uncorrelated variables is one of them. The approach was proposed by Kendall (1957), who implemented artificial orthogonalization into a regression analysis. The author demonstrated how substituting the original data with their orthogonal-principal components according to the mean squared error (MSE) produces more accurate estimates than those obtained using ordinary least squares (OLS) estimation. Massy (1965) also studied regression modelling and principal component analysis combination. An ex-

tensive review of the approach is presented by Jolliffe (2002). The PCR applications to GLMs to eliminate the impacts of multicollinearity were initially studied by Marx and Smith (1990), Smith and Marx (1990), and Marx (1992). Aguilera et al. (2006) suggested using PCR estimation to reduce the dimension of data with a binary response and to provide an accurate estimation of the parameters of the model while avoiding multicollinearity.

Another method to eliminate the negative impact of multicollinearity aside from the principal component approach is a biased estimation. The ridge estimation, a well-known biased method, was proposed by Hoerl and Kennard (1970) as an alternative to the OLS estimator in linear regression. This estimation method is a technique for introducing some degree of bias to reduce the variability of parameter estimates. It shrinks the regression coefficients towards zero by adding a positive biasing constant (tuning parameter). Many researchers studied the ridge estimator extensions in linear regression, some of which are Hoerl et al. (1975), Lawless (1976), Wichern and Churchill (1978), Skinner et al. (2003), and Alkhamisi and Shukur (2007) among others. Segerstedt (1992) proposed a ridge estimator for GLMs, Schaefer et al. (1984), Lee and Silvapulle (1988) studied a ridge estimator for logistic regression where the response variable follows a binomial distribution. All these researchers obtained the ridge estimator on the ML estimator at convergence, and the weight matrix in these ridge estimators depends on the ML estimate. However, Özkale et al. (2018) noted that the ridge estimator obtained this way is unsuitable since GLMs are nonlinear models. The authors developed an iterative ridge estimator for logistic regression using the penalized log-likelihood function of Le Cessie and Van Houwelingen (1992). Özkale (2016) also presented an iterative biased estimator for logistic regression models. Månsson and Shukur (2011) proposed a Poisson ridge estimator to overcome the instability of the ML method for Poisson regression and discussed

the performance of several tuning parameters. Zaldivar (2018) extended the Poisson ridge estimator by Månsson and Shukur (2011) and compared fifty different tuning parameters for Poisson regression model to the ML estimator by considering Monte Carlo simulation. Abdella et al. (2019) presented a penalized likelihood estimation for the COM-Poisson model. Mammadova and Özkale (2021b) provided an iterative closed-form solution to the ridge estimator given by Abdella et al. (2019), and Sami et al. (2022) proposed COM-Poisson ridge regression estimator, which is ridge estimator obtained at the final iteration of ML estimator.

Despite being a popular technique for dealing with multicollinearity, the ridge estimator is controversial since it depends on the ridge tuning value. However, the excess amount of options can present difficulties at times. An estimator proposed by Liu (1993) is less complicated than the ridge estimator due to the simplicity of tuning parameter selection. Liu estimator itself is a combination of two estimators which are ridge and shrunken estimators. Several approaches were developed based on the Liu estimator over the years. Urgan and Tez (2008) developed a Liu-type estimator for logistic regression, and Özkale (2016) proposed an iterative Liu estimator to reduce the effect of collinearity in logistic regression. Kurtoğlu and Özkale (2016) developed a first-order approximated Liu estimator to resolve multicollinearity in GLMs. Mansson et al. (2012) and Qasim et al. (2018) suggested different methods for obtaining the Liu tuning parameter in Poisson regression. Månsson (2013) also obtained the Liu estimator for the negative binomial regression model. Qasim et al. (2020a) introduced some new tuning parameters for the Liu estimator in linear regression. Recently, Mammadova and Özkale (2022) presented Liu estimator for COM-Poisson model.

Besides the aforementioned methods, researchers also investigated a combination of two approaches which carries the idea that merging two successful methods

can strengthen efficiency. One of these combinations is an *r-k* class estimator. Initially suggested by Baye and Parker (1984) in linear regression, the estimator unites to principal components regression and ridge estimation methods. A comparative study on the *r-k* class estimator was conducted by Özkale and Kaçıranlar (2008), Dawoud and Kaçıranlar (2017), and Şiray and Sakallıoğlu (2012). Later, Özkale and Arıcan (2016) adjusted the *r-k* class estimator for logistic regression models. Abbasi and Özkale (2021) developed the iterative *r-k* class estimator for GLMs. The authors showed the superiority of proposed approaches to ML and ridge estimators in terms of the mean square.

The issue of multicollinearity is also addressed in profile monitoring. Houshmand and Javaheri (1998) studied ridge deviance residual control charts to overcome some drawbacks of process monitoring methods under multicollinearity in linear profiles. Amiri et al. (2014) proposed a new multivariate statistic for linear profiles considering the correlation between predictors and used a multivariate EWMA chart for monitoring. Marcondes Filho and Sant'Anna (2016) proposed residual-based control charts for monitoring count data with correlated predictors by combining principal component analysis with Poisson regression. Park et al. (2018) also adapted the PCR approach for the process monitoring and constructed an *r*-chart, Park et al. (2020) utilized randomized residuals to build a Shewhart chart for COM-Poisson profile monitoring. Later Rao et al. (2020) studied a mixed EWMA and CUSUM chart for the COM-Poisson profile. Shewhart, EWMA, and CUSUM charts based on ridge deviance residuals were introduced by Mammadova and Özkale (2021b) for monitoring Poisson and the COM–Poisson profiles. Jamal et al. (2021) adapted randomized quantile and deviance residuals based on CUSUM and EWMA charts for monitoring real-time highway safety surveillance data set by considering it as the COM-Poisson profile. Mammadova and Özkale (2022) extended the idea of deviance residual-based

control charts. The authors proposed Shewhart, CUSUM, and EWMA charts based on the Liu-deviance residuals for GLPs with dispersed count response under multicollinearity.

1.1. Aims and scope

This study covers various methods to identify an out-of-control situation in a particular count profile with residual-based control charts under multicollinearity. In available studies, the researchers are mostly inspired by regression modelling techniques and regression-based monitoring approaches in developing profile monitoring methods due to the similarities.

In this study we,

- modelled the data with the COM-Poisson model, overcome the limitations of Poisson distribution;
- estimated model parameters by utilizing alternative estimation methods (PCR, ridge, Liu, and *r-k* class estimation) that adjusted for the COM-Poisson model to reduce the impact of the multicollinearity;
- defined deviance-type residuals based on the PCR, ridge, Liu, and *r-k* class estimators;
- established PCR, ridge, Liu, and *r-k* deviance-based Shewhart, CUSUM, and EWMA charts to detect shifts of the any size;
- evaluated the performance of the suggested methods through comparative performance analysis, which include extensive simulation studies and real-life examples.

1.2. Organization of the thesis

The remainder of this thesis is organized as follows:

Chapter 2 provides general information regarding GLM and COM-Poisson model as its specific case, as well as the deviance residuals derived from the model and diagnostic procedures for multicollinearity. Parameter estimation for the COM-Poisson model under conditions of independent and correlated predictors is also presented. The parameter estimation under multicollinearity covers the calculation details for the proposed PCR, ridge, Liu, and *r-k* class estimators, along with tuning parameters for the ridge, Liu, and *r-k* class estimators. Residual-based control charts for monitoring COM-Poisson profiles are discussed in Chapter 3. Chapter 4 presents simulation studies for the performance evaluation of the proposed ridge, Liu, PCR, and *r-k* deviance-based Shewhart, CUSUM, and EWMA charts. The analysis of real-life "laminated plastic plywood" (*LPP*), "bike-sharing application" (*BikeShare*), and "semiconductor manufacturing" (*SECOM*) data sets using the monitoring techniques covered in the study is provided in Chapter 5. Finally, the last chapter of this study includes detailed conclusions.

2. GENERALIZED LINEAR MODELS

Assume that the pair data set $(y_i, x_i), i = 1, 2, \ldots, n$ is given where y_i is the ith observation of $Y_{n\times 1}$ response variable of non-normal distribution, $x_i = (x_{i1}, x_{i2}, \ldots, x_{ip})'$ is the ith row of $X_{n\times p}$ predictor matrix. The relationship between predictor and response variable can be modeled through GLM. The GLM is the generalization of an ordinary linear model that enables modelling data with a response variable of non-normal distribution, particularly the distributions that belong to the exponential family. A diverse range of continuous and discrete distributions, including count as well as the normally distributed data are covered by exponential family distribution that has the probability density function of

$$f(y_i, \theta_i, \phi) = exp\left(\frac{y_i\theta_i - b(\theta_i)}{a(\phi)} + c(y_i, \phi)\right) \tag{2.1.}$$

where θ_i and ϕ are the natural and dispersion parameters respectively, and $a(\circ)$, $b(\circ)$, and $c(\circ)$ are known functions.

The logarithm of the likelihood function of Eq. (2.1.) is

$$l(y_i, \theta_i, \phi) = \sum_{i=1}^{n} \frac{y_i\theta_i - b(\theta_i)}{a(\phi_i)} + \sum_{i=1}^{n} c(y_i, \phi_i).$$

The expected value and the mean of the response are respectively as

$$E(y_i) = \mu_i = b'(\theta_i) = \frac{\partial b(\theta_i)}{\partial \theta_i},$$
$$var(y_i) = b''(\theta_i)a(\phi) = \frac{\partial^2 b(\theta_i)}{\partial \theta_i^2}.$$

According to McCullagh and Nelder (1989), there exists a function that connects the predictors with the expected value of the response variable:

$$\eta_i = h(\mu_i) = x_i'\beta \tag{2.2.}$$

where $\beta = (\beta_1, \beta_2, \ldots, \beta_p)'$ is the unknown vector of parameters[1]. The function $h(\circ)$ in Eq. (2.2.) is known as a link function. The formulation of the link function depends on the distribution of the response variable. Since the exponential family distribution covers a wide range of distributions, several link functions exists that express the relationship between predictor and response variables. McCullagh and Nelder (1989) presented some of the link functions with respective distribution.

2.1. GLMs with count response: COM-Poisson model

COM-Poisson model is the particular case of the GLM where the response variable follows the COM-Poisson distribution. The model facilitates the analysis of count data with under- or overdispersion, as well as the equidispersion.

After the introduction by Conway and Maxwell (1962), conjugate analysis of the distribution is performed by Boatwright et al. (2003). Minka et al. (2003) and Shmueli et al. (2005) discussed some statistical and probabilistic properties, while Nadarajah (2009) investigated the distributional properties from the mathematical point of view. Another extensive study on the COM-Poisson distribution was presented by Li et al. (2020).

The probability density function of the COM-Poisson distribution is defined as

[1]The model that expresses the relationship may contain an intercept β_0. In that case, the unknown vector of parameters becomes $\beta = (\beta_0, \beta_1, \beta_2, \ldots, \beta_p)'$ and the array of the 1 should be included in the predictor matrix as the first column, making the total number of predictors $q = p + 1$.

$$f(y_i) = \frac{\mu_i^{y_i}}{(y_i!)^{\nu}} \frac{1}{Z(\mu_i, \nu)}, y_i = 0, 1, 2, \ldots, i = 1, 2, \ldots, n \tag{2.3.}$$

where $\mu_i \geq 0$ is the centering parameter, $\nu \geq 0$ is the shape parameter, $Z(\mu_i, \nu) = \sum_{s=0}^{\infty} \frac{\mu_i^s}{(s!)^{\nu}}$ is a normalization parameter s is the element of the whole numbers set. ν is also known as dispersion parameter. Overdispersion in the data set is represented by $\nu < 1$, equidispersion by $\nu = 1$, and underdispersion by $\nu > 1$.

Based on the values of centering and shape parameter, COM-Poisson distribution converges to different distributions. When $v = 0$ and $\mu_i < 1$, then $Z(\mu_i, v) = 1/(1-\mu_i)$, the COM-Poisson distribution yields in geometric distribution; as $v \to \infty$, $Z(\mu_i, v) \to 1 + \mu_i$, the distribution approaches a Bernoulli distribution. $Z(\mu_i, v)$ does not converge when $v = 0$ and $\mu_i \leq 1$, which means that distribution is undefined (Shmueli et al. 2005). In case of the equidispersion ($v = 1$), the normalization parameter is $Z(\mu_i, v) = exp(\mu_i)$, and probability density function given by Eq. (2.3.) becomes

$$f(y_i) = \frac{\mu_i^{y_i}}{y_i! exp(\mu_i)}, y_i = 0, 1, 2, \ldots, i = 1, 2, \ldots, n$$

which is an ordinary Poisson distribution.

Researchers model the data with COM-Poisson response through log-link function (e.g. Lord et al., 2008; Guikema and Goffelt, 2008; Sellers and Shmueli, 2010; Sellers, 2012; Francis et al., 2012 etc.) since the condition of $\mu_i \geq 0$ has to be satisfied.

2.2. Parameter estimation

2.2.1. Uncorrelated predictors

The way of estimating unknown β parameters of the COM-Poisson model is through a log-likelihood function of the COM-Poisson distribution that is provided by Sellers and Shmueli (2010) as

$$l(\beta; y, v) = \nu \sum_{i=1}^{n} y_i log(\mu_i) - \nu \sum_{i=1}^{n} log(y_i!) - \sum_{i=1}^{n} log\left(Z(\mu_i; \nu)\right). \tag{2.4.}$$

Jowaheer and Khan (2009) reviewed ML and quasi-likelihood estimation for COM-Poisson model. Sellers and Shmueli (2010) and Francis et al. (2012) proposed using the iteratively reweighted least squares (IRLS) technique presented by Nelder and Wedderburn (1972) and Wood (2017). The closed form solution for IRLS estimator, known as ML estimator, later delivered by Mammadova and Özkale (2021b) as

$$\hat{\beta}_{ML}^{(t+1)} = (X'\hat{V}_{ML}^{(t)}X)^{-1}X'\hat{V}_{ML}^{(t)}z_{ML}^{(t)} \tag{2.5.}$$

where t is the iteration step, $z_{ML}^{(t)} = X\hat{\beta}_{ML}^{(t)} + (\hat{V}_{ML}^{(t)})^{-1}(y - \hat{\mu}_{ML}^{(t)})$ is the working response, and $\hat{V}_{ML}^{(t)}$ is the weight matrix evaluated at $\hat{\beta}_{ML}^{(t)}$. Following the successful iterations, $\hat{\beta}_{ML}$ at convergence is obtained as $\hat{\beta}_{ML} = \left(X'\hat{V}_{ML}X\right)^{-1}X'\hat{V}_{ML}z_{ML}$.

Initially, the weighted matrix for the COM-Poisson model is introduced by Sellers and Shmueli (2010) and later elaborated by Francis et al. (2012) as

$$V = \sum_{s=0}^{\infty} \frac{\left[\frac{v(v-1)s^2(exp(\mu))^{2s}\left(\frac{(exp(\mu))^s}{s!}\right)^{v-2}}{(s!)^2} + \frac{vs^2(exp(\mu))^s\left(\frac{(exp(\mu))^s}{s!}\right)^{v-1}}{s!} \right]}{\sum_{s=0}^{\infty}\left(\frac{(exp(\mu))^s}{s!}\right)^v} - \sum_{s=0}^{\infty} \frac{\left[\frac{vs(exp(\mu))^s\left(\frac{(exp(\mu))^s}{s!}\right)^{v-1}}{s!} \right]^2}{\sum_{s=0}^{\infty}\left[\left(\frac{(exp(\mu))^s}{s!}\right)^v\right]^2}. \tag{2.6.}$$

2.2.2. Correlated predictors

In the case of uncorrelated predictors, the ML estimator proves to be a reliable method. But, because of the challenges that multicollinearity poses with the computation of the inverse of $X'V_{ML}X$ matrix, which is essential for ML estimation, alternative approaches are required. In this section, we present a few remedies to this issue for the COM-Poisson model.

2.2.2.1. *PCR estimator*

A suitable alternative to the ML estimation in the case of multicollinearity is the PCR estimation. The PCR estimator addresses the multicollinearity problem by generating a new set of uncorrelated variables using the singular value decomposition (SVD) technique discussed in GLMs by Smith and Marx (1990), Aguilera et al. (2006), Özkale and Arıcan (2016), and Abbasi and Özkale (2021). Jolliffe (2002) stated that the SVD is effective in terms of both computation and interpretation in PCR. The author also brought up the significance of standardization of the predictor variables to zero mean and unit variance to remove the scale dependence of principal components.

In brief, SVD can be described as follows: let us express linear predictor η as $\eta = X\beta = XTT'\beta = X^*\omega$ where $X^* = XT$ and $\omega = T'\beta$. T is an orthogonal matrix through $T'X'\hat{V}_{ML}XT = \hat{\psi} = diag(\hat{\psi}_1, \hat{\psi}_2, \ldots, \hat{\psi}_p)$ and $\hat{\psi}_1 = \hat{\psi}_{max} \geq \hat{\psi}_2 \geq \ldots \hat{\psi}_p = \hat{\psi}_{min}$ are the eigenvalues of the $X'\hat{V}_{ML}X$ matrix. X^* matrix can be partitioned as $X^* = [X_r^* \quad X_{p-r}^*]$, where $X_r^* = XT_r \quad (r \leq p)$ is the matrix of the principal components that will be retained in the model. ω, T, and $\hat{\psi}$ are partitioned as $\omega = [\omega_r \quad \omega_{p-r}]$, $\quad T = [T_r \quad T_{p-r}]$, and $\hat{\psi} = [\hat{\psi}_r^*, \hat{\psi}_{p-r}^*]$ where $\hat{\psi}_r^* = X_r^{*'}\hat{V}_{ML}X_r^* = diag(\hat{\psi}_1, \ldots, \hat{\psi}_r)$, $\hat{\psi}_{p-r}^* = X_{p-r}^{*'}\hat{V}_{ML}X_{p-r}^* = diag(\hat{\psi}_{r+1}, \ldots, \hat{\psi}_p)$, and r is the number of principal components that will be included in the model.

To determine the r value, several methods have been proposed in the literature in the context of linear regression. However, the most frequently used one is the one that Jolliffe (2002) recommended which is known as percentage of total variance (*PTV*). The *PTV* was also used by Aguilera et al. (2006) in the context of GLMs. We here can also use the *PTV* measure which is given by $PTV = \left(\frac{\sum_{i=1}^{r}\hat{\psi}_i}{\sum_{i=1}^{p}\hat{\psi}_i}\right) \times 100$ where $\hat{\psi}_i$, $i = 1, ..., p$ are the eigenvalues of $X'\hat{V}_{ML}X$.

By using SVD, Abbasi and Özkale (2021) obtained the PCR estimator in GLMs which was originally introduced by Marx and Smith (1990) in linear regression. We adjusted it for the COM-Poisson model as

$$\hat{\beta}_{PCR}^{(t+1)} = T_r \left(T_r'X'\hat{V}_{ML}^{(t)}XT_r\right)^{-1} T_r'X'\hat{V}_{ML}^{(t)}z_{PCR}^{(t)} \tag{2.7.}$$

where $z_{PCR}^{(t)} = XT_rT_r'\hat{\beta}_{PCR}^{(t)} + \left(\hat{V}_{ML}^{(t)}\right)^{-1}\left(y - \mu_{PCR}^{(t)}\right)$ is evaluated at $\hat{\beta}_{PCR}^{(t)}$. The $\hat{\beta}_{PCR}$ estimator at convergence is $\hat{\beta}_{PCR} = T_r\left(T_r'X'\hat{V}_{ML}XT_r\right)^{-1}T_r'X'\hat{V}_{ML}z_{PCR}$.

2.2.2.2. *Ridge estimator*

To obtain ridge estimator for COM-Poisson model, Mammadova and Özkale (2021b) defines the penalized log-likelihood function as

$$l(\beta; y, v, k) = l(\beta; y) - \frac{1}{2}\beta'\beta \tag{2.8.}$$

where $k > 0$ is a Lagrangian parameter. The penalty presented in the equation subtracted from log-likelihood function pulls or shrinks the final estimates away from the ML estimates. Following Mammadova and Özkale (2021b), we obtain the first and second order derivatives of Eq. (2.8.), respectively as

$$\frac{\partial l(\beta; y, v, k)}{\partial \beta} = X'(y - \mu) - k\beta$$
$$\frac{\partial l^2(\beta; y, v, k)}{\partial \beta \partial \beta'} = -(X'VX + kI_p).$$

where V is the weight matrix and I is the identity matrix in Eq. (2.6.).

Then we apply the Newton-Raphson iterative method to find estimators. The ridge estimator for COM-Poisson model in the $(t+1)^{th}$ iteration is

$$\hat{\beta}_{ridge}^{(t+1)} = (X'\hat{V}_{ridge}^{(t)}X + kI_p)^{-1}X'\hat{V}_{ridge}^{(t)}z_{ridge}^{(t)} \tag{2.9.}$$

where $z_{ridge}^{(t)} = X\hat{\beta}_{ridge}^{(t)} + (\hat{V}_{ridge}^{(t)})^{-1}(y - \hat{\mu}_{ridge}^{(t)})$ is the working response and $\hat{V}_{ridge}$ is the weight matrix in Eq. (2.6.) evaluated at $\hat{\beta}_{ridge}$. The ridge estimator of β at convergence has the form of $\hat{\beta}_{ridge} = \left(X'\hat{V}_{ridge}X + kI_p\right)^{-1} X'\hat{V}_{ridge}z_{ridge}$.

2.2.2.3. *Liu estimator*

Liu estimator is another biased estimator, proved to be useful in case of multicollinearity. In recent study, Mammadova and Özkale (2022) presented Liu estimation method for COM-Poisson model. Following Kurtoğlu and Özkale (2016), the authors defined the objective function as

$$\begin{aligned} P(\beta;y,v,\theta) &= l(\beta;y,v) - \frac{1}{2}\sum_{i=0}^{p}(\beta_i - \theta\hat{\beta}_{ML,i})^2 \\ &= (v\sum_{i=1}^{n} y_i log(\mu_i) - \sum_{i=1}^{n} log(Z(\mu_i,v)) - v\sum_{i=1}^{n} log(y_i!) - \frac{1}{2}\sum_{i=0}^{p}(\beta_i - \theta\hat{\beta}_{ML,i})^2 \end{aligned} \tag{2.10.}$$

where $0 < \theta < 1$ is the Liu tuning parameter and $\hat{\beta}$ is the ML estimator at final iteration. The first and second-order derivatives of Eq. (2.10.) with respect to β are, respectively as

$$\frac{\partial P(\beta;y,v,\theta)}{\partial\beta} = X'(y-\mu) - \beta + \theta\hat{\beta}_{ML}$$

and

$$\frac{\partial^2 P(\beta;y,v,\theta)}{\partial\beta\partial\beta'} = -(X'VX + I),$$

where V is the weight matrix given in Eq. (2.6.).

The application of Newton-Raphson method gives

$$\begin{aligned} \hat{\beta}_{Liu}^{(t+1)} &= \hat{\beta}_{Liu}^{(t)} + \left(X'\hat{V}_{Liu}^{(t)}X + I\right)\left(X'(y-\hat{\mu}_{Liu}^{(t)}) - \hat{\beta}_{Liu}^{(t)} + \theta\hat{\beta}_{ML}\right) \\ &= \left(X'\hat{V}_{Liu}^{(t)}X + I\right)^{-1}\left(X'\hat{V}_{Liu}^{(t)}X\hat{\beta}_{Liu}^{(t)} + X'(y-\hat{\mu}_{Liu}^{(t)}) + \theta\hat{\beta}_{ML}\right) \end{aligned} \tag{2.11.}$$

where $\hat{V}_{Liu}$ is the weight matrix given in Eq. (2.6.) obtained at $\hat{\beta}_{Liu}$. After simplifications, Eq. (2.11.) becomes

$$\hat{\beta}_{Liu}^{(t)} = (X'\hat{V}_{Liu}^{(t)}X + I)^{-1}(X'\hat{V}_{Liu}^{(t)}z_{Liu}^{(t)} + \theta\hat{\beta}_{ML}) \tag{2.12.}$$

which is the COM-Poisson Liu estimator where $z_{Liu}^{(t)} = X\hat{\beta}_{Liu}^{(t)} + (\hat{V}_{Liu}^{(t)})^{-1}(y - \hat{\mu}_{Liu}^{(t)})$ is the working response, $z_{Liu}^{(t)}, \hat{V}_{Liu}^{(t)}$, and $\hat{\mu}_{Liu}^{(t)}$ are evaluated at $\hat{\beta}_{Liu}^{(t)}$. The COM-Poisson Liu estimator at convergence is $\hat{\beta}_{Liu} = (X'\hat{V}_{Liu}X + I)^{-1}(X'\hat{V}_{Liu}z_{Liu} + \theta\hat{\beta}_{ML})$ where $\hat{V}_{Liu}$ and z_{Liu} are evaluated at the final iteration.

2.2.2.4. *r-k class estimator*

As mentioned before, the *r-k* class estimator is a combination of the PCR and ridge estimators. Abbasi and Özkale (2021) adjusted the *r-k* class estimator proposed by Baye and Parker (1984) and obtained the *r-k* class estimator for GLMs. We adapt the estimator defined by Abbasi and Özkale (2021) and obtain it for the COM-Poisson model by updating the weight matrix defined by Eq. (2.6.) as

$$\hat{\beta}_{r-k}^{(t+1)} = T_r\left(T_r'X'\hat{V}_{ML}^{(t)}XT_r + kI_r\right)^{-1}T_r'X'\hat{V}_{ML}^{(t)}z_{r-k}^{(t)} \tag{2.13.}$$

where k is the tuning parameter and $z_{r-k}^{(t)} = XT_rT_r'\hat{\beta}_{r-k}^{(t)} + \left(\hat{V}_{ML}^{(t)}\right)^{-1}\left(y - \mu_{r-k}^{(t)}\right)$.

If the successive estimates $\hat{\beta}_{r-k}^{(t)}$ converge to, say $\hat{\beta}_{r-k}$, as t tends to infinity, we obtain the COM-Poisson *r-k* class estimator at convergence as $\hat{\beta}_{r-k} = T_r\left(T_r'X'\hat{V}_{ML}XT_r + kI_r\right)^{-1}T_r'X'\hat{V}_{ML}z_{r-k}$ where $\hat{V}_{r-k}$ and z_{r-k} are evaluated at the final iteration.

2.3. Tuning parameters for biased estimators

The value of the tuning parameter plays an important role in biased estimation. It should be as small as possible, but at the same time, large enough to give good estimate because the increasing value pulls the estimator away from its true value. In this section, we present some tuning parameters that are available in literature for ridge, Liu, and *r-k* class estimators.

2.3.1. Tuning parameter for the ridge and *r-k* class estimators

Numerous studies were conducted in the literature on the selection of tuning parameter for ridge estimator. Some of the selection methods are estimation-oriented, while others are prediction-oriented. The earliest simple way of obtaining ridge tuning parameter was proposed by Hoerl et al. (1975). Kibria (2003) suggested ridge tuning parameter based on geometric mean and median. Later, Alkhamisi and Shukur (2007), motivated by the work of Kibria (2003) studied a slightly different approach. The authors proposed to calculate the ridge tuning parameter based on the eigenvalues of $X'X$ matrix. Mammadova and Özkale (2021a) adopted these well-known estimate-focused tuning parameter calculation techniques and obtained the ridge tuning parameter estimators for Poisson model as

$$k_1 = \frac{p}{\hat{\beta}'_{ML}\hat{\beta}_{ML}} \tag{2.14.a}$$

$$k_2 = \left(\frac{1}{\prod \hat{\beta}_{ML,i}}\right)^{\frac{1}{p}} \tag{2.14.b}$$

$$k_3 = median\left(\frac{1}{\hat{\beta}^2_{ML,i}}\right) \tag{2.14.c}$$

$$k_4 = max\left(\frac{1}{\hat{\beta}^2_{ML,i}} + \frac{1}{\hat{\psi}_i}\right) \tag{2.14.d}$$

$$k_5 = median\left(\frac{1}{\hat{\beta}^2_{ML,i}} + \frac{1}{\hat{\psi}_i}\right) \tag{2.14.e}$$

$$k_6 = \frac{v}{\sum \hat{\psi}_i \hat{\beta}^2_{ML,i}} + \frac{1}{\hat{\psi}_{max}} \tag{2.14.f}$$

where $\hat{\beta}_{ML}$ is the ML estimator vector at convergence, $\hat{\psi}_i$ is the ith eigenvalue of the $X'\hat{V}_{ML}X$ matrix.

By involving the dispersion to Eqs. (2.14.a) - (2.14.f), we obtain ridge tuning parameters for COM-Poisson model as

$$k_{CMP,1} = \frac{vp}{\hat{\beta}'_{ML}\hat{\beta}_{ML}} \tag{2.15.a}$$

$$k_{CMP,2} = \left(\frac{v}{\prod \hat{\beta}_{ML,i}}\right)^{\frac{1}{p}} \tag{2.15.b}$$

$$k_{CMP,3} = median\left(\frac{v}{\hat{\beta}^2_{ML,i}}\right) \tag{2.15.c}$$

$$k_{CMP,4} = max\left(\frac{v}{\hat{\beta}^2_{ML,i}} + \frac{1}{\hat{\psi}_i}\right) \tag{2.15.d}$$

$$k_{CMP,5} = median\left(\frac{v}{\hat{\beta}^2_{ML,i}} + \frac{1}{\hat{\psi}_i}\right) \tag{2.15.e}$$

$$k_{CMP,6} = \frac{v}{\sum \hat{\psi}_i \hat{\beta}^2_{ML,i}} + \frac{1}{\hat{\psi}_{max}} \tag{2.15.f}$$

Recently, Abbasi and Özkale (2021) adopted tuning parameter proposed by Hoerl and Kennard (1970) for the estimation of the *r-k* class estimator in GLMs. By adjusting the same tuning parameter for COM-Poisson regression models, we obtain

$$k = \frac{rv}{\hat{\beta}^{(0)'} T_r T_r' \hat{\beta}^{(0)}} \tag{2.16.}$$

where $\hat{\beta}^{(0)}$ is the initial value of the regression coefficients.

2.3.2. Tuning parameter for the Liu estimator

There are several approaches for obtaining the Liu tuning parameter in the context of GLMs. Urgan and Tez (2008), Månsson et al. (2012), Kurtoğlu and Özkale

(2016), Özkale (2016), Qasim et al. (2018), Qasim et al. (2020b), Algamal and Asar (2020) mentioned different Liu tuning parameter selection methods in GLMs or special regression model forms of GLMs. The commonly used method to obtain the tuning parameter value is based on minimizing the scalar MSE criterion of the estimators under consideration.

The aforementioned studies have also used the scalar MSE criterion to acquire the value of the tuning parameter. Therefore, to obtain the value of the tuning parameter, we modify the calculation of the tuning parameter selection method proposed by Kurtoğlu and Özkale (2016) to the COM-Poisson Liu estimator, which lies in the interval of $(0,1)$:

$$\hat{\theta} = 1 - h_\theta \frac{\sum_{j=1}^{p} \frac{v}{\hat{\psi}_j(\hat{\psi}_j+1)}}{\sum_{j=1}^{p} \frac{\hat{\alpha}_j^{(0)}}{(\hat{\psi}_j+1)^2}},$$

where h_θ provides the following inequality

$$0 < h_\theta < \frac{\sum_{j=1}^{p} \frac{\hat{\alpha}_j^{(0)}}{(\hat{\psi}_j+1)^2}}{\sum_{j=1}^{p} \frac{v}{\hat{\psi}_j(\hat{\psi}_j+1)}}$$

with $\hat{\psi}_j$ be the eigenvalue of the $X'\hat{V}_{ML}^{(0)}X$ matrix and $\hat{\alpha}^{(0)} = T'\beta^{(0)}$, where T is a $p \times p$ orthogonal matrix with columns constitute the eigenvectors of the $X'\hat{V}_{ML}^{(0)}X$ matrix.

Kurtoğlu and Özkale (2016) stated that h_θ satisfies

$$0 < h_\theta < min\left[\frac{2(n-p)}{n-p+2}\left(1 - \frac{2}{\sum_{j=1}^{p} \frac{\hat{\psi}_{min}(\hat{\psi}_{min}+1)}{\hat{\psi}_j(\hat{\psi}_j+1)}}\right), \frac{\sum_{j=1}^{p} \frac{(\hat{\alpha}_j^{(0)})^2}{\hat{\psi}_j+1)^2}}{\sum_{j=1}^{p} \frac{v}{\hat{\psi}_j(\hat{\psi}_j+1)}}\right] \qquad (2.17.)$$

if $\sum_{j=1}^{p} \frac{\hat{\psi}_{min}(\hat{\psi}_{min}+1)}{\hat{\psi}_j(\hat{\psi}_j+1)} > 2$. If the data set fails to meet the condition, then h_θ can be

chosen arbitrarily from the $(0,1)$ interval.

2.4. Iterative estimation algorithms

Repetitive calculations are necessary to obtain the iterative estimators described in Sections 2.2.1. and 2.2.2. While initial values required to start the iterative process, the convergence criterion should be defined to stop it. The initial fitted values for the iterative estimation can be chosen as $\mu_i^{(0)} = exp(x_i\beta^{(0)})$, where $\beta^{(0)}$ is the known value or an estimator of β for any method in COM-Poisson regression and the computations are repeated until the convergence criterion has met.

The following algorithms describe the computing process of each estimator.

Algorithm 1. ML estimation

1. Set $t = 0$
2. Set initial parameter vector $\beta^{(0)}$
3. Calculate $\hat{\mu}^{(0)}$, $\hat{V}^{(0)}$, and $\hat{z}^{(0)}$
4. Calculate $\hat{\beta}_{ML}^{(0)}$
5. Set convergence criterion, begin **while** loop
6. Update $\hat{\mu}_{ML}^{(t)}$, $\hat{V}_{ML}^{(t)}$, and $\hat{z}_{ML}^{(t)}$
7. Set $\hat{\beta}_{ML}^{(t+1)}$=$\hat{\beta}_{ML}^{(t)}$
8. Calculate $\hat{\beta}_{ML}^{(t+1)}$ as in Eq. (2.5.)
9. Set $t \rightarrow t+1$
10. End **while** loop

Algorithm 2. PCR estimation

1. Set $t = 0$
2. Set initial parameter vector $\beta^{(0)}$
3. Calculate $\hat{\mu}^{(0)}$ and $\hat{V}^{(0)}$
4. Apply SVD, obtain r and T_r
5. Calculate $\hat{\beta}^{(0)}_{PCR}$
6. Set convergence criterion, begin **while** loop
7. Update $\hat{\mu}^{(t)}_{PCR}$, $\hat{V}^{(t)}_{PCR}$, and $\hat{z}^{(t)}_{PCR}$
8. Set $\hat{\beta}^{(t+1)}_{PCR}$=$\hat{\beta}^{(t)}_{PCR}$
9. Calculate $\hat{\beta}^{(t+1)}_{PCR}$ as in Eq. (2.13.)
10. Set $t \to t+1$
11. End **while** loop

Algorithm 3. Ridge estimation

1. Set $t = 0$
2. Set initial parameter vector $\beta^{(0)}$
3. Calculate $\hat{\mu}^{(0)}$, $\hat{V}^{(0)}$, and $\hat{z}^{(0)}$
4. Calculate tuning parameter k
5. Calculate $\hat{\beta}^{(0)}_{ridge}$
6. Set convergence criterion, begin **while** loop
7. Update $\hat{\mu}^{(t)}_{ridge}$, $\hat{V}^{(t)}_{ridge}$, and $\hat{z}^{(t)}_{ridge}$
8. Set $\hat{\beta}^{(t+1)}_{ridge}$=$\hat{\beta}^{(t)}_{ridge}$
9. Calculate $\hat{\beta}^{(t+1)}_{ridge}$ as in Eq. (2.9.)
10. Set $t \to t+1$
11. End **while** loop

Algorithm 4. Liu estimation

1. Set $t = 0$
2. Set initial parameter vector $\beta^{(0)}$
3. Calculate $\hat{\mu}^{(0)}$, $\hat{V}^{(0)}$, and $\hat{z}^{(0)}$
4. Obtain tuning parameter θ as in Section 2.3.2.
5. Calculate $\hat{\beta}_{Liu}^{(0)}$
6. Set convergence criterion, begin **while** loop
7. Update $\hat{\mu}_{Liu}^{(t)}$, $\hat{V}_{Liu}^{(t)}$, and $\hat{z}_{Liu}^{(t)}$
8. Set $\hat{\beta}_{Liu}^{(t+1)}$=$\hat{\beta}_{Liu}^{(t)}$
9. Calculate $\hat{\beta}_{Liu}^{(t+1)}$ as in Eq. (2.9.)
10. Set $t \to t+1$
11. End **while** loop

Algorithm 5. r-k class estimation

1. Set $t = 0$
2. Set initial parameter vector $\beta^{(0)}$
3. Calculate $\hat{\mu}^{(0)}$ and $\hat{V}^{(0)}$
4. Apply SVD, obtain r and T_r
5. Calculate tuning parameter k
6. Calculate $\hat{\beta}_{r-k}^{(0)}$
7. Set convergence criterion, begin **while** loop
8. Update $\hat{\mu}_{r-k}^{(t)}$, $\hat{V}_{r-k}^{(t)}$, and $\hat{z}_{r-k}^{(t)}$
9. Set $\hat{\beta}_{r-k}^{(t+1)}$=$\hat{\beta}_{r-k}^{(t)}$
10. Calculate $\hat{\beta}_{r-k}^{(t+1)}$ as in Eq. (2.13.)
11. Set $t \to t+1$
12. End **while** loop

2.5. Multicollinearity diagnostics

Farrar and Glauber (1967) mention that the independence among the predictor variables is almost non-existent. So, the first thing that leads to multicollinearity is the human factor, in other words, a poor experiment design. Also, the difficulties in the analysis depend on the severity of the problem. Gunst and Webster (1975) specifies three causes of multicollinearity that are

(1) an over-defined model,
(2) sampling techniques,
(3) physical constraints on the model and/or population.

The authors emphasize the importance of early detection of multicollinearity for reliable analysis results. Mackinnon and Puterman (1989) point out that examination of the usual correlation matrix is not always sufficient for detecting signs of multicollinearity. Instead, in GLMs, the diagnostics should be based on an estimated information matrix. They mentioned that the problem of multicollinearity leads to a computationally unstable. It also has an indirect effect on inference and prediction statistics, such as deviance. Moreover, multicollinearity might manifest itself in the form of unexpected algebraic signs of the estimated coefficients or significant standard errors of estimates of the essential variables. According to Paul (2006), the effect of multicollinearity can be reduced but not completely eliminated.

Different methods of multicollinearity diagnostics were investigated in the literature (see, Belsley et al., 1980; Mansfield and Helms, 1982; Schroeder et al., 1990; Mackinnon and Puterman, 1989; Paul, 2006; Daoud, 2017; Özkale, 2021). Schroeder et al. (1990) suggested diagnostics with visual inspection of pairwise correlations of variables. But since visual inspection is frequently insufficient to diagnose multicollinearity, reviewing variance inflation factor (*VIF*) values, and evalu-

ating the eigenvalues by using condition number (*CN*) metric for detecting multicollinearity is also an option.

Marquardt (1970) defined the *VIF* of each term as the factors that increase variances of the corresponding parameter due to the correlation among predictors. According to Dobson (2002), in practice, one or more *VIF* values higher than 5 or 10 indicate the multicollinearity among predictors. *CN* on the other hand, originally utilized by Riley (1955), and later applied to GLM by Mackinnon and Puterman (1989). It is accepted that $CN > 10$ is a clear sign of the multicollinearity.

These methods can be utilized in addition to examination of pairwise correlation of predictors to inspect presence of the multicollinearity during COM-Poisson modelling.

The adjusted *VIF* values for the COM-Poisson model based on the different estimation methods can be calculated as

$$VIF_{ML} = diag\left[(X'\hat{V}_{ML}X)^{-1}\right] \tag{2.18.}$$

$$VIF_{PCR} = diag\left[(T_r'X'\hat{V}_{ML}XT_r)^{-1}T_r'X'\hat{V}_{ML}XT_r(T_r'X'\hat{V}_{ML}XT_r)^{-1}\right] \tag{2.19.}$$

$$VIF_{ridge} = diag\left[(X'\hat{V}_{ridge}X + kI_p)^{-1}X'\hat{V}_{ridge}X(X'\hat{V}_{ridge}X + kI_p)^{-1}\right] \tag{2.20.}$$

$$\begin{aligned} VIF_{Liu} =& diag[(X'\hat{V}_{Liu}X + \theta I_p)^{-1}(X'\hat{V}_{Liu}X + I_p)X'\hat{V}_{Liu}X(X'\hat{V}_{Liu}X + I_p) \\ & (X'\hat{V}_{Liu}X + \theta I_p)^{-1}] \end{aligned} \tag{2.21.}$$

$$VIF_{r-k} = diag\left[(T_r'X'\hat{V}_{ML}XT_r + kI_p)^{-1}T_r'X'\hat{V}_{ML}XT_r(T_r'X'\hat{V}_{ML}XT_r + kI_p)^{-1}\right] \quad (2.22.)$$

The *CN* values for the evaluation of eigenvalues of the COM-Poisson model based on the ML, ridge, and Liu estimation methods can be obtained as

$$CN_{est} = \sqrt{\frac{\hat{\psi}_{est,max}}{\hat{\psi}_{est,min}}} \quad (2.23.)$$

where $\hat{\psi}_{max}$ and $\hat{\psi}_{min}$ are the eigenvalues of information matrix obtained through SVD and "*est*" in the index shows the estimation method that utilized for the modelling.

2.6. Deviance residuals

Deviance residual for the *i*th observation of the GLMs is defined as 1/2 exponent of two times of the difference between the log-likelihood of the fitted and the log-likelihood of the saturated model (Dobson, 2002). In other words, the signed square root of the individual contribution to the likelihood ratio statistic is deviance residual. The value of the deviance residual increases or decreases depending on the sign of the difference between the actual and fitted values.

The general form of the *i*th deviance residual for the COM-Poisson model defined by Sellers and Shmueli (2010) is as

$$d_i = sign(y_i - \hat{\mu}_i) \times \left[2\left(l(y_i, y_i; v) - l(\widehat{E(y_i)}, y_i; v)\right)\right]^{1/2} \quad (2.24.)$$

where $l(\widehat{E(y_i)}, y_i; v)$ and $l(y_i, y_i; v)$ are the log-likelihood of the fitted and saturated models, respectively, $\widehat{E(y_i)} = \hat{\mu}_i^{1/v} - \frac{v-2}{2v}$ and $\hat{\mu}_i$ is the fitted response obtained by using ML estimator of the β at convergence. Eq. (2.24.) is the direct computation of deviance residual (see Sellers and Shmueli, 2010). The authors also gave the approximated deviance residual[2] as follows (see also Jamal et al., 2021)

$$d_i = sign(y_i - \hat{\mu}_i) \times \left[2 \left(y_i \hat{v} log \left(\left(y_i + \frac{\hat{v}-1}{2\hat{v}} \right) / \left(\hat{\mu}_i + \frac{\hat{v}-1}{2\hat{v}} \right) \right) + log \left(Z \left(\left(\hat{\mu}_i + \frac{\hat{v}-1}{2\hat{v}} \right)^{\hat{v}}, \hat{v} \right) / Z \left(\left(y_i + \frac{\hat{v}-1}{2\hat{v}} \right)^{\hat{v}}, \hat{v} \right) \right) \right) \right]^{1/2}$$

which exists in the constraint that $y > c$ for $\hat{v} < \frac{1}{2c+1}; c \in N^+$. In calculation of log-likelihood for saturated model for deviance residuals, Sellers and Shmueli (2010) suggested to set normalization parameter $Z = 1$ when $v < 1$ and $y_i = 0$, $i = 1, 2, \ldots, n$ to facilitate computation.

The ith standardized deviance residual obtained by Sellers and Shmueli (2010) is

$$sd_i = sign(y_i - \hat{\mu}_i) \times \left[2 \left(l(y_i, y_i; \hat{v}) - l(\widehat{E(y_i)}, y_i; \hat{v}) \right) / (1 - h_{ii}) \right]^{1/2} \qquad (2.25.)$$

where h_{ii} is the ith diagonal element of the projection matrix for the ML estimation, $H = \hat{V}_{ML}^{1/2} X (X' \hat{V}_{ML} X)^{-1} X' \hat{V}_{ML}^{1/2}$.

Following Sellers and Shmueli (2010), the ith deviance residual based on PCR, ridge, Liu, and *r-k* class estimators can be expressed by using the log-likelihood functions of the fitted model provided in Eq. (2.4.) with the appropriate estimator instead of the ML estimator.

[2]Throughout the thesis, the term "deviance" in a single form without any specification of estimation method refers to the residuals derived from the fitted models where the ML estimation method is applied.

Following McCullagh and Nelder (1989), the residuals given by Eq. (2.24.) can be standardized as

$$sd_{est,i} = sign(y_i - \hat{\mu}_i) \times \left[2 \left(l(y_i, y_i; \hat{v}) - l(\widehat{E(y_i)}, y_i; \hat{v}) \right) / (1 - h_{est,ii}) \right]^{1/2} \quad (2.26.)$$

where $h_{est,ii}$ is the ith diagonal element of the corresponding projection or quasi-projection[3]

$$\begin{aligned}
H_{ML} &= \hat{V}_{ML}^{1/2} X (X' \hat{V}_{ML} X)^{-1} X' \hat{V}_{ML}^{1/2} \\
H_{PCR} &= \hat{V}_{ML}^{1/2} X T_r (T_r' X' \hat{V}_{ML} X T_r)^{-1} T_r' X' \hat{V}_{ML}^{1/2} \\
H_{ridge} &= \hat{V}_{ridge}^{1/2} X (X' \hat{V}_{ridge} X + k I_p)^{-1} X' \hat{V}_{ridge}^{1/2} \\
H_{Liu} &= \hat{V}_{Liu}^{1/2} X (X' \hat{V}_{Liu} X + I_p)^{-1} (X' \hat{V}_{Liu} X + \theta I_p) (X' \hat{V}_{Liu} X)^{-1} X' \hat{V}_{Liu}^{1/2} \\
H_{r-k} &= \hat{V}_{ML}^{1/2} X T_r (T_r' X' \hat{V}_{ML} X T_r + k I_r)^{-1} T_r' X' \hat{V}_{ML}^{1/2}.
\end{aligned}$$

[3]If the projection matrix is not idempotent, it is called as quasi-projection matrix (Tripp, 1983; Özkale, 2013).

3. MONITORING COM-POISSON PROFILES

Control charts are widely used tools for SPC to monitor the quality characteristics. This chapter contains general information regarding control charts, the emergence of residual-based control charts, in brief, residual-based control charts for monitoring COM-Poisson profile with uncorrelated and correlated predictors and the performance evaluation metrics for these control charts.

Subsections 3.1 and 3.2 cover the origination of the control charts and metrics to assess their effectiveness. The deviance-based Shewhart, CUSUM, and EWMA charts for monitoring are given in Subsection 3.3. Subsection 3.3 also covers the proposed methods to monitor the COM-Poisson profiles that aim to lessen the negative effect of multicollinearity to reach a more reliable result. These monitoring methods include fitting the COM-Poisson profile under multicollinearity using the PCR, ridge, Liu, and *r-k* class estimation methods discussed in Subsection 2.2.2 and constructing the adjusted residual-based Shewhart, CUSUM, and EWMA charts for the monitoring. The PCR deviance, ridge deviance, Liu deviance, and *r-k* deviance based on Shewhart charts are proposed as an alternative to the deviance-based Shewhart chart for identifying medium to high shifts in the profile process with correlated predictors. In contrast, the goal of using the proposed CUSUM and EWMA charts based on the PCR deviance, ridge deviance, Liu deviance, and *r-k* deviance residuals is to identify shifts, including in small sizes in the process in the case of multicollinearity.

3.1. Control charts as a process monitoring tool

Maintaining a control condition is necessary for industrial processes. Shewhart (1931), an originator of the control chart concept, defined statistical control as the following: ”*phenomenon will be said to be controlled when, through the use of*

past experience, we can predict, at least within limits, how the phenomenon may be expected to vary in the future".

Earlier in 1924, W. A. Shewhart introduced the Shewhart chart as a simple tool to identify and eliminate anomalies in the process, therefore improving the process by removing variability. The proposed control chart has upper and lower control limits constructed based on the statistical properties of the quality characteristics. The observations exceeded the control limits were considered as process variations or shifts. According to Shewhart (1931), there are various types of process variations that fall into two categories: common and special causes of variation[1]. While common causes variations manifest as random ups and downs, variations due to special causes such as equipment failure can appear in the form of up and down trends.

Although the Shewhart chart is effective in the detection of medium to large variations in the process, it is impractical for identifying small-sized shifts. Page (1954) proposed a sensitive CUSUM chart that utilizes the past information available from previously plotted points. Later, Roberts (1959) introduced the EWMA chart, an alternative to the CUSUM chart. EWMA charts also accumulate current and past information from the observations that make the control chart effective in detecting small shifts. Since then, several modifications and extensions of these control charts are investigated.

3.2. Performance of the control charts

Based on the metrics used for performance evaluation, a control chart can be assessed to be effective. One of these metrics is the run length (*RL*). The *RL* corresponds to the number of observations until the first out-of-control observation is

[1]Originally, Shewhart (1926) used the terminology of chance and assignable causes. Today, writers prefer to use the terminology of the common cause instead of the chance cause and special cause instead of the assignable cause.

identified by the control chart. The mean of the run length is known as the average run length (*ARL*). *ARL* is classified as in-control (ARL_0) and out-of-control (ARL_1). ARL_0 is expected to be substantially large. Generally, the control limits of the control charts are determined such that $ARL_0 = 370$, which is equal to the false alarm rate of 0.0027, which means that the control chart will have false alarm about every 370 observation on the average. On the other hand, the small ARL_1 is the most desirable, considering that we want to quickly identify out-of-control observations.

Along with the *ARL*, the standard deviation of the run length (*SDRL*) can also be used to measure the performance of control charts. A good control chart is expected to have a small *SDRL* value as well.

3.3. Residual-based control charts for COM-Poisson profiles

In profile monitoring, residual-based control charts are an extension of the traditional control charts where residuals from the profile are used to inspect the stability.

The residual-based control charts are originated from cause-selecting control charts. Initially, by reviewing the process as a sum of sub-processes, Zhang (1984) aimed to check the process stability by considering current sub-process data as a response and data from previous sub-processes as the predictors. The monitoring process is carried out by establishing a relationship between response and predictors and obtaining residuals. Afterwards, these residuals are used to identify unwanted changes in the process. Wade and Woodall (1993) emphasize that the relationship between the variables need not be linear for this technique to work. It can be applied to any functional relationship if the assumption of normality for the residuals can be established.

This idea later extended to the GLP framework, following the statement

made by Pierce and Schafer (1986) that the deviance residuals are asymptotically normally distributed. While deviance residuals act as monitored observations for residual-based Shewhart charts, they are used to calculate control chart statistics for CUSUM and EWMA charts.

3.3.1. Residual-based Shewhart chart

Mammadova and Özkale (2021b) defined the control limits for the Shewhart chart based on the deviance and ridge deviance residuals, respectively as

$$CL_{ML} = \hat{\mu}^0_{ML} \pm l\hat{\sigma}^0_{ML}, \tag{3.1.}$$

$$CL_{ridge} = \hat{\mu}^0_{ridge} \pm l\hat{\sigma}^0_{ridge} \tag{3.2.}$$

where $\hat{\mu}^0_{ML}$ and $\hat{\sigma}^0_{ML}$ correspond to the in-control mean and in-control standard deviation of the deviance residuals and $\hat{\mu}^0_{ridge}$ and $\hat{\sigma}^0_{ridge}$ are the in-control mean and in-control standard deviation of the ridge deviance residuals. l is the control chart constant and must be chosen carefully because it determines the width of the control limits. High l values result in a wide control range and make the identification of out-of-control observations difficult. A small l value, on the other hand, narrows the control range and leads to falsely recognized out-of-control observations. It is usually recommended to select the l for Shewhart based on the prespecified ARL_0 value (Montgomery, 2020). Another implementation of biased estimation to profile monitoring was suggested by Mammadova and Özkale (2022). The authors proposed Liu deviance-based Shewhart chart to monitor COM-Poisson profile under multicollinearity and defined the control limits of this chart as

$$CL_{Liu} = \hat{\mu}^0_{Liu} \pm l\hat{\sigma}^0_{Liu} \tag{3.3.}$$

where μ^0_{Liu} and σ^0_{Liu} are the in-control mean and the standard deviation of the Liu deviance residuals when the process is in control. We define control limits for Shewhart charts based on the PCR and *r-k* deviance residuals as

$$CL_{PCR} = \hat{\mu}^0_{PCR} \pm l\hat{\sigma}^0_{PCR}, \tag{3.4.}$$

$$CL_{r-k} = \hat{\mu}^0_{r-k} \pm l\hat{\sigma}^0_{r-k} \tag{3.5.}$$

$\hat{\mu}^0_{PCR}$ and $\hat{\sigma}^0_{PCR}$ are the in-control mean and in-control standard deviation of PCR deviance residuals and $\hat{\mu}^0_{r-k}$ and $\hat{\sigma}^0_{r-k}$ are the in-control mean and in-control standard deviation of *r-k* deviance residuals.

We will refer to deviance-based Shewhart charts as Shewhart$_{ML}$ and PCR, ridge, Liu, and *r-k* deviance-based Shewhart charts as Shewhart$_{PCR}$, Shewhart$_{ridge}$, Shewhart$_{Liu}$, and Shewhart$_{r-k}$, respectively to prevent the confusion.

3.3.2. Residual-based CUSUM and EWMA charts

Montgomery (2020) describes the CUSUM and EWMA charts as alternatives to the Shewhart chart when the detection of small shifts is significant. An extension of the traditional CUSUM and EWMA charts was defined on the basis of deviance, ridge deviance, and Liu deviance residuals by Mammadova and Özkale (2021b, 2022). Required formulas to construct these control charts are presented in

Tables 3.1 and 3.2.

Table 3.1. Control chart statistics of the deviance, ridge deviance, and Liu deviance-based CUSUM and EWMA charts.

Control chart	**Control chart statistic**
CUSUM$_{ML}$	$C^-_{ML,i} = min[0, \hat{\mu}^0_{ML} - K - d_{ML,i} + C^-_{ML,i-1}], i = 1,2,\ldots,n$
	$C^+_{ML,i} = max[0, d_{ML,i} - \hat{\mu}^0_{ML} - K + C^+_{ML,i-1}], i = 1,2,\ldots,n$
	$C^-_{ML,0} = C^+_{ML,0} = 0$
CUSUM$_{ridge}$	$C^-_{ridge,i} = min[0, \hat{\mu}^0_{ridge} - K - d_{ridge,i} + C^-_{ridge,i-1}], i = 1,2,\ldots,n$
	$C^+_{ridge,i} = max[0, d_{ridge,i} - \hat{\mu}^0_{ridge} - K + C^+_{ridge,i-1}], i = 1,2,\ldots,n$
	$C^-_{ridge,0} = C^+_{ridge,0} = 0$
CUSUM$_{Liu}$	$C^-_{Liu,i} = min[0, \hat{\mu}^0_{Liu} - K - d_{Liu,i} + C^-_{Liu,i-1}], i = 1,2,\ldots,n$
	$C^+_{Liu,i} = max[0, d_{Liu,i} - \hat{\mu}^0_{Liu} - K + C^+_{Liu,i-1}], i = 1,2,\ldots,n$
	$C^-_{Liu,0} = C^+_{Liu,0} = 0$
EWMA$_{ML}$	$z_{ML,i} = \lambda d_{ML,i} + (1-\lambda) z_{ML,i-1}, i = 1,2,\ldots,n;$
	$z_{ML,0} = \hat{\mu}^0_{ML}$
EWMA$_{ridge}$	$z_{ridge,i} = \lambda d_{ridge,i} + (1-\lambda) z_{ridge,i-1}, i = 1,2,\ldots,n;$
	$z_{ridge,0} = \hat{\mu}^0_{ridge}$
EWMA$_{Liu}$	$z_{Liu,i} = \lambda d_{Liu,i} + (1-\lambda) z_{Liu,i-1}, i = 1,2,\ldots,n;$
	$z_{Liu,0} = \hat{\mu}^0_{Liu}$

In Tables 3.1 and 3.2, deviance-based charts are referred to as CUSUM$_{ML}$ and EWMA$_{ML}$, ridge deviance-based charts as CUSUM$_{ridge}$ and EWMA$_{ridge}$, and Liu deviance-based charts as CUSUM$_{Liu}$ and EWMA$_{Liu}$. $\hat{\mu}^0_{ML}$, $\hat{\mu}^0_{ridge}$, and $\hat{\mu}^0_{Liu}$ are in-control means, $\hat{\sigma}^0_{ML}$, $\hat{\sigma}^0_{ridge}$, and $\hat{\sigma}^0_{Liu}$ are in-control standard deviations of deviance, ridge deviance, and Liu deviance residuals, accordingly. K and h are the reference and the decision value of the CUSUM chart, respectively. $0 < \lambda \leq 1$ is the smoothing parameter of the EWMA chart while L is the EWMA control limit constant.

Even if the biased estimation alleviates the multicollinearity problem, some-

Table 3.2. Control limits of the deviance, ridge deviance, and Liu deviance-based CUSUM and EWMA charts.

Control chart	**Control chart limits**
CUSUM$_{ML}$	$CL_{ML} = \pm h\hat{\sigma}^0_{ML}$
CUSUM$_{ridge}$	$CL_{ridge} = \pm h\hat{\sigma}^0_{ridge}$
CUSUM$_{Liu}$	$CL_{Liu} = \pm h\hat{\sigma}^0_{Liu}$
EWMA$_{ML}$	$CL_{ML} = \hat{\mu}^0_{ML} \pm L\hat{\sigma}^0_{ML}\sqrt{(\lambda/(2-\lambda))(1-(1-\lambda))^{2i}}, i = 1,2,\ldots,n$
EWMA$_{ridge}$	$CL_{ridge} = \hat{\mu}^0_{ridge} \pm L\hat{\sigma}^0_{ridge}\sqrt{(\lambda/(2-\lambda))(1-(1-\lambda))^{2i}}, i = 1,2,\ldots,n$
EWMA$_{Liu}$	$CL_{Liu} = \hat{\mu}^0_{Liu} \pm L\hat{\sigma}^0_{Liu}\sqrt{(\lambda/(2-\lambda))(1-(1-\lambda))^{2i}}, i = 1,2,\ldots,n$

times it causes computational difficulties as it depends on the tuning parameter. For this reason, ridge and Liu deviance-based control charts can be improved by defining the CUSUM and EWMA charts' statistics based on the PCR and *r-k* deviance residuals for COM-Poisson profiles.

Control chart statistics for the PCR and *r-k* deviance-based CUSUM charts can be defined as

$$\begin{aligned} C^-_{PCR,i} &= min[0, \hat{\mu}^0_{PCR} - K - d_{PCR,i} + C^-_{PCR,i-1}], i = 1,2,\ldots,n, \\ C^+_{PCR,i} &= max[0, d_{PCR,i} - \hat{\mu}^0_{PCR} - K + C^+_{PCR,i-1}], i = 1,2,\ldots,n \end{aligned} \tag{3.6.}$$

and

$$\begin{aligned} C^-_{r-k,i} &= min[0, \hat{\mu}^0_{r-k} - K - d_{r-k,i} + C^-_{r-k,i-1}], i = 1,2,\ldots,n, \\ C^+_{r-k,i} &= max[0, d_{r-k,i} - \hat{\mu}^0_{r-k} - K + C^+_{r-k,i-1}], i = 1,2,\ldots,n \end{aligned} \tag{3.7.}$$

respectively, where $\hat{\mu}^0_{PCR}$ and $\hat{\mu}^0_{r-k}$ correspond to the in-control mean of the PCR and *r-k* deviance residuals, $\hat{\sigma}^0_{PCR}$ and $\hat{\sigma}^0_{r-k}$ correspond to the in-control standard deviation

of the PCR and *r-k* deviance residuals, respectively. The starting values are taken as zero: $C^{-}_{PCR,0} = C^{+}_{PCR,0} = 0$, $C^{-}_{r-k,0} = C^{+}_{r-k,0} = 0$.

The control limits for the CUSUM$_{PCR}$ and CUSUM$_{r-k}$ charts are

$$CL_{PCR} = \pm h\hat{\sigma}^{0}_{PCR}, \tag{3.8.}$$

$$CL_{r-k} = \pm h\hat{\sigma}^{0}_{r-k}. \tag{3.9.}$$

Modified control chart statistics for the EWMA chart based on the PCR deviance residuals (EWMA$_{PCR}$) and EWMA chart based on the *r-k* deviance residuals (EWMA$_{r-k}$) are respectively as

$$z_{PCR,i} = \lambda d_{PCR,i} + (1-\lambda) z_{PCR,i-1}, i = 1,2,\ldots,n, \tag{3.10.}$$

$$z_{r-k,i} = \lambda d_{r-k,i} + (1-\lambda) z_{r-k,i-1}, i = 1,2,\ldots,n \tag{3.11.}$$

where the initial values $z_{PCR,0}$ and $z_{r-k,0}$ are the in-control mean of the corresponding deviance residuals. Respective control limits for EWMA$_{PCR}$ and EWMA$_{r-k}$ are

$$CL_{PCR} = \hat{\mu}^{0}_{PCR} \pm L\hat{\sigma}^{0}_{PCR}\sqrt{(\lambda/(2-\lambda))(1-(1-\lambda))^{2i}}, i = 1,2,\ldots,n, \tag{3.12.}$$

$$CL_{r-k} = \hat{\mu}^{0}_{r-k} \pm L\hat{\sigma}^{0}_{r-k}\sqrt{(\lambda/(2-\lambda))(1-(1-\lambda))^{2i}}, i = 1,2,\ldots,n. \tag{3.13.}$$

The selection of the K and h combination for the CUSUM chart as well as the λ and L combination for the EWMA chart is a sensitive task because these combinations affect the performance of the control chart. Hawkins (1993), for example, in his study, gave a table of reference values for the CUSUM chart that will achieve a particular *ARL*. Montgomery (2020) mentioned that, $h = 4$ or $h = 5$ and $K = 0.5\sigma_0$ generally provide a CUSUM chart with good *ARL* against 1σ shift in normal distributed processes. Lucas and Saccucci (1990) presented optimal combinations of different λ and L that effectively minimize the ARL_1 of the EWMA chart. Montgomery (2020), on the other hand, emphasizes that $0.05 \leq \lambda \leq 0.25$ perform efficiently in practice.

4. SIMULATION STUDY

In this chapter, we analyzed COM-Poisson profiles with multicollinearity for various combinations to evaluate the effectiveness of the approaches presented in this study. Simulations are carried out in *Matlab* and/or *R* for a fixed number of observations and correlation levels, various combinations of predictor number, dispersion levels, shift types, and shift sizes. A detailed procedure for conducting a simulation study is illustrated in Subsection 4.1.

4.1. Design of the simulation study

A simulation study in general consists of two stages. While Stage 1 aims to determine control chart limits for the in-control process that meet desired ARL_0 condition, performance evaluation of the control charts by using the information obtained in Stage 1 is executed in Stage 2.

A description of each stage is presented in the following paragraphs and on the flowcharts given by Figs. 4.1 and 4.2. An algorithm based on the flowchart shown in Fig. 4.1 is executed for the comparative analysis of Shewhart charts. CUSUM and EWMA charts are subjected to comparison by using the algorithm based on the flowchart presented in Fig. 4.2.

The Stage 1 analysis is conducted by following the algorithm given below:

(1) Set sample size, dispersion and correlation levels, and the β for generating the response variable.

(2) Generate correlated predictors by following McDonald and Galarneau (1975) as

$$x_{ij} = (1-\rho^2)^{1/2} w_{ij} + \rho w_{ip}, i = 1,2,\ldots,n, j = 1,2,\ldots,p \qquad (4.1.)$$

where w_{ij} is a random standard normal number, ρ^2 is the desired correlation between any two predictors. Then these variables are standardized as suggested by Lesaffre and Marx (1993) and Mackinnon and Puterman (1989).

(3) Set $ARL_0 = 0$ and initialize the control chart constants as $l = 0$ for Shewhart, $h = 0$ for CUSUM, and $L = 0$ for EWMA.

(4) Generate the COM-Poisson distributed response variable y as $y \sim COM-Poisson(exp(X\beta), v)$ where X is the correlated predictor matrix.

(5) Use log-link function to model the relationship between predictor matrix and response variable.

(6) Estimate the parameters for the monitoring process according to the algorithms given in Section 2.4. by using the OLS estimator as an initial value and $||\hat{\beta}_{est}^{(t)} - \hat{\beta}_{est}^{(t-1)}|| \leq 1 \times 10^{-6}$ as convergence criterion where $\hat{\beta}_{est}$ is any estimator used.

(7) Compute respective deviance residuals as given in Eq. (2.24.). We set normalization parameter Z, in calculation of log-likelihood for saturated model for deviance residuals equal to one when $v < 1$ and $y_i = 0, i = 1, 2, \ldots, n$.

(8) Calculate control chart statistics and establish control chart limits.

(9) Compare each control chart statistic to the lower and upper control limits of the respective control chart and obtain the *RL*.

(10) Reset the counter to zero and repeat the steps (2) - (9), $N = 500$ times. Then calculate the average of the *RL*, which is ARL_0. If the desired ARL_0 is not achieved, increase the control chart constant by 0.001 and repeat the steps until the approximate value of desired ARL_0 is determined.

(11) Record the control limits of each control chart when desired ARL_0 is achieved.

The following algorithm is performed in Stage 2 to analyze the performance of each control chart:

(1) Repeat steps (1) and (2) as in Stage 1;

(2) Generate the shifted $n \times 1$ response variable y as $y \sim COM-Poisson(\mu_1, v)$ by adding shift to the mean parameter. Two types of shifts are considered for the simulations. These are

   (a) **Additive shift**: $\mu_1 = exp(X\beta) + \delta\hat{\sigma}^0_{ML}$ where δ is a shift size, $\hat{\sigma}^0_{ML}$ is a in-control standard deviation of the deviance residual.

   (b) **Multiplicative shift**: $\mu_1 = exp(X(\beta + \delta\hat{\sigma}^0_{ML}))$ adds shift to regression coefficients in the same size.

(3) Repeat the steps (5) - (7) of Stage 1.

(4) Calculate control chart statistics and compare each control chart statistic to the control limits calculated using the control chart constants determined in Stage 1.

(5) Obtain RL and repeat steps (2) - (5), $N = 500$ times.

(6) Calculate ARL_1 and $SDRL$.

(7) Record final results.

4.2. Performance of ridge deviance-based control charts

An analysis based on the underdispersed data and a simulation study is conducted for a thorough investigation of the impact of the tuning parameter on the

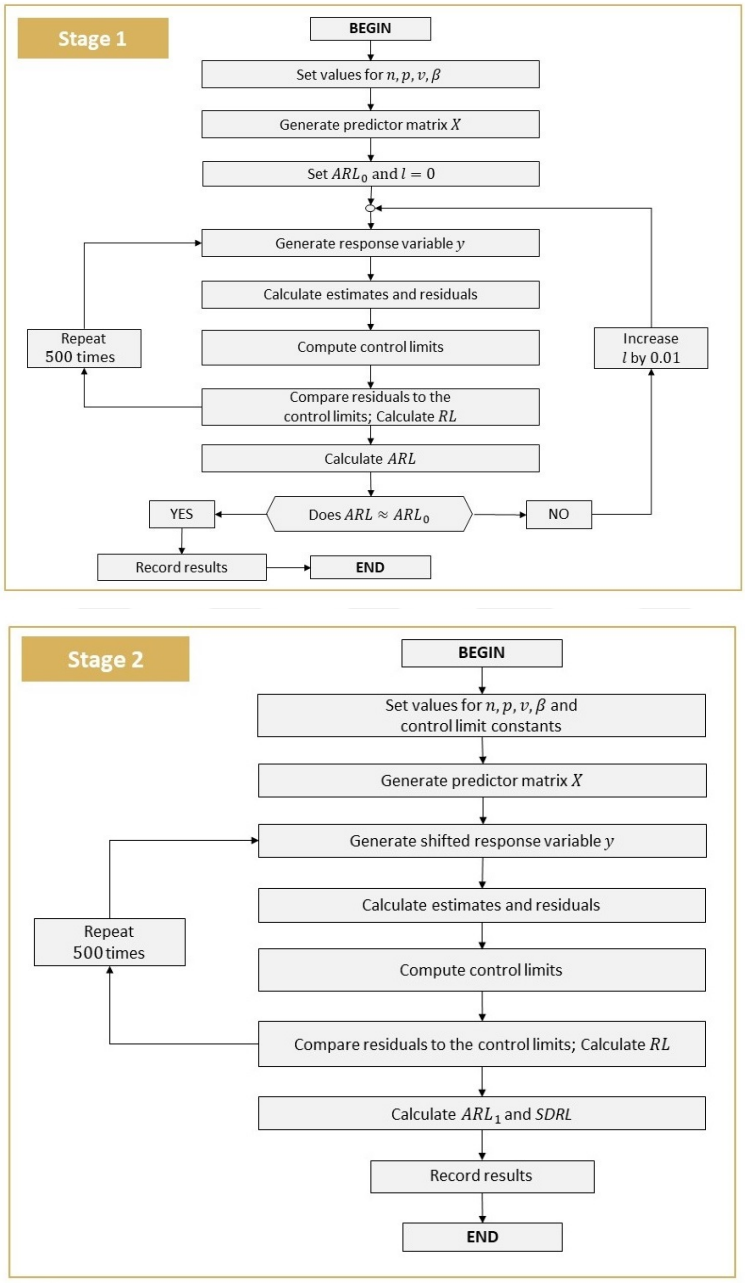


Figure 4.1. Simulation flowchart for comparative analysis of Shewhart charts.

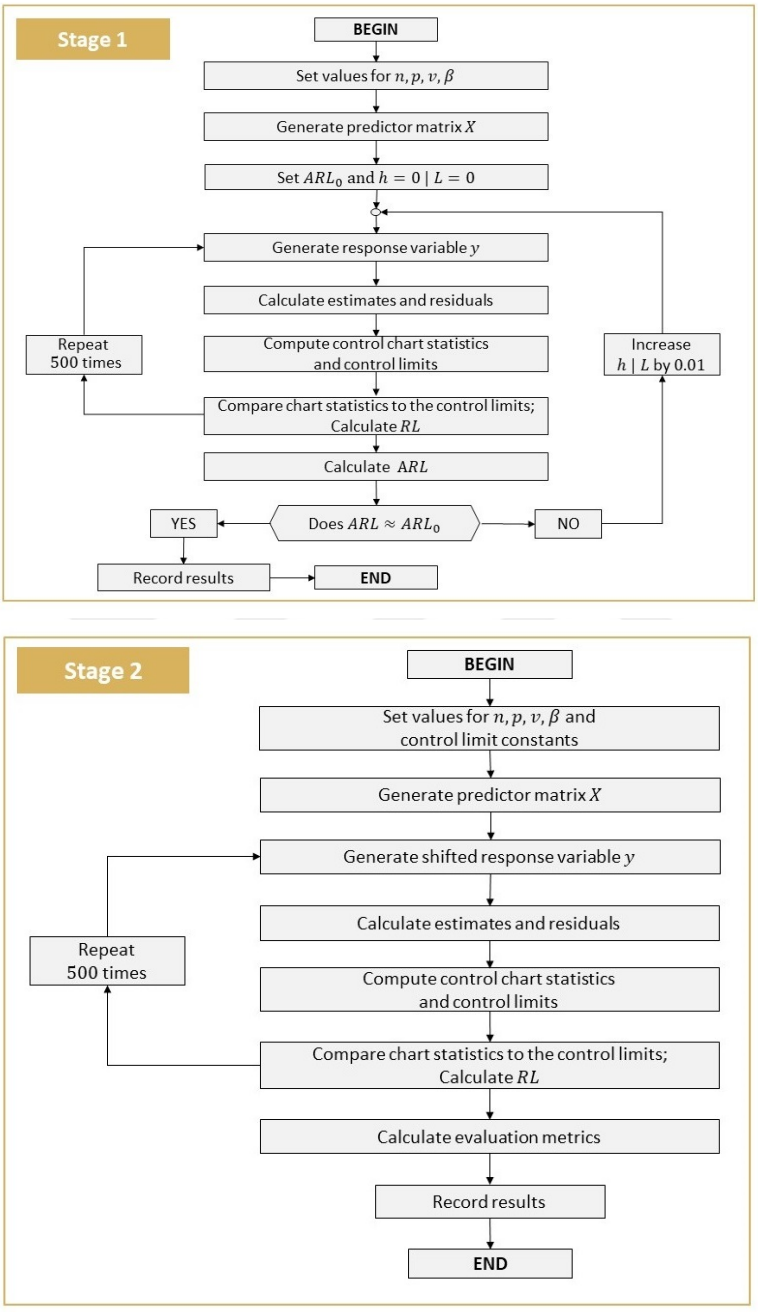


Figure 4.2. Simulation flowchart for comparative analysis of CUSUM and EWMA charts.

effectiveness of the suggested ridge deviance-based control charts.

4.2.1. Ridge deviance-based control charts for monitoring COM-Poisson profile

In this Subsection we present a comparative analysis of the ridge deviance residual-based control charts. We consider COM-Poisson profile where response is underdispersed. The analysis is carried out by setting number of the simulation repetitions $N = 1$ and following the steps in Subsection 4.1.

We start performance analysis by generating correlated predictor matrix and response variable. Each element of the $X_{200\times5} = [1, x_i']$ predictor matrix is generated as in Eq. (4.1.) with $\rho^2 = 0.90$. Response variable from COM-Poisson distribution is generated by arbitrarily setting $\beta = (0.005, 0.5, 0.15, -0.15, 0.7, -0.7)$ and $\nu = 1.3$. The data set is modelled through the log-link function, and ML and ridge estimators are obtained for the model. Tuning parameter is computed as $\hat{k} = (pv)/(\hat{\beta}_{ML}'\hat{\beta}_{ML}) = 3.7209$ following Eq. (2.15.a) where $\hat{\beta}_{ML}$ is the ML estimator in convergence.

The condition number for ML and ridge estimators are $CN_{ML} = 3396.1$ and $CN_{ridge} = 2.2514$ for $\hat{k} = 3.7209$. VIF_{ML} values are [54.6459, 99.7724, 16.5634, 121.3653, 211.7423, 261.2297] and VIF_{ridge} are [0.04334, 0.01771, 0.01807, 0.01784, 0.01695, 0.01742]. Noticeable improvements in the *VIF* values and condition numbers of ML and ridge estimators indicate that the ridge estimator alleviates the degree of multicollinearity.

Assuming the simulated data set is under control, control chart constants are determined under the progress explained by Fig. 4.1 such that $ARL_0 \approx 200$[1] and results are presented in Table 4.1.

The settings from Stage 1 are used to generate the data set in the same size

[1] ARL_0 is selected based on the size of the data set.

Table 4.1. Stage 1 analysis results for simulated COM-Poisson profile data.

	Deviance	**Ridge deviance**
Shewhart	$l = 5.15$	$l = 5.27$
CUSUM, $K = 0.5$	$h = 7.20$	$h = 7.36$
EWMA, $\lambda = 0.2$	$L = 1.96$	$l = 2.01$
in-control $\hat{\mu}^0$	5.2496	5.2479
in-control $\hat{\sigma}^0$	2.8653	2.4088

for Stage 2. But for Stage 2, the response variable is generated by adding a shift to the 90^{th} observation before being rounded to the nearest integer. The shift is the sum of the original observation with five times the standard deviation of the corresponding variable, whereas the 90^{th} observation is selected due to having the maximum value among responses.

Following the steps in Fig. 4.1 and 4.2 regarding Stage 2, after the ML as well as the ridge estimator with $k = 3.7209$ is obtained, the deviance and ridge deviance residuals are computed. Control limits for control charts are constructed based on Table 4.1.

The results for each control chart in terms of the first signal (the first control chart statistic outside the control area) and ARL_1 for COM–Poisson profile is given in Table 4.2.

Table 4.2. Stage 2 analysis results for simulated COM-Poisson profile data.

	First signal		$\boldsymbol{ARL_1}$	
	Deviance	Ridge deviance	Deviance	Ridge deviance
Shewhart	36	90	1.0204	1.0152
CUSUM, $K = 0.5$	36	90	1.2121	1.1905
EWMA, $\lambda = 0.20$	1	1	1.0471	1.0363

According to the first signal, Shewhart$_{ridge}$ and EWMA$_{ridge}$ charts correctly detected the shifted observation. EWMA$_{ridge}$, as well as the EWMA$_{ML}$, signalled in the first observation. All the ridge deviance-based control charts outperformed the corresponding deviance-based control charts in terms of ARL_1 value.

Shewhart, CUSUM, and EWMA charts based on deviance and ridge deviance residuals for monitoring COM–Poisson profile are given in Fig. 4.3. Deviance and ridge deviance control charts exhibit a similar pattern, as seen in Fig. 4.3.

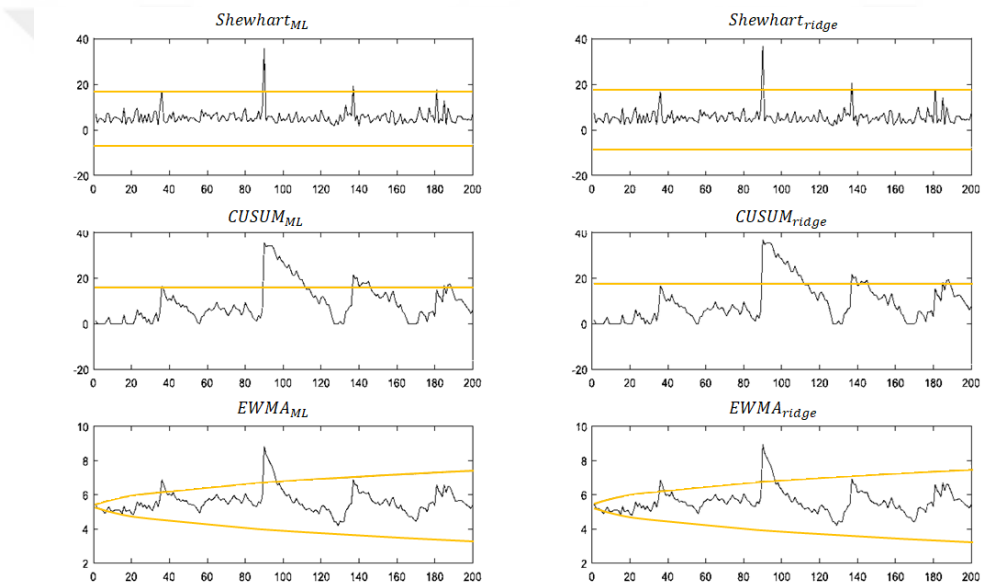


Figure 4.3. Performance analysis of deviance and ridge deviance-based control charts during monitoring COM-Poisson profile, $\rho^2 = 0.90$.

4.2.2. Effect of ridge tuning parameter on profile monitoring

An extensive simulation study is carried out to evaluate the impact of tuning parameter selection on the performance of the ridge deviance-based control charts by monitoring a Poisson profile as an equidispersed case of the COM-Poisson profile.

For start, $p = 2,3,4$ predictors each with $n = 50,100,200,500$ and $\rho^2 = 0.90, 0.99$ are generated by following Eq. (4.1.). An intercept is added to predictor matrix for the modelling. Response variable form Poisson distribution with mean parameter $\mu = exp(X\beta)$ is generated by setting $\beta = [0.5, \beta_i]$ where $\beta_i = 1, i = 1, \ldots, p$.

Stage 1 analysis is conducted for prespecified $ARL_0 \approx 370$. Ridge deviance-based control charts were constructed based on the tuning parameters given in Section 2.3.1. by Eqs. (2.14.a) - (2.14.f). Control chart constants that obtained at the end of the Stage 1 are presented in Tables 4.3 and 4.4. The k in the second row of the name field of the tables shows which method for calculation of the tuning parameter is utilized.

The response variable for Stage 2 is generated under various shifts in sizes $\delta = 0.5, 1.5, 2.5$. Along with the additive shift, three different multiplicative shifts are considered. To determine the impact of various regression coefficients on the performance of the control chart, the multiplicative shift in intercept, in regression coefficients except for intercept, and in all regression coefficients including the intercept are investigated in the simulation.

Stage 2 results of the deviance and ridge deviance-based Shewhart, CUSUM, and EWMA charts are presented in Tables 4.5 - 4.12 when the response variables are imposed to additive and multiplicative shifts. Each table contains the markings referred to as the minimum ARL_1 values of control charts for all the combinations of n, p, and k. Two types of marks are:

- '$\times$' means in that combination, the deviance-based control chart shows the best performance;
- '$\circ$' shows which ridge deviance-based control chart is the best depending on the tuning parameter.

Table 4.3. Stage 1 analysis results regarding ridge tuning parameter selection, $\rho^2 = 0.90$.

Control chart	***n***	***p***	**Deviance**	**Ridge deviance**					
				k_1	k_2	k_3	k_4	k_5	k_6
Shewhart	50	2	2.810	2.790	2.810	2.810	2.800	2.830	2.770
		3	3.000	2.940	2.920	2.950	2.820	3.030	2.940
		4	3.110	3.070	3.060	3.065	2.830	3.150	3.090
	100	2	2.895	2.870	2.930	2.880	2.830	2.990	3.110
		3	3.250	3.040	3.040	3.035	2.820	3.120	3.050
		4	3.250	3.210	3.200	3.180	2.820	3.260	3.250
	200	2	2.940	2.960	2.940	2.945	3.025	3.020	3.130
		3	3.100	3.110	3.110	3.097	2.840	3.130	3.060
		4	3.250	3.230	3.220	3.202	2.770	3.210	3.110
	500	2	3.000	2.980	2.990	2.973	2.790	3.040	3.110
		3	3.130	3.130	3.110	3.108	2.840	3.150	3.090
		4	3.250	3.250	3.230	3.223	3.250	3.260	3.110
CUSUM	50	2	6.500	3.573	3.070	4.141	4.705	3.350	4.300
		3	7.650	3.815	3.040	4.617	6.080	3.385	5.020
		4	9.000	4.100	3.100	7.001	6.255	3.610	5.590
	100	2	4.980	4.061	3.600	3.530	4.910	3.683	4.900
		3	5.425	3.914	3.590	3.605	5.155	3.745	4.408
		4	6.005	4.467	3.800	3.655	5.570	3.800	5.800
	200	2	4.630	4.052	4.010	3.720	6.010	4.135	4.012
		3	4.915	4.200	4.020	4.762	5.010	4.405	4.175
		4	5.700	4.470	4.145	4.952	5.140	4.465	4.800
	500	2	4.505	4.373	4.360	4.210	4.380	4.455	4.303
		3	4.715	4.370	4.330	4.377	4.490	4.475	4.306
		4	4.623	4.464	4.385	4.255	4.530	4.455	4.551
EWMA	50	2	3.951	5.110	4.050	4.505	4.045	4.100	4.100
		3	3.981	5.380	4.250	4.965	4.350	4.450	4.300
		4	4.530	5.480	4.475	5.320	5.180	4.150	4.340
	100	2	3.640	4.670	3.600	3.715	3.570	3.700	3.580
		3	3.951	4.860	3.855	3.720	4.250	3.750	3.800
		4	3.853	5.010	4.315	3.855	3.995	4.000	3.850
	200	2	3.070	4.130	3.150	3.155	3.505	3.250	3.100
		3	3.110	4.210	3.215	3.200	3.420	3.150	3.100
		4	3.170	4.220	3.225	3.300	3.270	3.320	3.250
	500	2	2.560	3.510	2.515	2.500	2.775	2.500	2.500
		3	2.510	3.560	2.540	2.550	2.560	2.550	2.525
		4	2.570	3.620	2.650	2.575	2.710	2.575	2.550

Table 4.4. Stage 1 analysis results regarding ridge tuning parameter selection, $\rho^2 = 0.99$.

Control chart	***n***	***p***	**Deviance**	**Ridge deviance**					
				k_1	k_2	k_3	k_4	k_5	k_6
	50	2	2.790	2.800	2.810	2.810	2.780	2.880	2.880
		3	2.960	2.950	2.940	3.040	2.990	3.020	3.040
		4	3.120	3.120	3.100	3.080	3.190	3.270	3.270
	100	2	2.940	2.900	2.910	2.890	2.915	2.950	2.950
		3	3.080	3.070	3.070	3.120	3.110	3.180	3.120
Shewhart		4	3.245	3.250	3.220	3.270	3.230	3.290	3.270
	200	2	2.990	2.950	2.990	3.000	2.970	2.975	2.980
		3	3.130	3.120	3.080	3.132	3.110	3.140	3.145
		4	3.255	3.250	3.270	3.280	3.255	3.320	3.320
	500	2	2.990	3.005	2.975	3.033	2.990	3.000	3.000
		3	3.140	3.140	3.100	3.160	3.160	3.160	3.160
		4	3.280	3.270	3.280	3.280	3.273	3.290	3.320
	50	2	6.000	6.010	3.070	3.081	3.580	4.870	5.050
		3	7.000	6.990	3.050	3.163	4.160	5.540	4.550
		4	3.450	7.830	3.140	3.250	4.700	6.220	5.300
	100	2	3.500	4.310	3.660	3.350	3.380	4.195	4.290
		3	3.530	4.430	3.585	3.720	3.735	4.750	4.700
CUSUM		4	3.660	5.180	3.620	4.010	3.740	4.970	7.300
	200	2	4.700	4.120	4.000	4.131	3.920	4.010	4.550
		3	4.000	4.790	4.025	4.225	4.200	5.200	6.712
		4	5.300	4.450	4.150	4.281	4.210	4.330	7.075
	500	2	4.270	4.330	4.268	4.235	4.340	4.310	4.350
		3	4.500	4.355	4.400	4.428	4.420	4.550	4.390
		4	4.510	4.530	4.650	4.406	4.560	4.560	4.406
	50	2	5.105	5.040	5.070	5.030	5.030	5.095	5.070
		3	5.360	5.290	5.310	5.240	5.240	5.160	5.280
		4	5.615	5.500	5.420	5.540	5.390	5.355	5.540
	100	2	4.615	4.620	4.620	4.570	4.540	4.670	4.570
		3	4.655	4.860	4.630	4.735	4.805	4.685	4.860
EWMA		4	5.005	5.040	4.820	4.920	4.985	4.775	4.920
	200	2	4.105	4.110	4.130	4.050	4.070	4.090	4.050
		3	4.120	4.220	4.190	4.160	4.290	4.005	4.160
		4	4.185	4.210	4.230	4.200	4.200	4.330	4.200
	500	2	3.420	3.530	3.520	3.450	3.450	3.680	3.530
		3	3.605	3.570	3.535	3.540	3.540	3.515	3.570
		4	3.610	3.590	3.700	3.510	3.595	3.545	3.510

Table 4.5. Stage 2 analysis of ridge deviance-based control charts with different tuning parameters in case of additive shift, $\rho^2 = 0.90$.

			Shewhart							**CUSUM**							**EWMA**						
n	p	δ	Deviance	Ridge deviance						Deviance	Ridge deviance						Deviance	Ridge deviance					
				k_1	k_2	k_3	k_4	k_5	k_6		k_1	k_2	k_3	k_4	k_5	k_6		k_1	k_2	k_3	k_4	k_5	k_6
	2	0.5						○						○								○	
	2	1.5						○						○								○	
	2	2.5						○						○						○			
	3	0.5		○										○							○		
50	3	1.5		○										○							○		
	3	2.5		○										○							○		
	4	0.5					○							○							○		
	4	1.5				○								○							○		
	4	2.5				○								○							○		
	2	0.5					○							○							○		
	2	1.5					○							○							○		
	2	2.5					○							○							○		
	3	0.5						○							○						○		
100	3	1.5						○		×					○						○		
	3	2.5						○		×					○						○		
	4	0.5		○						×				○								○	
	4	1.5		○						×				○						○			
	4	2.5		○						×						○						○	
	2	0.5		○											○						○		
	2	1.5	×	○											○						○		
	2	2.5	×	○											○						○		
	3	0.5			○					×	○									○			
200	3	1.5			○					×	○									○			
	3	2.5			○					×	○									○			
	4	0.5		○											○						○		
	4	1.5		○						×						○					○		
	4	2.5		○									○								○		
	2	0.5					○							○							○		
	2	1.5					○							○							○		
	2	2.5					○							○							○		
	3	0.5							○					○							○		
500	3	1.5							○						○						○		
	3	2.5							○						○						○		
	4	0.5				○								○						○			
	4	1.5			○									○						○			
	4	2.5				○							○							○			

Table 4.6. Stage 2 analysis of ridge deviance-based control charts with different tuning parameters in case of multiplicative shift in intercept, $\rho^2 = 0.90$.

			Shewhart							**CUSUM**							**EWMA**					
n	p	δ	Deviance	Ridge deviance					Deviance	Ridge deviance						Deviance	Ridge deviance					
				k_1	k_2	k_3	k_4	k_5	k_6		k_1	k_2	k_3	k_4	k_5	k_6		k_1	k_2	k_3	k_4	k_5	k_6
	2	0.5						○								○						○	
	2	1.5						○						○						○			
	2	2.5						○						○						○			
	3	0.5		○										○							○		
50	3	1.5		○										○							○		
	3	2.5		○										○							○		
	4	0.5			○									○							○		
	4	1.5				○										○			○				
	4	2.5				○								○								○	
	2	0.5					○							○					○				
	2	1.5					○							○					○				
	2	2.5				○								○					○				
	3	0.5			○					×					○				○				
100	3	1.5		○						×					○						○		
	3	2.5						○							○				○				
	4	0.5		○						×				○								○	
	4	1.5		○						×				○								○	
	4	2.5		○						×				○								○	
	2	0.5	×	○											○						○		
	2	1.5	×	○											○						○		
	2	2.5	×					○							○						○		
	3	0.5			○					×		○							○				
200	3	1.5			○					×	○								○				
	3	2.5			○										○						○		
	4	0.5		○						×			○								○		
	4	1.5				○				×						○			○				
	4	2.5		○											○				○				
	2	0.5					○							○					○				
	2	1.5					○							○						○			
	2	2.5					○							○					○				
	3	0.5							○							○			○				
500	3	1.5							○							○			○				
	3	2.5							○						○				○				
	4	0.5				○							○							○			
	4	1.5				○							○							○			
	4	2.5				○									○					○			

Table 4.7. Stage 2 analysis of ridge deviance-based control charts with different tuning parameters in case of multiplicative shift in regression coefficients intercept included, $\rho^2 = 0.90$.

			Shewhart							**CUSUM**						**EWMA**						
n	p	δ	Deviance	Ridge deviance						Deviance	Ridge deviance					Deviance	Ridge deviance					
				k_1	k_2	k_3	k_4	k_5	k_6		k_1	k_2	k_3	k_4	k_5	k_6	k_1	k_2	k_3	k_4	k_5	k_6
	2	0.5		○											○						○	
	2	1.5						○							○				○			
	2	2.5						○						○							○	
	3	0.5				○								○						○		
50	3	1.5		○										○						○		
	3	2.5				○								○						○		
	4	0.5				○								○				○				
	4	1.5					○							○				○				
	4	2.5				○								○				○				
	2	0.5				○				×				○						○		
	2	1.5				○								○						○		
	2	2.5				○								○						○		
	3	0.5						○		×					○					○		
100	3	1.5						○							○					○		
	3	2.5						○							○					○		
	4	0.5		○						×				○							○	
	4	1.5		○										○							○	
	4	2.5		○										○							○	
	2	0.5	×	○											○					○		
	2	1.5	×	○											○					○		
	2	2.5	×	○											○					○		
	3	0.5			○										○					○		
200	3	1.5			○										○					○		
	3	2.5						○							○						○	
	4	0.5				○									○					○		
	4	1.5				○									○					○		
	4	2.5		○											○					○		
	2	0.5		○												○				○		
	2	1.5					○							○						○		
	2	2.5					○							○						○		
	3	0.5							○					○						○		
500	3	1.5							○					○						○		
	3	2.5							○						○					○		
	4	0.5				○								○					○			
	4	1.5				○									○				○			
	4	2.5				○								○					○			

Table 4.8. Stage 2 analysis of ridge deviance-based control charts with different tuning parameters in case of multiplicative shift in regression coefficients intercept excluded, $\rho^2 = 0.90$.

			Shewhart							**CUSUM**						**EWMA**						
n	p	δ	Deviance	Ridge deviance						Deviance	Ridge deviance					Deviance	Ridge deviance					
				k_1	k_2	k_3	k_4	k_5	k_6		k_1	k_2	k_3	k_4	k_5	k_6	k_1	k_2	k_3	k_4	k_5	k_6
	2	0.5							○							○				○		
	2	1.5							○							○				○		
	2	2.5						○						○						○		
	3	0.5		○										○							○	
50	3	1.5							○					○							○	
	3	2.5				○								○							○	
	4	0.5				○								○				○				
	4	1.5					○							○				○				
	4	2.5				○								○								○
	2	0.5				○				×				○							○	
	2	1.5				○								○							○	
	2	2.5				○								○							○	
	3	0.5							○						○						○	
100	3	1.5							○						○						○	
	3	2.5							○						○						○	
	4	0.5		○										○								○
	4	1.5		○										○								○
	4	2.5	×	○										○								○
	2	0.5	×						○						○						○	
	2	1.5	×	○											○						○	
	2	2.5	×	○											○						○	
	3	0.5							○						○						○	
200	3	1.5							○						○						○	
	3	2.5						○							○							○
	4	0.5				○									○						○	
	4	1.5		○											○						○	
	4	2.5				○									○							○
	2	0.5							○						○						○	
	2	1.5							○						○						○	
	2	2.5							○						○						○	
	3	0.5						○							○						○	
500	3	1.5		○											○						○	
	3	2.5					○								○						○	
	4	0.5				○								○					○			
	4	1.5				○									○				○			
	4	2.5							○						○					○		

Table 4.9. Stage 2 analysis of ridge deviance-based control charts with different tuning parameters in case of additive shift, $\rho^2 = 0.99$.

			Shewhart							**CUSUM**							**EWMA**					
n	p	δ	Deviance	Ridge deviance						Deviance	Ridge deviance						Deviance	Ridge deviance				
				k_1	k_2	k_3	k_4	k_5	k_6		k_1	k_2	k_3	k_4	k_5	k_6		k_1	k_2	k_3	k_4	k_5	k_6
	2	0.5				○										○						○	
	2	1.5				○									○							○	
	2	2.5				○									○							○	
	3	0.5					○								○								o
50	3	1.5					○								○								o
	3	2.5					○								○								o
	4	0.5	×						○							○					○		
	4	1.5	×			○										○							o
	4	2.5	×			○										○					○		
	2	0.5							○	×						○			○				
	2	1.5							○	×						○						○	
	2	2.5							○	×						○						○	
	3	0.5							○							○					○		
100	3	1.5							○							○					○		
	3	2.5							○							○					○		
	4	0.5	×		○											○						○	
	4	1.5	×	○												○						○	
	4	2.5	×		○											○						○	
	2	0.5				○								○								○	
	2	1.5				○								○								○	
	2	2.5				○						○										○	
	3	0.5							○					○							○		
200	3	1.5				○									○								o
	3	2.5							○					○									o
	4	0.5				○						○									○		
	4	1.5				○					○										○		
	4	2.5				○						○									○		
	2	0.5				○						○										○	
	2	1.5				○										○						○	
	2	2.5				○									○							○	
	3	0.5					○								○								o
500	3	1.5					○								○								o
	3	2.5					○								○								o
	4	0.5	×						○						○	○					○		
	4	1.5	×			○										○							o
	4	2.5	×			○										○					○		

Table 4.10. Stage 2 analysis of ridge deviance-based control charts with different tuning parameters in case of multiplicative shift in intercept, $\rho^2 = 0.99$.

			Shewhart							**CUSUM**							**EWMA**					
n	p	δ	Deviance	Ridge deviance						Deviance	Ridge deviance						Deviance	Ridge deviance				
				k_1	k_2	k_3	k_4	k_5	k_6		k_1	k_2	k_3	k_4	k_5	k_6		k_1	k_2	k_3	k_4	k_5	k_6
	2	0.5	×						○						○				○				
	2	1.5				○										○			○				
	2	2.5				○									○							○	
	3	0.5							○						○								o
50	3	1.5							○						○								o
	3	2.5					○								○								o
	4	0.5							○							○					○		
	4	1.5	×						○							○					○		
	4	2.5	×						○							○					○		
	2	0.5							○	×						○			○				
	2	1.5							○	×						○						○	
	2	2.5							○	×						○			○				
	3	0.5							○							○					○		
100	3	1.5							○							○					○		
	3	2.5							○							○					○		
	4	0.5	×		○											○						○	
	4	1.5		○												○						○	
	4	2.5		○												○						○	
	2	0.5				○							○									○	
	2	1.5				○							○									○	
	2	2.5				○							○									○	
	3	0.5							○							○					○		
200	3	1.5							○				○										o
	3	2.5							○				○							○			
	4	0.5				○				×			○						○				
	4	1.5				○							○						○				
	4	2.5				○							○						○				
	2	0.5	×						○						○				○				
	2	1.5				○										○			○				
	2	2.5				○									○							○	
	3	0.5							○						○								o
500	3	1.5							○						○								o
	3	2.5					○								○								o
	4	0.5							○							○					○		
	4	1.5	×						○							○					○		
	4	2.5	×						○							○					○		

Table 4.11. Stage 2 analysis of ridge deviance-based control charts with different tuning parameters in case of multiplicative shift in regression coefficients intercept excluded, $\rho^2 = 0.99$.

			Shewhart							**CUSUM**							**EWMA**						
n	p	δ	Deviance	Ridge deviance						Deviance	Ridge deviance						Deviance	Ridge deviance					
				k_1	k_2	k_3	k_4	k_5	k_6		k_1	k_2	k_3	k_4	k_5	k_6		k_1	k_2	k_3	k_4	k_5	k_6
	2	0.5				○									○							○	
	2	1.5				○										○						○	
	2	2.5				○										○						○	
	3	0.5					○								○						○		
50	3	1.5					○								○								o
	3	2.5					○								○								o
	4	0.5	×			○										○					○		
	4	1.5	×			○										○					○		
	4	2.5	×			○										○						○	
	2	0.5						○		×						○			○				
	2	1.5			○					×						○			○				
	2	2.5			○					×						○			○				
	3	0.5						○								○					○		
100	3	1.5						○								○					○		
	3	2.5						○								○					○		
	4	0.5		○												○						○	
	4	1.5		○												○						○	
	4	2.5		○												○						○	
	2	0.5				○								○								○	
	2	1.5				○								○								○	
	2	2.5				○								○								○	
	3	0.5						○						○					○				
200	3	1.5						○							○				○				
	3	2.5						○						○									o
	4	0.5				○								○				○					
	4	1.5				○								○						○			
	4	2.5				○								○						○			
	2	0.5				○									○							○	
	2	1.5				○										○						○	
	2	2.5				○										○						○	
	3	0.5					○								○						○		
500	3	1.5					○								○								o
	3	2.5					○								○								o
	4	0.5	×			○										○					○		
	4	1.5	×			○										○					○		
	4	2.5	×			○										○						○	

Table 4.12. Stage 2 analysis of ridge deviance-based control charts with different tuning parameters in case of multiplicative shift in regression coefficients intercept included, $\rho^2 = 0.99$.

			Shewhart							**CUSUM**							**EWMA**						
n	***p***	δ	Deviance	Ridge deviance						Deviance	Ridge deviance						Deviance	Ridge deviance					
				k_1	k_2	k_3	k_4	k_5	k_6		k_1	k_2	k_3	k_4	k_5	k_6		k_1	k_2	k_3	k_4	k_5	k_6
	2	0.5				○										○						○	
	2	1.5				○										○						○	
	2	2.5				○									○							○	
	3	0.5					○								○								o
50	3	1.5					○								○						○		
	3	2.5					○								○								o
	4	0.5	×						○							○					○		
	4	1.5	×			○										○				○			
	4	2.5	×			○										○						○	
	2	0.5			○					×						○			○				
	2	1.5			○					×						○			○				
	2	2.5			○											○			○				
	3	0.5							○							○					○		
100	3	1.5							○							○					○		
	3	2.5							○							○					○		
	4	0.5			○											○						○	
	4	1.5		○												○						○	
	4	2.5			○											○						○	
	2	0.5				○								○								○	
	2	1.5				○								○								○	
	2	2.5				○								○								○	
	3	0.5							○						○								o
200	3	1.5				○									○								o
	3	2.5							○					○									o
	4	0.5				○								○				○					
	4	1.5				○								○						○			
	4	2.5				○								○						○			
	2	0.5				○										○				○			
	2	1.5				○										○				○			
	2	2.5				○									○					○			
	3	0.5					○								○								o
500	3	1.5					○								○						○		
	3	2.5					○								○								o
	4	0.5	×						○							○					○		
	4	1.5	×			○										○				○			
	4	2.5	×			○										○						○	

The main conclusions of the detailed examination of Tables 4.5 - 4.12 are summarized as follows:

- *Residual-based Shewhart chart:*
  - The Shewhart$_{ridge}$ chart outperforms Shewhart$_{ML}$ regardless of the shift type, except for the cases $n = 200$, $p = 2$, $\rho^2 = 0.90$, and $n = 50, 100, 500$, $p = 4$, $\rho^2 = 0.99$.
  - It is evident that Shewhart$_{ridge}$ with k_1 outnumbers the others when $\rho^2 = 0.90$ and additive shift as well as the multiplicative shift present in intercept, and the predictors except for intercept.
  - When multiplicative shift presents in all predictors, in most cases when $\rho^2 = 0.90$ the Shewhart$_{ridge}$ charts based on the k_3 and k_6 have the smallest ARL_1 values. The Shewhart$_{ridge}$ based on the k_3 is the best in most combinations when $\rho^2 = 0.99$ regardless of the shift type.
- *Residual-based CUSUM chart:*
  - The CUSUM$_{ridge}$ shows better results than the CUSUM$_{ML}$ chart when the multiplicative shift is in the regression coefficients when $\rho^2 = 0.90$ and when $\rho^2 = 0.99$ unless $n = 100$ and $p = 2$.
  - When $\rho^2 = 0.90$, the CUSUM$_{ridge}$ chart based on the k_4 and k_5 constant has the best performance results among CUSUM$_{ridge}$ charts, especially when the shift is additive.
  - When $\rho^2 = 0.99$, the CUSUM$_{ridge}$ chart based on the k_5 and k_6 outperforms the others if there is a multiplicative shift in all

the predictors, including the intercept. In other cases, k_4 and k_6 appear more often than the others.

- The CUSUM$_{ridge}$ chart based on the k_6 seems to be particularly efficient when $n = 50, 100$, whereas k_4 shows similar results when $n = 200, 500$.

- *Residual-based EWMA chart:*

  - The EWMA$_{ridge}$ chart has the best performance regardless of the correlation, shift type, and size. Also, EWMA$_{ridge}$ based on k_4 outperforms other choices of tuning parameter in most of the combinations for both $\rho^2 = 0.90$ and $\rho^2 = 0.99$.

- *Degree of correlation:*

  - The degrees of correlation $\rho^2 = 0.90$ and $\rho^2 = 0.99$ do not seriously affect the performance of the control charts. That is, Shewhart, CUSUM, and EWMA charts show almost the same pattern both in cases of $\rho^2 = 0.90$ and $\rho^2 = 0.99$.

We further use another data generation process to see how the correlated data generation affects the results. We consider the no intercept regression model to see the effect of the intercept on the overall results. Simulation for no intercept model has been performed for $n = 200$, $p = 3$, and control limits are constructed such that $ARL_0 = 200$, assuming that all the samples are in-control. Inspired by Bozdogan (1987), we generated the second predictor uncorrelated, the first and the third predictors with 0.90 correlation in the following manner:

$$x_1 = 10 + \alpha w_{i2}$$

$$x_2 = 10 + w_{i1}$$

$$x_3 = 8(-1) + x_1 + \rho^2 w_{i2} + 0.5 w_{i3}$$

where ρ^2 is the desired correlation level, $\alpha = 1 - \rho^2$, and w_{ij}, $i = 1, 2, \ldots, 200$, $j = 1, 2, 3$ are random independent standard normal numbers.

The shifts considered for this simulation are additive and multiplicative shifts which are respectively as

- in β_1 which will show results for shifted correlated predictor,
- in β_2 which will show results for shifted uncorrelated predictor.

The performance analysis results are in Table 4.13. The second simulation shows that the Shewhart$_{ridge}$ chart shows better results than Shewhart$_{ML}$, which is coherent with the previous results. CUSUM$_{ridge}$ is better than CUSUM$_{ML}$ in all shift sizes when the shift is in the correlated predictor. The EWMA chart shows a different result when the intercept is excluded from the model. The EWMA$_{ML}$ has the best performance in all combinations except for the case where the medium-sized shift ($\delta = 1.5$) is in the correlated predictor. Also, according to the results, it is challenging to pinpoint precisely which tuning parameter is best for monitoring with Shewhart$_{ridge}$ and CUSUM$_{ridge}$ charts, but k_1 is unquestionably the best choice for the EWMA$_{ridge}$ regardless of the shift size and type.

4.3. Performance of PCR and *r-k* deviance-based control charts

In this section, we present a simulation study on the performance of PCR and *r-k* deviance-based control charts and compare the outcomes with those of deviance and ridge deviance-based control charts in terms of ARL_1 and *SDRL*.

Table 4.13. Performance of ridge deviance-based control charts with different tuning parameters under various shift for no intercept model.

Control chart	Shift type	δ	Deviance	Ridge deviance					
				k_1	k_2	k_3	k_4	k_5	k_6
Shewart	Additive	0.5				○			
		1.5							o
		2.5							o
	Multiplicative - correlated	0.5				○			
		1.5			○				
		2.5							o
	Multiplicative - ucorrelated	0.5				○			
		1.5			○				
		2.5			○				
CUSUM	Additive	0.5	×				○		
		1.5	×						o
		2.5	×	○					
	Multiplicative - correlated	0.5							o
		1.5					○		
		2.5						○	
	Multiplicative - uncorrelated	0.5	×	○					
		1.5					○		
		2.5					○		
EWMA	Additive	0.5	×	○					
		1.5	×	○					
		2.5	×	○					
	Multiplicative - correlated	0.5	×	○					
		1.5		○					
		2.5	×	○					
	Multiplicative - uncorrelated	0.5	×	○					
		1.5	×	○					
		2.5	×	○					

4.3.1. Residual-based Shewhart chart

4.3.1.1. *Stage 1 analysis*

Stage 1 analysis is conducted considering three different levels of dispersion: $v = 0.75$ (overdispersion), $v = 1$ (equidispersion), and $v = 1.5$ (underdispersion) for sample size $n = 750$ with $p = 2, 4, 7$, and $\rho^2 = 0.95, 0.99$ correlation levels.

Following the data generation where response variable generated by setting $\beta_i = 1, i = 1, \ldots, p$, first ML estimators for the COM-Poisson model are obtained. Then using $\hat{V}_{ML}$, PCR and *r-k* class estimators are calculated such that PCs are explain 95% of total variation or equivalently $PTV = 0.95\%$. Considering dimension reduction through application of PC method, the initial value in the calculation of PCR and *r-k* class estimators is set to be $\hat{\beta}^{(0)} = T_r T_r'(X'X)^{-1}X'y$. The tuning parameter selection method given in Eq. (2.16.) is used both for both the ridge and *r-k* class estimators to make the results comparable at the same tuning parameter. Then the deviance, ridge deviance, PCR deviance, and *r-k* deviance residuals are calculated. In-control mean $\hat{\mu}^0$, and in-control standard deviation $\hat{\sigma}^0$ of these residuals are used to obtain control limits that satisfy the $ARL_0 \approx 370$ condition.

Control chart constants, as well as the respective ARL_0 values for each combination are given in Table 4.14.

4.3.1.2. *Stage 2 analysis*

The algorithm based on the flowchart of Stage 2, presented in Fig. 4.1 is utilized for the performance analysis.

To assess the effects of the modifications on the control chart statistics, additive, as well as the multiplicative shift simultaneously in all regression coefficients each in sizes of $\delta = 0.5, 1.5, 2.5$ are considered where $\delta = 0.5$ refers to small, $\delta = 1.5$

Table 4.14. Stage 1 analysis results for residual-based Shewhart charts.

p	v	ρ^2	**ML**		**Ridge**		**PCR**		***r-k***	
			l	ARL_0	l	ARL_0	l	ARL_0	l	ARL_0
2	0.75	0.95	2.770	372.32	2.770	361.70	2.775	382.36	2.775	382.36
2	1	0.95	2.870	363.12	2.865	382.18	2.865	382.58	2.875	382.87
2	1.5	0.95	3.205	377.20	3.215	363.88	3.210	378.38	3.210	384.88
2	0.75	0.99	2.770	372.32	2.785	370.68	2.785	370.68	2.775	383.38
2	1	0.99	2.865	384.40	2.860	374.02	2.870	383.22	2.880	370.68
2	1.5	0.99	3.205	381.48	3.215	378.86	3.215	378.86	3.205	378.22
4	0.75	0.95	2.770	370.50	2.765	383.20	2.765	382.84	2.775	374.94
4	1	0.95	2.865	378.72	2.870	377.12	2.870	381.94	2.880	366.44
4	1.5	0.95	3.185	360.04	3.200	383.00	3.180	378.32	3.185	384.60
4	0.75	0.99	2.770	376.14	2.750	364.66	2.765	383.34	2.775	376.52
4	1	0.99	2.864	381.58	2.845	383.34	2.870	384.80	2.870	384.60
4	1.5	0.99	3.175	378.74	3.205	362.58	3.180	378.50	3.200	381.34
7	0.75	0.95	2.735	367.14	2.773	382.82	2.735	371.02	2.776	378.06
7	1	0.95	2.826	361.12	2.870	384.38	2.826	365.22	2.873	381.82
7	1.5	0.95	3.168	380.08	3.216	360.46	3.168	368.80	3.207	369.29
7	0.75	0.99	2.740	384.58	2.773	372.60	2.735	361.54	2.776	372.62
7	1	0.99	2.831	364.12	2.796	368.60	2.831	365.58	2.878	379.46
7	1.5	0.99	3.168	382.88	3.131	370.51	3.168	383.66	3.207	371.95

to moderate, and $\delta = 2.5$ to large shifts.

After the shifted data are generated, parameters are estimated. The deviance residuals are computed and evaluated by considering the in-control limits obtained in Stage 1, by using control chart constants given by Table 4.14.

Results of Stage 2 analysis are presented in Tables A.1 - A.4. The important conclusions of the extensive examination of Tables A.1 - A.4 are as follows:

- ***ARL_1 results***

– *Effect of additive shift*:

All combinations of Shewhart$_{r-k}$ show the best performance. With few exceptions, Shewhart$_{ridge}$ shows the same ARL_1 as Shewhart$_{r-k}$ when $p = 2$. This is valid for under-dispersed cases when $p = 4,7$, and $\rho^2 = 0.99$. When $p = 2,4$, almost in all combinations, Shewhart$_{ML}$ has the highest ARL_1 values. Regardless of correlation level, in the case of the small and moderate additive shifts when $p = 2,4$, $v = 1.5$, Shewhart$_{PCR}$ appears to have results with the highest values. When $\delta = 2.5$, and $p = 2,4$ regardless of the level of dispersion and correlation, with Shewhart$_{r-k}$ being the best, Shewhart$_{r-k}$ and Shewhart$_{ridge}$ share the first two places, while Shewhart$_{PCR}$ and Shewhart$_{ML}$ are alternate third and fourth in order.

ARL_1 values of all Shewhart charts increase as v increases at fixed ρ^2.

– *Effect of multiplicative shift*:

In the case of multiplicative shift Shewhart$_{r-k}$ chart outperforms other charts in most of the combinations. Exceptions appear when moderate or large shift is present, $\rho^2 = 0.95$, $p = 2$, $v = 0.75,1$, when small and moderate shift is present, $\rho^2 = 0.99$, $p = 7$, $v = 1.5$, $p = 4$, and regardless of the shift size when $\rho^2 = 0.95$, $p = 4$, $v = 1.5$. In these combinations, Shewhart$_{r-k}$ follows Shewhart$_{ridge}$ in terms of ARL_1. Moreover, when $p = 2$ and $v = 1.5$, irrespective of dispersion and correlation level Shewhart$_{r-k}$ and Shewhart$_{ridge}$ show the same performance.

Shewhart$_{PCR}$ mostly follows Shewhart$_{r-k}$ and/or Shewhart$_{ridge}$

when $\delta = 2.5$, while Shewhart$_{ML}$ almost in all cases has the highest ARL_1 value.

- Regardless of the shift type, for fixed p, v and ρ, ARL_1 values of all four control charts decrease as shift size increases. When additive shift presents, reduction appears to be between two to five times as shift changes from small size to moderate.
- While for $v = 4$, $\delta = 1.5, 2.5$, ARL_1 values of all Shewhart charts increase as v increases, for $v = 7$, $\delta = 0.5, 1.5, 2.5$, ARL_1 values of Shewhart$_{ML}$, Shewhart$_{ridge}$, Shewhart$_{PCR}$ charts increase as v increases at fixed ρ^2. However, for Shewhart$_{r-k}$ chart for all values of p, v, and δ except $p = 2$, $\delta = 0.5$, $\rho^2 = 0.95, 0.99$ and $p = 7$, $\delta = 2.5$, $\rho^2 = 0.95, 0.99$.

- ***SDRL* results**

  - *Effect of additive shift*:

    When the moderate shift is present, Shewhart$_{r-k}$ is the best among all four control charts with the smallest *SDRL* values. Exceptions are $p = 4$ and $v = 1.5$. Result pattern is very similar to the ARL_1 results when $\delta = 1.5, 2.5$. When shift size is small, $p = 2, 4$ and $v = 1, 1.5$. *SDRL* values of Shewhart$_{PCR}$ are the highest. But these values decrease as the shift size increases.

    For fixed p, when $\rho^2 = 0.95$ and small and moderate shifts are present in the data, *SDRL* values increase as the dispersion level increases. Moreover, the raise in *SDRL* based on increasing v is also valid for all combinations when $\rho^2 = 0.99$.

  - Except the cases $p = 2, 4$, $\delta = 2.5$, $\rho^2 = 0.95$, the *SDRL* values

of all Shewhart charts increase as v increases.

- *Effect of multiplicative shift*:

  After Shewhart$_{ridge}$, Shewhart$_{r-k}$ mostly shows the best or the second-best results. Results are the same when $p = 2$, $v = 2.5$, in case of moderate and large shifts regardless of the correlation level. Shewhart$_{PCR}$ mostly outperforms Shewhart$_{ML}$ when $\delta = 2.5$.

  When shift size is small, $\rho^2 = 0.99$ and $p = 7$, an increase appears in the *SDRL* values as the dispersion level increases. For fixed correlation levels, in the case of moderate and large shifts, *SDRL* values also increase as v increases when $p = 4$.

- Except the cases $p = 2$, $\delta = 0.5$, $\rho^2 = 0.95, 0.99$, and $p = 7$, $\delta = 2.5$, $\rho^2 = 0.95, 0.99$, *SDRL* of Shewhart$_{r-k}$ increases as v increases. The *SDRL* of Shewhart$_{ridge}$ increases as v increases for all cases of $p = 4, 7$.

4.3.2. Residual-based CUSUM and EWMA charts

4.3.2.1. *Stage 1 analysis*

Stage 1 analysis of residual-based CUSUM and EWMA charts is conducted as presented in Fig. 4.2 considering for sample size $n = 750$ with $p = 4, 7, 10$, and $\rho^2 = 0.95$ correlation and $v = 0.75, 1, 1.5$ dispersion levels. Response variable generated with regression coefficients $\beta_i = 1, i = 1, 2, .., p$.

Data generation is followed by modelling the data with log-link function and calculating the ML and ridge parameters of the COM-Poisson regression model. As in Section 4.3., $\hat{\beta}^{(0)} = T_r T_r'(X'X)^{-1}X'y$ is chosen as initial value for the PCR and *r-k*

class estimators. The number of PCs is decided based on the $PTV = 95\%$. The tuning parameter given in Eq. (2.16.) is used in obtaining the ridge and *r-k* class estimators. Then based on these computations, deviance residuals are calculated.

Control chart constants are obtained for the CUSUM chart with reference value $K = 0.5$ and for EWMA charts with smoothing parameters $\lambda = 0.05, 0.1, 0.2$ to see the impact of smoothing parameters on EWMA chart performance. Then, control chart statistics are computed and compared to the control limit of the corresponding control chart, where the control chart constant continued increasing by 0.001 in every run until the approximate value of desired $ARL_0 \approx 370$ is determined. Stage 1 results of simulation study are given in Table A.5. Table A.5 contains control chart constants for CUSUM and EWMA charts as well as corresponding in-control mean, in-control deviation, and ARL_0.

4.3.2.2. *Stage 2 analysis*

In Stage 2, control charts examined for shifted data. Considering the sensitivity of CUSUM and EWMA charts to small-sized shifts, shift size is set as $\delta = 0.25(0.25)1.5, 2.5, 3$.

The Stage 2 results of the simulation study are presented in Appendix, by Tables A.6 - A.9, and key findings are given in the following paragraphs based on the shift type for each control chart:

Results for CUSUM charts

- *Effect of additive shift*:

  - In all combinations, the CUSUM$_{r-k}$ chart outperformed other control charts. CUSUM$_{ML}$ in most of the combinations shows the worst performance. ARL_1 values of the CUSUM$_{PCR}$ chart

follows either CUSUM$_{r-k}$ or CUSUM$_{ridge}$ chart. This control chart has the highest ARL_1 values, especially when $p = 7, 10$, and $\delta \geq 2$ when the response is over-dispersed. CUSUM$_{ridge}$ has similar performance to CUSUM$_{PCR}$, mostly performing better than CUSUM$_{ML}$, except for a few combinations when $p = 4, 7$ and $v = 1, 1.5$.

- In case of overdispersion, for fixed shift size, as the predictor number increases, the performance of all CUSUM charts improves. The ARL_1 values are very close for $p = 4$ and $p = 7$ and generally decrease as shift size increases. For $v = 1$, while the ARL_1 findings for $p = 4$ and $p = 7$ are relatively similar for $\delta \leq 0.5$, the variations get higher for the other shift sizes by increasing the performance of all CUSUM charts. An increase in p also has a positive effect on performance. As in other cases, for $v = 1.5$, ARL_1 values decrease as p increases. Also, there is an increase in the performance of CUSUM charts when $p = 7$ for all δ and when $p = 4, 10$, for $\delta \geq 0.5$.
- For fixed δ and p, ARL_1 values decrease as dispersion of the response increases. It is also valid when shift size increases regardless of p and v, in general.
- The *SDRL* findings of the control charts share an almost similar pattern to ARL_1, especially regarding CUSUM$_{ML}$ and CUSUM$_{r-k}$. For fixed p and δ, the performance of CUSUM charts decreases as the value of v increases, and for fixed p and v, it increases as the shift size increases. CUSUM$_{r-k}$ outperforms other CUSUM charts in most of the combinations. In rare cases, it is exceeded

by CUSUM$_{ridge}$ when shift size is small and by CUSUM$_{PCR}$ in remaining combinations in terms of *SDRL*.

- *Effect of multiplicative shift*:

  - With very few variations, the performances of CUSUM charts are similar to the results when the response is additively shifted. In the presence of the multiplicative shift, CUSUM$_{r-k}$ outperforms other CUSUM charts in all considered cases. CUSUM$_{ridge}$ and CUSUM$_{PCR}$ charts also show similar performance. The exceptions are $p = 7$ and $v = 1.5$ for CUSUM$_{ridge}$ and $p = 4, 7$, and $v = 0.75$ for CUSUM$_{PCR}$. In these combinations, ARL_1 values of the control charts are the highest.
  - Regardless of the dispersion level, the performance of CUSUM charts increases as the predictor number increases. For $v = 0.75$, with the considerably small changes, performances of the CUSUM charts increase as shift size increases, except for $p = 7$. The dispersion level also affects the performance. Increased dispersion in the response variable causes lower performance irrespective of the predictor number.
  - Same as for ARL_1 results, the CUSUM$_{r-k}$ chart outperforms at least one of the CUSUM charts and is frequently followed by either CUSUM$_{ridge}$ or CUSUM$_{PCR}$, in terms of *SDRL*. Both CUSUM$_{ridge}$ and CUSUM$_{PCR}$ mostly have smaller *SDRL* values compared to CUSUM$_{ML}$. While the exception for CUSUM$_{ridge}$ is in some combinations of $p = 7$, the exception for CUSUM$_{PCR}$ including combinations of $p = 4$, and $p = 7, v \leq 1$.

- The *SDRL* values for CUSUM charts increase as v increases. In general, the performance of the control charts tends to improve as the predictor number increases. This is particularly evident when the response is under dispersed. The tendency of improving performance is also salient in the case of an increase in shift size.

Results for EWMA charts

- *Effect of additive shift*:

  - Based on ARL_1, EWMA$_{r-k}$ surpasses other EWMA charts regardless of the smoothing parameter. In some combinations of $v \leq 1$, EWMA$_{r-k}$ ($\lambda = 0.05$) demonstrates high ARL_1 values. On the contrary, EWMA$_{r-k}$ with $\lambda = 0.1$, and 0.2 are the best or second-best control chart. In cases where EWMA$_{r-k}$ ($\lambda = 0.1$) and EWMA$_{r-k}$ ($\lambda = 0.2$) is the second-best, EWMA$_{PCR}$ is outperformed by all EWMA type control charts. In terms of efficiency, EWMA$_{ridge}$ typically follows EWMA$_{r-k}$. Exceptions are when $\lambda = 0.1, p = 10$ and $\lambda = 0.2, p = 4,7$, both for the dispersion level is greater than or equal to one.
  - For cases with the overdispersed response, the performances of EWMA charts increase as the shift size increases, except for $\delta \leq 1.25$ and $p = 7$. An increase in performance is especially noticeable when $p = 10$. While EWMA ($\lambda = 0.05$) charts perform better when $p = 4$ with a significantly small shift size, EWMA charts with $p = 10$ perform much better in remaining combinations for $v = 1$. For $v = 1.5$, on the other hand, results

show a decrease in ARL_1 values depending on shift size. The only exception is when $p = 10$ and $\delta = 3$. An increase in the predictor numbers also have a positive impact on performances when $\delta \leq 2$. Apart from EWMA$_{r-k}$, ARL_1 values increase as the smoothing parameter for the EWMA chart gets larger, regardless of p, v, and δ.

- In terms of *SDRL*, when $\lambda = 0.05$, EWMA$_{r-k}$ commonly surpasses other EWMA charts, although EWMA$_{ML}$ has the highest results compared to others. The results of EWMA$_{r-k}$ is followed by either EWMA$_{ridge}$ or EWMA$_{PCR}$ chart. The number of cases where EWMA$_{ML}$ has the lowest result values is high for $\lambda = 0.1$ when compared to the result values of EWMA charts with $\lambda = 0.05, 0.2$.
- Based on the *SDRL* values, the performances of the control charts decrease as the dispersion increases and increase as the shift size increases in combinations of fixed delta and $p = 10$, regardless of the smoothing parameter. With the increasing predictor number and $\delta \geq 0.75$, the result for EWMA ($\lambda = 0.05$) charts becomes smaller. When the response is overdispersed and $\lambda = 0.1, 0.2$, the performance of the EWMA charts gets better as p increases. Results are inconsistent when $v \leq 1$.

- *Effect of multiplicative shift*:

  - Even though the performance of the EWMA charts is not particularly affected pattern-wise by increasing value of the smoothing parameter, EWMA charts with $\lambda = 0.2$ mostly have better

results in comparison to respective charts with $\lambda = 0.05, 0.1$. But, when $\lambda = 0.1$, the number of cases where EWMA_{ML} outperforms other charts is high. Some combinations with $\lambda = 0.2$, EWMA_{ridge}, and EWMA_{PCR} charts have the same performance. When $\lambda = 0.05, 0.1$, EWMA_{r-k} is either the best or the second-best control chart in terms of the ARL_1. This control chart has the highest results when $\lambda = 0.2$, $v = 1.5$, and $p = 4, 7$. EWMA_{ridge} (0.05) is mostly positioned as second or third, except when $p = 10$, $v = 0.75$, and $\delta \leq 0.5$. EWMA_{PCR} (0.05), on the other hand, has high ARL_1 values when the response is overdispersed and $p = 7$, and when a response is underdispersed and $p = 7, 10$. Regardless of the smoothing parameter, EWMA_{ML} is a control chart mainly with the worst performance.

- Regardless of the value of v, the performance of the EWMA charts with $\lambda = 0.1, 0.2$ increases as the predictor number increases. When the smoothing parameter is 0.05, while EWMA_{r-k} also displays a similar pattern, for the rest of the charts, this is viable only if $\delta \leq 1.5$. Moreover, increasing shift size positively affects performance. When $p = 10$, the ARL_1 values of all EWMA charts get larger as the dispersion level goes from 0.75 to 1.5.
- Although in a few combinations, EWMA_{r-k} has high values when $\lambda = 0.05, 0.1$, the control chart surpasses at least two EWMA charts in terms of *SDRL* when $\lambda = 0.2$. In contrast, while $\text{EWMA}_{ML}(\lambda = 0.05)$ and $\text{EWMA}_{ML}(\lambda = 0.2)$ provide the poorest outcomes in the majority of combinations, EWMA_{ridge}

($\lambda = 0.1$) replaces it in the case of $\lambda = 0.1$, except for $p = 10$. EWMA$_{PCR}$ ($\lambda = 0.2$) outperforms at least one EWMA chart in its category.

- For fixed v and δ, slightly different *SDRL* values of EWMA charts when $p = 4, 7$ decrease in a visible manner when $p = 10$. In general, the performance of the control charts increases as p increases. An increase in shift size also positively affects the performance. This change especially has a higher influence on the results when $\lambda = 0.2$ and $p = 10$. The increasing value of the v also results in an increase in the *SDRL* values for $p = 10$.

4.4. Performance of Liu deviance-based control charts

In this section, a simulation study experiment is performed to evaluate the performance of Liu deviance-based control charts over deviance and ridge deviance-based control charts.

4.4.1. *Stage 1 analysis*

For the simulation study, predictor matrix is generated following Eq. (4.1.) with $n = 750$, $p = 2, 4$, and $\rho^2 = 0.99$. After generating predictors, a constant term is added to the model. 750×1 predictor variable from COM-Poisson distribution is generated by setting $\beta_i = 1, i = 0, 1, \ldots, q$. Dispersion is selected as $v = 0.5, 1, 1.5$, to reflect the over-, equi-, and underdispersion, respectively and fixed for the entire simulation.

Along with the optimal tuning parameter $\hat{\theta}_{opt}$ for Liu estimator, arbitrarily selected $\theta = 0.5$, and $\theta = 0.85$ values also used for Liu estimation. h_θ is set to

be equal to 0.99 if condition given in Eq. (2.17.) is not satisfied. Two different tuning parameters given by Eq. (2.15.a) and Eq. (2.15.e) are used to obtain the ridge estimator.

Once ML, ridge, and Liu estimators are obtained, corresponding deviance residuals are calculated. Control limits for the control charts are constructed such that $ARL_0 \approx 370$. The control chart constants for different combinations of p and v are given in Table 4.15.

4.4.2. *Stage 2 analysis*

The out-of-control data set is generated with an additive shift, a multiplicative shift in all regression coefficients, and a multiplicative shift solely in the intercept for Stage 2 analysis each in sizes of $\delta = 0.5, 1.5, 2.5$.

Results from Stage 2 are presented in Appendix by Tables B.10 - B.15. The key findings of the results obtained in Tables B.10 - B.15 are described in the following paragraphs.

- *Results for Shewhart charts*:
  - It is found that Shewhart$_{Liu}$, and Shewhart$_{ridge}$ charts have better ARL_1 results compared to Shewhart$_{ML}$. Most of the cases, the performances of Shewhart$_{Liu}$ and Shewhart$_{ridge}$ are similar, but when $v = 0.5$, either Shewhart$_{ridge(k_1)}$ or Shewhart$_{ridge(k_5)}$ outperform other charts. This case is obvious at $p = 4$. When $p = 4$ and $v = 0.5$, Shewhart$_{Liu(\hat{\theta}_{opt})}$ follows Shewhart$_{ridge}$ charts.
  - In terms of *SDRL*, Shewhart$_{Liu}$ and Shewhart$_{ridge}$ show better performance than Shewhart$_{ML}$. When $p = 4$ and $v = 0.5$, *SDRL* results of either Shewhart$_{ridge(k_1)}$ or Shewhart$_{ridge(k_5)}$ are the best

Table 4.15. Stage 1 analysis results for residual-based control charts with respective ARL_0 values.

Method	p	v	**Shewhart**		**CUSUM,** $K = 0.5$		**EWMA** ($\lambda = 0.2$)	
			l	ARL_0	h	ARL_0	L	ARL_0
ML	2	0.5	3.039	372.233	4.660	375.820	3.251	361.220
	2	1	2.852	369.300	5.010	370.780	3.020	360.620
	2	1.5	2.749	369.700	5.640	366.480	2.980	368.660
	4	0.5	3.341	369.867	6.525	375.400	3.298	369.940
	4	1	2.837	371.133	6.110	360.660	3.142	374.480
	4	1.5	2.726	375.533	5.982	368.380	3.010	372.680
Ridge (k_1)	2	0.5	2.921	371.967	4.554	380.820	3.137	367.040
	2	1	2.831	375.533	4.902	375.440	2.876	360.720
	2	1.5	2.913	368.667	5.534	365.080	2.837	361.720
	4	0.5	3.481	367.700	6.436	375.280	3.085	367.180
	4	1	2.827	364.300	6.002	360.660	2.994	366.940
	4	1.5	2.730	361.167	5.873	368.360	2.844	366.420
Ridge (k_5)	2	0.5	2.931	365.667	4.553	380.840	3.201	373.100
	2	1	2.831	374.900	4.904	367.400	2.920	375.500
	2	1.5	2.913	368.667	5.534	365.100	2.880	368.680
	4	0.5	3.578	382.067	6.436	375.280	3.198	369.940
	4	1	2.827	364.300	6.002	360.660	3.039	363.240
	4	1.5	2.730	361.167	5.873	375.360	2.910	375.180
Liu ($\hat{\theta}_{opt}$)	2	0.5	3.000	368.920	4.553	380.820	3.162	378.000
	2	1	2.710	369.300	4.902	375.440	2.908	365.480
	2	1.5	2.996	378.360	5.534	365.080	2.872	375.880
	4	0.5	3.710	365.780	6.436	375.300	3.140	372.240
	4	1	2.960	362.400	6.002	360.660	3.029	375.220
	4	1.5	2.910	375.560	5.873	375.360	2.903	368.180
Liu ($\theta = 0.5$)	2	0.5	2.981	369.160	4.553	380.820	3.181	366.580
	2	1	2.695	369.300	4.902	375.440	2.913	365.500
	2	1.5	2.955	363.880	5.534	365.080	2.876	368.660
	4	0.5	3.700	361.860	6.436	375.300	3.190	375.980
	4	1	2.985	360.860	6.002	360.660	3.036	364.740
	4	1.5	2.895	378.060	5.873	368.360	2.906	372.680
Liu ($\theta = 0.85$)	2	0.5	2.985	369.160	4.553	380.820	3.201	366.580
	2	1	2.695	369.300	4.902	367.440	2.920	365.500
	2	1.5	2.955	363.880	5.534	365.080	2.880	368.660
	4	0.5	3.700	361.860	6.436	367.300	3.198	369.940
	4	1	2.985	360.860	6.002	360.660	3.042	374.480
	4	1.5	2.895	368.060	5.873	375.360	2.910	372.680

followed by Shewhart$_{Liu(\hat{\theta}_{opt})}$. The order of Shewhart$_{Liu(\hat{\theta}_{opt})}$ and Shewhart$_{Liu(0.5)}$ or Shewhart$_{Liu(0.85)}$ change when the additive shift size is 0.5 and 1.5.

- When shift type and p are fixed, as v increases ARL_1 and $SDRL$ values of Shewhart$_{ML}$, Shewhart$_{Liu}$, and Shewhart$_{ridge}$ charts increase.
- When v is fixed, ARL_1 and $SDRL$ values increase as p changes from 2 to 4 for Shewhart$_{ML}$, Shewhart$_{Liu}$, and Shewhart$_{ridge}$ charts.
- When p and v are fixed, as shift size increases, ARL_1 values of Shewhart$_{ML}$, Shewhart$_{Liu}$ and Shewhart$_{ridge}$ charts decrease. This case is valid for all types of shifts. In terms of $SDRL$, Shewhart$_{Liu}$ and Shewhart$_{ridge}$ charts decrease as shift size increases when p and v are fixed.

• *Results for CUSUM charts*:

- At least one of CUSUM$_{Liu}$ and CUSUM$_{ridge}$ charts outperforms the CUSUM$_{ML}$ chart in terms of ARL_1. Only when $v = 0.5$, $p = 4$, and shift size is 2.5, the CUSUM$_{ML}$ chart produces slightly better ARL_1 result than either CUSUM$_{Liu}$ or CUSUM$_{ridge}$ at multiplicative shift type.
- Generally, CUSUM$_{ridge}$ dominates CUSUM$_{Liu}$ in the sense of ARL_1, but there are few cases where CUSUM$_{Liu}$ is better than one of CUSUM$_{ridge}$ in terms of ARL_1 results, depending on the tuning parameter.

- There is no obvious case where one CUSUM chart is better than the others in terms of the *SDRL*.
- When shift size and p are fixed, as v increases, ARL_1 and *SDRL* values of CUSUM_{ML}, CUSUM_{Liu}, and CUSUM_{ridge} increase.
- ARL_1 values of CUSUM_{ML}, CUSUM_{Liu}, and CUSUM_{ridge} increase as p goes from 2 to 4 when shift size and v are fixed. This result is also valid for the *SDRL* values of all CUSUM charts except the multiplicative shift type for $v = 0.5$.
- ARL_1 and *SDRL* values decrease as as shift size increases for CUSUM_{ML}, CUSUM_{Liu}, and CUSUM_{ridge} when p and v are fixed.
- When the shift is additive, CUSUM_D chart is outperformed by CUSUM_{ridge}, $\text{CUSUM}_{Liu(0.5)}$, and $\text{CUSUM}_{Liu(0.85)}$.

• *Results for EWMA charts*:

- When the ARL_1 criterion is considered, for all combinations EWMA_{ridge} and EWMA_{Liu} outperform EWMA_{ML}. EWMA_{ridge} for either k_1 or k_5 is the best in having the smallest ARL_1 except in the cases of all multiplicative shift types when shift size is 2.5, $p = 2$, $v = 1.5$. EWMA_{Liu} chart follows EWMA_{ridge} chart, but there are cases where EWMA_{Liu} and EWMA_{ridge} perform the same in terms of ARL_1 criterion.
- Examination of *SDRL* presents that EWMA_{Liu} and EWMA_{ridge} outperform EWMA_{ML} in most of the combinations except for $\text{EWMA}_{Liu(\hat{\theta}_{opt})}$ when $p = 4$, $v = 0.5$. At $p = 4$, $v = 0.5$ for all shift types, $\text{EWMA}_{Liu(\hat{\theta}_{opt})}$ gives the worst *SDRL* results or the

SDRL results equal to EWMA_{ML}. In some circumstances, at least one EWMA_{Liu} dominates at least one EWMA_{ridge}.

- As the value of dispersion increases for fixed p and shift size, ARL_1 and *SDRL* for all EWMA charts increase.
- Increase in the shift size at fixed shift type and p results in a decrease of ARL_1 and *SDRL*.
- ARL_1 and *SDRL* for all EWMA charts increase as p goes from 2 to 4 when shift type and v are fixed.

5. REAL DATA ANALYSIS

In this chapter, we considered three different real-life data. Laminated plastic plywood (i.e. *LPP*) data set is used to illustrate the performance of ridge deviance-based control charts and the effect of tuning parameters on the overall performance. Through reconstructed semiconductor manufacturing (i.e. *SECOM*) data set, we examined the efficiency of principal component-based approaches. The performance of Liu deviance-based control charts is evaluated and compared to the deviance and ridge deviance-based control chart via bike-sharing application (i.e. *BikeShare*) data set. All analysis is carried out in *R* software.

5.1. *"LPP"* data set analysis

This section covers the investigative analysis of the performance of ridge deviance-based control charts. We conducted this analysis based on the findings in Section 4.2.2.

Marcondes Filho and Sant'Anna (2016) used the "*LPP*" data set[1] to assess the influence of input variables on the number of defects in manufactured plywoods with a principal components-based control chart. Sami et al. (2022) considered data to compare ridge estimation for the COM-Poisson model to ML estimation in terms of MSE, where the ridge estimator was obtained by adding bias to the ML estimator.

The data set consists of a number of defects (response variable) in manufactured laminated plastic plywoods - a wooden plate of a particular size - with respective four input data points (predictors). A descriptive summary of predictor and response variables of the data set is given in Table 5.1.

The data set is analyzed according to the Fig 5.1.

[1] The data set can be accessed from the appendix of Marcondes Filho and Sant'Anna (2016).

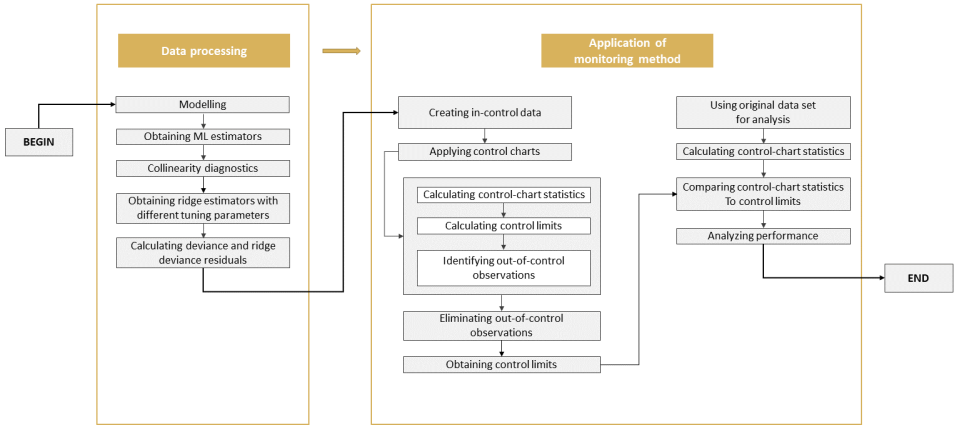


Figure 5.1. Analysis of *LPP* data set.

Table 5.1. Descriptive statistics for *LPP* data set.

	Variable	**mean**	**std. dev.**	**min**	**max**	**unit**
y	Number of defects	14.28	44.006	0	404	–
x_1	Volumetric shrinkage	9.6255	1.224	7.46	12.39	%
x_2	Assembly time	14.992	1.152	12.62	17.9	min
x_3	Wood density	0.5366	0.0157	0.5	0.57	g/cm^3
x_4	Drying temperature	124.6329	14.793	86.97	155.71	C^o

5.1.1. Data processing

Following standardization of the predictor variables, we obtained the dispersion value for the response variable. Since the estimated dispersion $v = 1.0806$ is very close to 1, we modelled the data with a log-link function for Poisson regression.

ML estimator for the no-intercept model is calculated iteratively by using OLS estimator as an initial value and $||\hat{\beta}_{est}^{(t)} - \hat{\beta}_{est}^{(t-1)}|| \leq 1 \times 10^{-6}$ as a convergence criterion. Next, we determined VIF_{ML} and CN_{ML} values based on the scaled informa-

tion matrix, $X'\hat{V}_{ML}X$ as in Eq. (2.23.). The VIF_{ML} values are [99.88565, 97.79919, 16.01773, 20.28182], whereas $CN_{ML} = 1846.153$. The results show a clear sign of multicollinearity.

Ridge estimators with tuning parameters given by Eqs. (2.14.a) - (2.14.f) are obtained iteratively for the no intercept model through the respective algorithm in Section 2.4.. Tuning parameters are $\hat{k}_1 = 6.570068 \times 10^{-6}$, $\hat{k}_2 = 3.338249 \times 10^{-5}$, $\hat{k}_3 = 8.242533 \times 10^{-6}$, $\hat{k}_4 = 2.224697 \times 10^{-2}$, $\hat{k}_5 = 6.012126 \times 10^{-4}$, and $\hat{k}_6 = 4.437456 \times 10^{-5}$. Deviance and ridge deviance residuals from four fitted models are calculated, and each ridge deviance residual is based on different tuning parameters compared to the deviance residuals. Maximum and minimum values of the difference between deviance and ridge deviance residuals, as well as the first five residuals with the highest difference value, are given in Table 3. Table results confirm that the highest tuning parameter produces ridge deviance residuals that are far from deviance residuals.

Table 5.2. Comparison of deviance residuals calculated from the models with ML and ridge estimators.

	[min. value, max. value]	**First 5 observations with the highest difference**
$d_{ML} - d_{ridge(k_1)}$	[-0.0005039735, 0.00007420893]	(27, 39, 54, 59, 61)
$d_{ML} - d_{ridge(k_2)}$	[-0.0005039735, 0.00037509710]	(27, 39, 54, 59, 61)
$d_{ML} - d_{ridge(k_3)}$	[-0.0005039735, 0.00009306913]	(27, 39, 54, 59, 61)
$d_{ML} - d_{ridge(k_4)}$	[-0.0005039735, 0.04608902000]	(39, 54, 59, 61, 69)
$d_{ML} - d_{ridge(k_5)}$	[-0.0081328651, 0.00608257400]	(27, 39, 54, 59, 61)
$d_{ML} - d_{ridge(k_6)}$	[-0.0006684280, 0.00049754790]	(27, 39, 54, 59, 61)

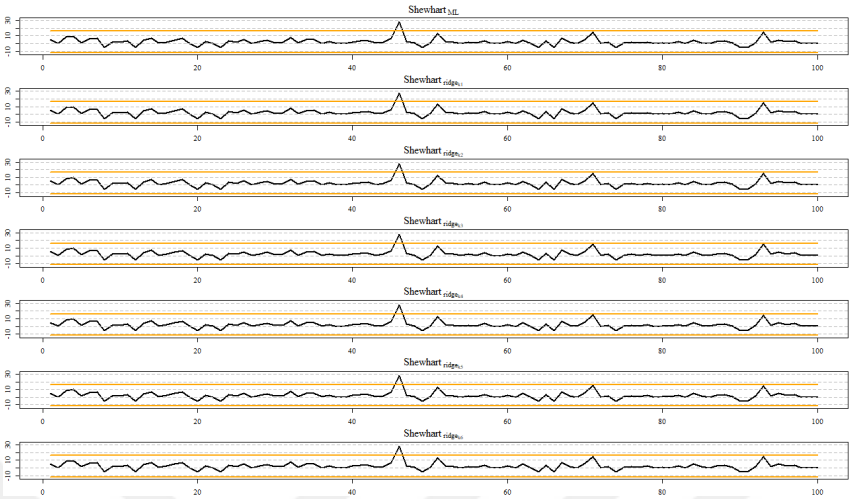


Figure 5.2. Monitoring of the Poisson profile with residual-based Shewhart charts.

5.1.2. Monitoring process

Assuming that the original data set is out-of-control, we create in-control data set by using the entire data set to obtain more precise measurement results during performance analysis. We set $l = 3$ for Shewhart, $K = 0.5$ with $h = 4$ for CUSUM, and $\lambda = 0.1$ with $L = 2.7$ for the EWMA chart, which are the values presented by Montgomery (2020) that satisfy the $ARL_0 \approx 370$ condition. Constructed control charts are given by Figures 5.2 - 5.4.

While in Figs. 5.2 - 5.4, control chart statistics exhibit a similar pattern, slight changes are decisive. Detailed examination revealed that Shewhart charts identified one (46^{th} observation), and CUSUM charts identified seven (46-48^{th}, 51-54^{th} observations) as out-of-control. None of the control chart statistics exceeded the control limits of EWMA charts.

The out-of-control observations later removed from the data set to create an in-control data set. According to Table 5.3, after the elimination mean of the process data is changed approximately by 0.35 units.

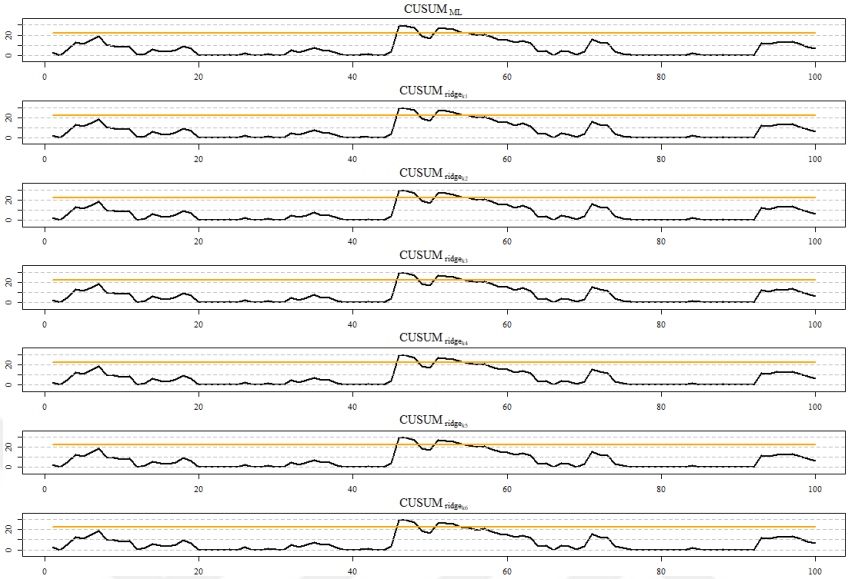


Figure 5.3. Monitoring of the Poisson profile with residual-based CUSUM charts.

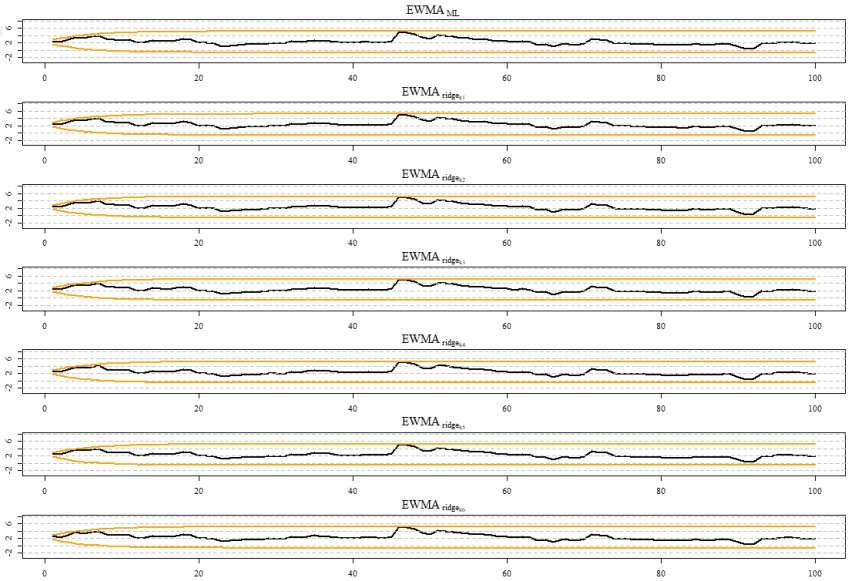


Figure 5.4. Monitoring of the Poisson profile with residual-based EWMA charts.

Table 5.3. Change in the mean of the process data.

	Mean of the original process data	**Mean of the in-control process data**
deviance	2.299373	1.945436
ridge deviance, k_1	2.299374	1.945436
ridge deviance, k_2	2.299374	1.945440
ridge deviance, k_3	2.299374	1.945437
ridge deviance, k_4	2.299107	1.945584
ridge deviance, k_5	2.299382	1.945500
ridge deviance, k_6	2.299374	1.945441

The built-in functions of the "*SPC*" package are used to construct the control limits based on the in-control data set. l for Shewhart charts, h for CUSUM charts for $K = 0.5$, and L for EWMA charts for $\lambda = 0.1$ is reported in Table 5.4.

Table 5.4. Control chart constants for in-control Poisson profile.

	l	h	L
deviance	1.575754	3.156618	10.85020
ridge deviance, k_1	1.575754	3.156624	10.85020
ridge deviance, k_2	1.575755	3.156647	10.85022
ridge deviance, k_3	1.575754	3.156625	10.85020
ridge deviance, k_4	1.575803	3.159948	10.85085
ridge deviance, k_5	1.575775	3.157075	10.85048
ridge deviance, k_6	1.575756	3.156647	10.85022

With these control limits and the original data set, we assess the performance of deviance and ridge deviance residual-based Shewhart, CUSUM, and EWMA charts in terms of ARL_1. ARL_1 values are calculated by using the built-in functions of the *"SPC"* package.

Results presented in Table 5.5 are consistent with the simulation study re-

Table 5.5. Performance analysis of residual-based control charts for monitoring Poisson profile in terms of ARL_1.

	Shewhart	**CUSUM**	**EWMA**
deviance	3.295474	1.358106	34.33659
ridge deviance, k_1	3.295472	1.358105	34.33669
ridge deviance, k_2	3.295466	1.358101	34.33706
ridge deviance, k_3	3.295472	1.358105	34.33671
ridge deviance, k_4	3.295378	1.357774	34.39436
ridge deviance, k_5	3.295359	1.358027	34.34430
ridge deviance, k_6	3.295464	1.358099	34.33722

sults of the no intercept model in Section 4.2.2. While ridge deviance residual-based Shewhart and CUSUM charts show superior performance compared to the deviance residual-based Shewhart and CUSUM charts, the EWMA chart performs the exact opposite.

Shewhart$_{ridge}$ and CUSUM$_{ridge}$ charts with k_4 and k_5 tuning parameters and EWMA$_{ridge}$ chart with k_1 tuning parameters are the best among respective ridge residual-based control charts. Also, with small ARL_1 values, residual-based CUSUM charts outperform residual-based Shewhart and EWMA charts.

5.2. *"SECOM"* data set analysis

A modern semiconductor manufacturing process is equipped with high technology. The monitoring of the process is carried out on a continuous basis through the collection of signals/variables from sensors and/or process measurement points. Each type of signal can be considered a feature to improve the quality of semiconductors.

The data set presented in this section is generated from a similar process. After being measured by the 590 sensors, each of the 1567 instances of the production

line was subjected to a Pass/Fail test. Test result associated with a specific date time stamp is either -1 or 1, where -1 stands for pass and 1 for failure. The null values are described using "*NaN*". The final data set is the 1567×591 matrix which consists of 590 features and a class.

Moldovan et al. (2017, 2018) and Kim et al. (2017) used a data set to illustrate different machine learning algorithms for classification problems. Cao et al. (2020) applied a mixture of two refinement methods to detect quality issues in the data set. Via data set, Takahashi et al. (2019) demonstrated simplified machine learning implementation to reduce the time spent on failure prediction in manufacturing processes. Kwon and Kim (2020) adapted iterative feature selection for failure prediction and preferred the data set to evaluate the performance of the proposed method.

Inspired by the aforementioned studies, we designed the analysis process of the *SECOM* data set with deviation residual-based control charts. Our purpose is to determine if the PCR and *r-k* deviance residuals-based control charts outperform the control charts based on deviance and ridge deviance residuals. The analysis of the data is conducted in *R* mostly by using *"COMPoissonReg"* and *"SPC"* packages.

But since the response is binary, we made rearrangements and reconstructed the data set to make it suitable for count data analysis. The rearrangement is performed differently for the comparative analysis of residual-based CUSUM and EWMA charts taking into account the sensitivity of these control charts to small-sized changes in the process mean.

The process steps can be summarized with the flowchart given in Fig. 5.5.

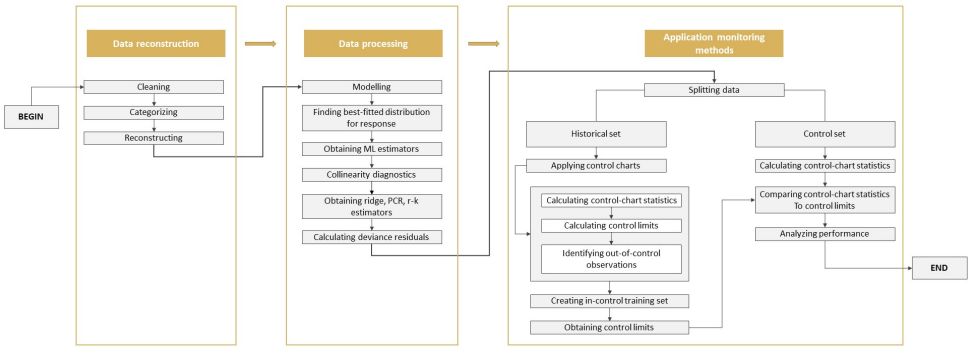


Figure 5.5. Analyzing *SECOM* data set.

5.2.1. Analysis with residual-based Shewhart chart

5.2.1.1. *Data reconstruction*

For the analysis of *SECOM* data set with residual-based Shewhart chart, we reconstructed data in following manner:

1. All missing values are replaced with the previous value;
2. The number of predictors is reduced by maintaining continuous variables only and removing the rest. As a result, initial predictor matrix $X_{1567\times590}$ become $X_{1567\times444}$;
3. The 24-hour period was divided into 8 different groups which is called as time frame. Time frame variable created based on the time stamp and the corresponding time intervals are

$1 \rightarrow 01:00-03:59$	$5 \rightarrow 13:00-15:59$
$2 \rightarrow 04:00-06:59$	$6 \rightarrow 16:00-18:59$
$3 \rightarrow 07:00-09:59$	$7 \rightarrow 19:00-21:59$
$4 \rightarrow 10:00-12:59$	$8 \rightarrow 22:00-00:59(nextday)$

4. The data and the time frame are combined to create "date and time frame" (DTF), e.g. 19-7-2008-4 stands for date 19-7-2008 and time frame 4;
5. The response variable is created by summing the number of passes in the respective DTF. On the other hand, the corresponding predictors are generated by taking the average of each predictor variable in the respective DTF. The resulting data set consists of a 476×444 predictor matrix and a 476×1 response vector of counts;
6. Among predictors with the absolute value of pairwise correlation value higher than 0.9999 were selected to be included in the analysis to ensure severe multicollinearity. 13 predictor that fall into this criteria are selected among 444 predictors and these 13 predictors are the sensors numbered 3, 33, 35, 139, 151, 171, 173, 251, 274, 286, 306, 308, and 389. The final form of the data set is a matrix of $[Y_{476\times1}, X_{476\times13}]$.

5.2.1.2. *Data processing*

Kim et al. (2017) mentioned that the data distribution is very irregular in each feature and needed standardization. Taking into account this statement and multicollinearity, prior to the modelling data set, we scaled the X matrix.

Following the standardization, the COM-Poisson, Negative Binomial, and Poisson distributions are utilized to determine the best-fitting distribution for the count response. Log-likelihood, Akaike information criterion (AIC), and Bayesian information criterion (BIC) values for each model are computed by using "*MASS*" and "*COMPoissonReg*" packages. Diagnostic analyses of the distributions are presented in Table 5.6. Results in Table 5.6 show that COM–Poisson distribution is the best-fitting distribution for response in terms of all three measures. The dispersion

for the response variable is estimated as $v = 0.3555$ which indicates that response is overdispersed.

Table 5.6. Diagnostic analysis of best-fitted distribution for response variable of *SECOM* data set for application of the residual-based Shewhart charts.

	Log-likelihood	**AIC**	**BIC**
COM-Poisson	-1149.4683	2326.9367	2379.0871
Negative Binomial	-1335.0334	2698.0668	2750.2172
Poisson	-1658.4254	3326.8507	3397.0012

By setting the initial value as $\hat{\beta}_{OLS}$ and convergence criterion as $||\hat{\beta}_{est}^{(t)} - \hat{\beta}_{est}^{(t-1)}|| \leq 1 \times 10^{-6}$, we obtained the ML estimator, as well as the weight matrix $\hat{V}_{ML}$ in the final iteration. To examine the collinearity among predictors, we calculated the CN_{ML} based on the scaled information matrix, $X'\hat{V}_{ML}X$. The $CN_{ML} = 1846.153 > 10$, indicates severe multicollinearity.

Considering Eq. (2.16.), the tuning parameter is calculated as $\hat{k} = 0.1073862$ and it is used for both ridge and *r-k* estimators, to make different estimators comparable at the same tuning parameter. The number of principal components that explain approximately 90% of the overall variance is obtained as 5. Next, ridge, PCR, and *r-k* class estimators as well as the deviance residuals based on these estimators are computed.

Table 5.7 and Fig. (5.6) show how different estimation methods affect the residuals and in which observations they are most affected relative to each other. In Fig. (5.6), different combinations of differences between d_{ML}, d_{ridge}, d_{PCR}, d_{rk} are plotted against the observation number. The figure presents that the differences are much more explicit in $d_{ML} - d_{PCR}$, $d_{ML} - d_{r-k}$, $d_{ridge} - d_{PCR}$, $d_{ridge} - d_{r-k}$ which shows the effect of applying the principal components methods. The ranges of the

differences in Fig. 5.6(a) and 5.6(f) are lower than that of Fig. 5.6(b) - 5.6(e). According to the numerical values of the differences in Table 5.7, the biggest change occurs between d_{ML} and d_{PCR}, whereas the lowest one occurs between d_{PCR} and d_{r-k}. Thus, Table 5.7 and Fig. 5.6 show that different estimation methods produce residuals with different values.

Table 5.7. Comparison of deviance residuals calculated from the models with ML, ridge, PCR, and *r-k* class estimators.

	[min. value, max. value]	**First 10 observations with the highest difference**
$d_{ML} - d_{ridge}$	[-0.04028026, 0.05188635]	(5, 19, 84, 89, 184, 217, 362, 407, 461, 475)
$d_{ML} - d_{PCR}$	[-0.28292939, 0.25309909]	(12, 15, 18, 184, 280, 294, 296, 314, 322, 474)
$d_{ML} - d_{r-k}$	[-0.27277291, 0.24067092]	(12, 15, 18, 184, 280, 294, 296, 314, 322, 474)
$d_{ridge} - d_{PCR}$	[-0.27806437, 0.2412572]	(12, 15, 143, 278, 280, 294, 296, 314, 322, 422)
$d_{ridge} - d_{r-k}$	[-0.2679079, 0.2412572]	(12, 15, 143, 278, 280, 294, 296, 314, 322, 422)
$d_{PCR} - d_{r-k}$	[-0.01242816, 0.01015648]	(12, 165, 278, 280, 294, 296, 314, 322, 352, 423)

5.2.1.3. *Monitoring process*

Since we do not have any prior information about the state of the data, we split the data set into two which we call as historical and control sets. The historical set is assigned approximately 10% of the residuals (first 47 residuals) and the control set is assigned as the remaining residuals (last 429 residuals). Considering that the Shewhart charts will perform better with large shifts, data split rate was determined with the difference between the mean of the two data sets being maximum.

The historical set is used to determine the control limits while the control set is utilized to see the performance of the control charts.

The control chart constants are derived from in-built functions of the *"SPC"*

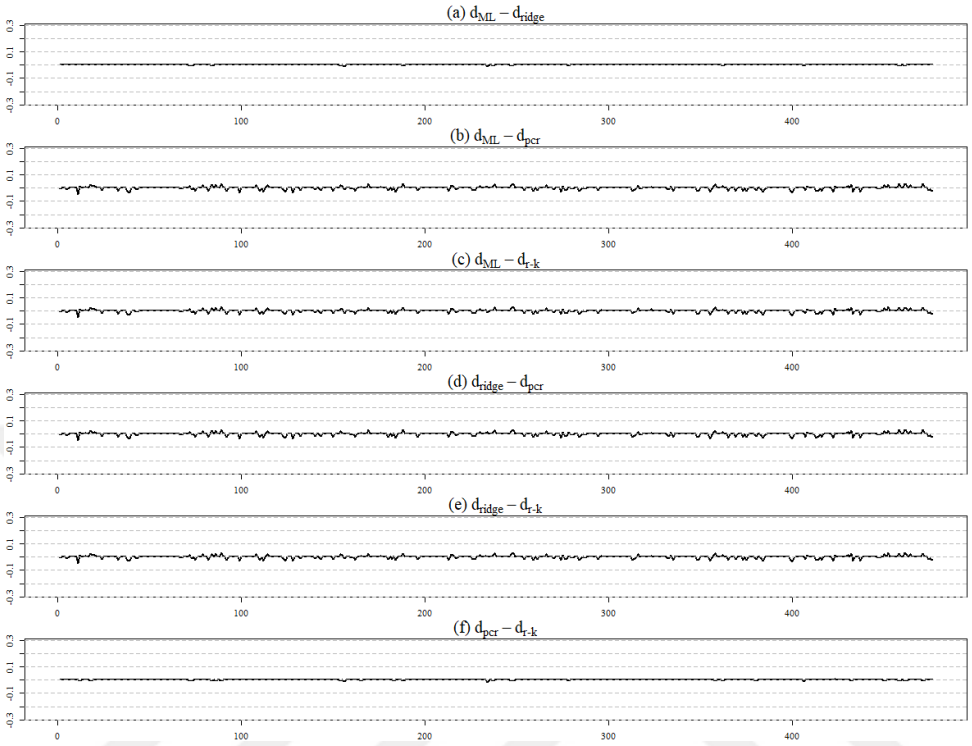


Figure 5.6. Graph of residual differences against the observation numbers.

package such that $ARL_0 \approx 370$ by using the mean and standard deviation of deviance residuals corresponding to the historical set. Then by using these constants, we constructed the control limits as in Eqs. (3.1.) - (3.2.) and Eqs.(3.4.) - (3.5.) to roughly determine the out-of-control observations. Shewhart$_{ML}$, Shewhart$_{ridge}$, Shewhart$_{PCR}$, as well as Shewhart$_{r-k}$ chart identified the 2^{nd}, 23^{th}, 28^{th}, 34^{th}, 44^{th}, and 46^{th} observations as out-of-control.

To create in-control data from the historical set, we eliminated all six out-of-control observations and computed the mean and standard deviations of the remaining 41 deviance residuals. Then, by using the in-built functions from the "*SPC*" package for these in-control residuals, control limits for Shewhart charts are established such that $ARL_0 \approx 370$. The lower and upper limits of control charts are computed as given

in Table 5.8.

Table 5.8. Control chart constant and control limits calculated using the corresponding l, $ARL_0 \approx 370$.

	l	LCL	UCL
Shewhart$_{ML}$	1.054048	0.070199	0.635587
Shewhart$_{ridge}$	1.054379	0.073213	0.63504
Shewhart$_{PCR}$	1.056782	0.088333	0.637654
Shewhart$_{r-k}$	1.056711	0.088085	0.637384

After the control limits are computed, control chart statistics corresponding to the control set are compared to these control limits and in-built functions of the *"SPC"* package executed to obtain the ARL_1 values. Control charts established based on the control data are presented in Fig. 5.7. Although control charts in Fig. 5.7 seem to be similar, slight differences between the residuals exist as demonstrated by Table 5.7. The difference in the performance of these control charts can be seen clearly in terms of ARL_1 values. The ARL_1 values of Shewhart$_{ML}$, Shewhart$_{ridge}$, Shewhart$_{PCR}$, and Shewhart$_{r-k}$ charts are respectively as $2.26825, 2.25433, 2.20371, 2.20365$ which indicate that Shewhart$_{r-k}$ is the best among all four control charts and it is followed by Shewhart$_{PCR}$, while Shewhart$_{ML}$ chart shows the worst performance among all control charts.

This real life application demonstrated that with the application of the *r-k* class estimator to Shewhart charts, the performances of Shewhart control charts have improved over Shewhart$_{ML}$, Shewhart$_{ridge}$ and Shewhart$_{PCR}$ under multicollinearity.

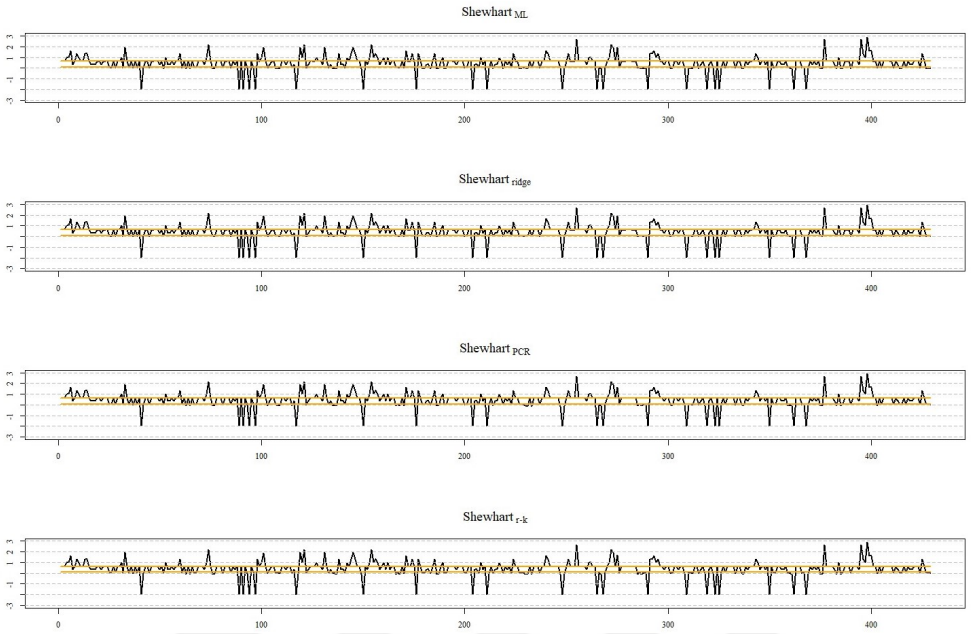


Figure 5.7. Control charts established based on the control set.

5.2.2. Analysis with residual-based CUSUM and EWMA charts

5.2.2.1. *Data reconstruction*

For the analysis of *SECOM* data set with residual-based CUSUM and EWMA charts, we reconstructed data by following steps 1 - 5 given in Section 5.2.1.1. and then selected the variables with the absolute value of the pairwise correlation between 0.948 and 0.952 to be included in the analysis[2]. We get the predictor matrix X in dimension 476×8 where the predictors in the model are values recorded by sensors numbered 93, 95, 98, 103, 116, 198, 470, and 523.

[2]Thereby, we secured multicollinearity and the final data produced the least change in the mean of the in-control historical and the mean of the control set.

5.2.2.2. *Data processing*

After the standardization of predictor matrix, three count data modelling techniques are utilized to determine the best-fitting distribution for the response variable. Log-likelihood, AIC, and BIC values for the COM-Poisson, Negative Binomial, and Poisson models are given in Table 5.9. The COM-Poisson distribution is recognized as the best fitting distribution due to its high log-likelihood and low AIC and BIC values. An estimated dispersion for the response variable is computed as $v = 0.2019$, which indicates overdispersion.

Table 5.9. Diagnostic analysis of best-fitted distribution for response variable of *SECOM* data set for application of the residual-based CUSUM and EWMA charts.

	Log-likelihood	**AIC**	**BIC**
COM-Poisson	-1028.77204	2075.54409	2106.86743
Negative Binomial	-1331.30338	2680.60676	2711.93010
Poisson	-1666.44804	3342.89608	3382.21942

After it is seen that the response variable follows COM-Poisson distribution, we go on the analysis corresponding to this distribution. ML estimator is first obtained by utilizing the OLS estimator as an initial value and $||\hat{\beta}_{est}^{(t)} - \hat{\beta}_{est}^{(t-1)}|| \leq 1 \times 10^{-6}$ is used as convergence criterion.

Scaled information matrix is examined for the multicollinearity. We calculated the eigenvalues of scaled information matrix as 64.2714, 56.7976, 54.6487, 48.30560, 1.5845, 1.4329, 1.4186, 1.3268 and the variance inflation factor (*VIF*) values as 28.49139, 28.50746, 29.49110, 29.49507, 28.37309, 28.51614, 28.56399, 28.34829. Since all *VIF* values are larger than 10, they indicate that all the predictor variables are involved in multicollinearity.

The tuning parameter for the ridge and *r-k* class estimators is obtained as $\hat{k} = 0.001536528$ by using Eq. (2.16.). The number of principal components that explain approximately 99% of the overall variance is obtained as 7. Then the ML, ridge, PCR, and *r-k* deviance residuals are calculated as in Eq. (2.24.).

The residuals with respect to each other are compared to see the difference between them. The absolute value of the differences of the residuals was taken, and the minimum and maximum values of these obtained values and the top ten highest values were tabulated in Table 5.10. Table 5.10 shows how the different estimation methods affect the residuals and in which observations they are most effective relative to each other. Also, while the closest residual values to each other are between d_{PCR} and d_{r-k}, it is followed by d_{ML} and d_{ridge} and it is clear that the other residual differences are more than these two. The highest range is between d_{ML} and d_{r-k}.

Table 5.10. Comparison of deviance residuals calculated from the models with ML, ridge, PCR, and *r-k* class estimators.

	[min. values, max. values]	**First 10 observations with the highest differences**
$\mid d_{ML} - d_{ridge} \mid$	[0.000000008102, 0.00898]	(73, 155, 156, 234, 278, 323, 359, 362, 406, 423)
$\mid d_{ML} - d_{PCR} \mid$	[0.00000001433, 0.04814]	(11, 39, 89, 99, 128, 248, 355, 384, 400, 461)
$\mid d_{ML} - d_{r-k} \mid$	[0.0000001098, 0.04512]	(11, 39, 89, 99, 128, 248, 384, 400, 452, 461)
$\mid d_{ridge} - d_{PCR} \mid$	[0.00000006621, 0.04977]	(11, 39, 89, 99, 128, 188, 248, 355, 400, 461)
$\mid d_{ridge} - d_{r-k} \mid$	[0.00000002929, 0.04675]	(11, 39, 89, 99, 128, 248, 384, 400, 452, 461)
$\mid d_{PCR} - d_{r-k} \mid$	[0.0000000668, 0.01509]	(73, 99, 156, 234, 278, 323, 359, 362, 406, 423)

5.2.2.3. *Monitoring process*

As in Section 5.2.1.3. we split the data set into historical and control sets. The first 25% of the data set (first 119 residuals) forms the historical set and is used

to create the data set of the in-control state, while the last 75% of the data set (last 357 residuals) forms the control set and is used to examine the performance of the control charts.

Once the historical and control sets are determined, the following steps are taken separately for CUSUM and EWMA charts to create a historical set which is used to construct the in-control control limits, and a control set which is used for the analysis:

1. Creating in-control data from historical set
   (a) Utilizing in-built functions of the *"SPC"* package with the mean and standard deviation of deviance residuals of the historical set, we obtained the control limits that met the $ARL_0 \approx 200$ criterion;
   (b) We calculated the CUSUM chart statistics with $K = 0.5$ and EWMA chart statistics with smoothing parameters of $\lambda = 0.05, 0.1, 0.2$ of ML, ridge, PCR, and *r-k* deviance-based control charts;
   (c) We compared the control chart statistics with the control limits of the corresponding control chart. Results are given in Table 5.11 and Table 5.12 for CUSUM and EWMA charts respectively.

   Table 5.11 shows that the 80 observations exceeded the upper control limit of the CUSUM_{ML} and CUSUM_{ridge} charts while 79 observations for the CUSUM_{PCR} and CUSUM_{r-k} charts. On the other hand, Table 5.12 shows that EWMA with $\lambda = 0.05$ detected two (2^{nd} and 3^{rd}) observations while EWMA with $\lambda = 0.1$ detected only one (2^{nd}) observation as

out-of-control observation. EWMA_{ML} and EWMA_{ridge} detected one (2^{nd}) observation whereas EWMA_{PCR} and EWMA_{r-k} detected two (2^{nd} and 88^{th}) observations when $\lambda = 0.2$.

Table 5.11. Control limits and number of out-of-control observations identified by respective CUSUM chart.

	Control limits	**Number of out-of-control observations**
CUSUM_{ML}	$\pm$ 1.697833	80
CUSUM_{ridge}	$\pm$1.698043	80
CUSUM_{PCR}	$\pm$1.696883	79
CUSUM_{r-k}	$\pm$1.697169	79

Table 5.12. Control limit constants and number of out-of-control observations identified by respective EWMA chart.

	Control limit constant			**Number of out-of-control observations**		
	$\lambda = 0.05$	$\lambda = 0.1$	$\lambda = 0.2$	$\lambda = 0.05$	$\lambda = 0.1$	$\lambda = 0.2$
EWMA_{ML}	4.839887	4.274365	3.84603	2	1	1
EWMA_{ridge}	4.839496	4.274089	3.845839	2	1	1
EWMA_{PCR}	4.843432	4.276866	3.84776	2	1	2
EWMA_{r-k}	4.842814	4.27643	3.847458	2	1	2

(d) We pooled the out-of-control observations detected by ML, ridge, PCR, and *r-k* deviance-based control charts and eliminated the unique ones to create the in-control historical set. 80 observations were eliminated for monitoring with the CUSUM chart and three observations were eliminated for the EWMA chart;

(e) By obtaining the control limits meeting $ARL_0 = 200$, we calculated the mean and standard deviation of each in-control historical set such that the results are given in Table 5.13 and Table 5.14.

Table 5.13. CUSUM chart limits, in-control mean, and standard deviation of the historical set.

	Control limits	$\hat{\mu}^0$	$\hat{\sigma}^0$
CUSUM_{ML}	± 3.011428	0.615378	0.271395
CUSUM_{ridge}	± 3.009625	0.615453	0.271221
CUSUM_{PCR}	± 3.004797	0.615778	0.270584
CUSUM_{r-k}	± 3.001579	0.61591	0.270273

Table 5.14. EWMA chart limit constants, in-control mean, and standard deviation of the historical set.

	$\lambda = 0.05$	$\lambda = 0.1$	$\lambda = 0.2$	$\hat{\mu}^0$	$\hat{\sigma}^0$
EWMA_{ML}	2.651935	2.776787	2.856777	0.549335	0.328883
EWMA_{ridge}	2.651731	2.776636	2.856673	0.549269	0.328982
EWMA_{PCR}	2.650594	2.775801	2.856099	0.549929	0.328395
EWMA_{r-k}	2.650289	2.775577	2.855944	0.549825	0.328533

2. Analysis for the control set

(a) We calculated the control chart statistics for each chart by using test data;

(b) We compared the control limits obtained from the historical set with the control chart statistics obtained in (a);

(c) We analyzed the performance of the control chart in terms

of ARL_1 and ARL_1 values are derived by using the appropriate functions of the *"SPC"* package. Results are presented in Table 5.15.

Table 5.15. Performance analysis of CUSUM and EWMA charts with *SECOM* data set, ARL_1.

	ML	***ridge***	***PCR***	***r-k***
CUSUM	5.232221	5.230022	5.212231	5.208366
EWMA, $\lambda = 0.05$	26.04584	26.04308	25.87346	25.87023
EWMA, $\lambda = 0.1$	37.30165	37.29657	37.04754	37.04124
EWMA, $\lambda = 0.2$	54.93462	54.92688	54.58413	54.57429

Performance evaluation of the control charts is as follows:

To see the direction of the shift, differences between the mean of in-control historical set and control set is given by Table 5.16. Compared to the in-control mean of the historical set, it is observed that the mean of the control set reduced. Then, it is acceptable to say that a negative shift has occurred. Negative change is particularly evident in Fig. 5.8 since control chart statistics are positioned on the bottom part of the zero line and in Figs. 5.9, 5.10, and 5.11 since they show a downward trend.

Table 5.16. The difference in the mean of the residuals from the in-control control set and historical set.

	d_{ML}	d_{ridge}	d_{PCR}	d_{r-k}
CUSUM	-0.24073	-0.24081	-0.24015	-0.24029
EWMA	-0.17469	-0.17463	-0.1743	-0.17421

The visualized analysis of the control set is conducted by plotting CUSUM and EWMA chart statistics against the observation number for the control set, as well

as respective control limits calculated from Table 5.13 and Table 5.14 and we show the outcomes with Fig. 5.8 and Figs. 5.9 - 5.11. Figs. 5.9 - 5.11 show the effect of the smoothing parameter for the EWMA chart.

Table 5.15 shows that both CUSUM$_{r-k}$ and EWMA$_{r-k}$ are the best in comparison to corresponding control charts based on the ML, ridge, and PCR deviance residuals in terms of ARL_1. The CUSUM$_{PCR}$ and EWMA$_{PCR}$ charts follow CUSUM$_{r-k}$ and EWMA$_{r-k}$, respectively and the CUSUM$_{ML}$ and EWMA$_{ML}$ have the highest ARL_1 values.

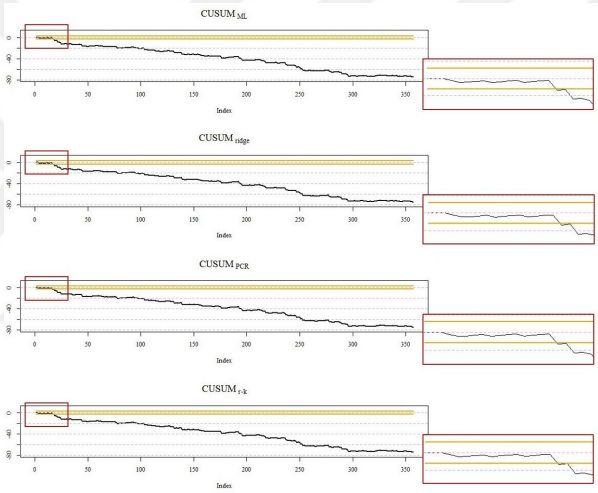


Figure 5.8. Analysis of control set with CUSUM charts.

5.3. *"BikeShare"* data set analysis

To illustrate the use of the Liu deviance-based monitoring method for the COM-Poisson profile, we use data from a bike-sharing application data set. The bike-sharing application system is a bike rental service where the whole process is automated. The automation makes it easier to gather information about the number of rides by casual and registered users for every hour, the weekday of a ride, a working

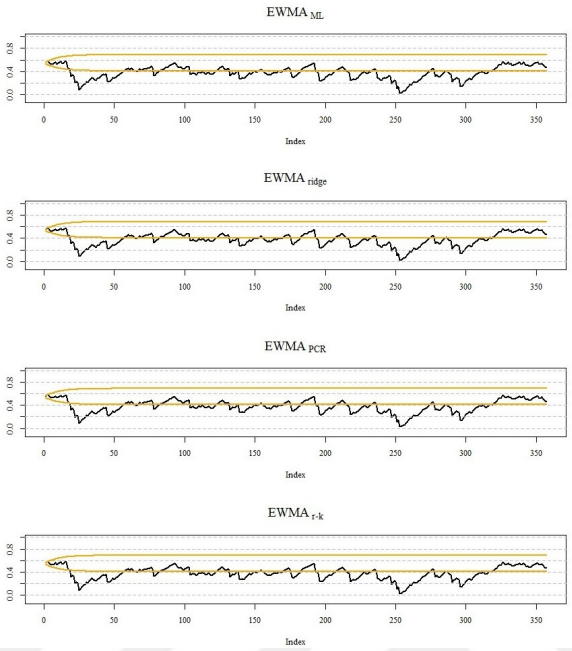


Figure 5.9. Analysis of control set with EWMA charts with $\lambda = 0.05$.

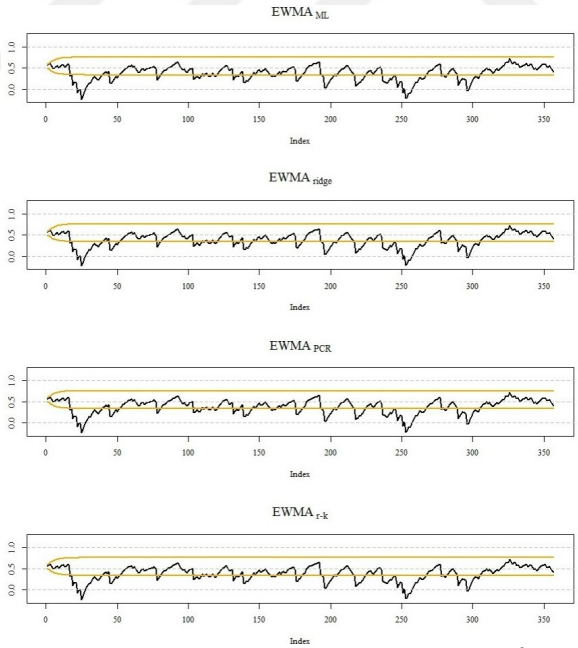


Figure 5.10. Analysis of control set with EWMA charts with $\lambda = 0.1$.

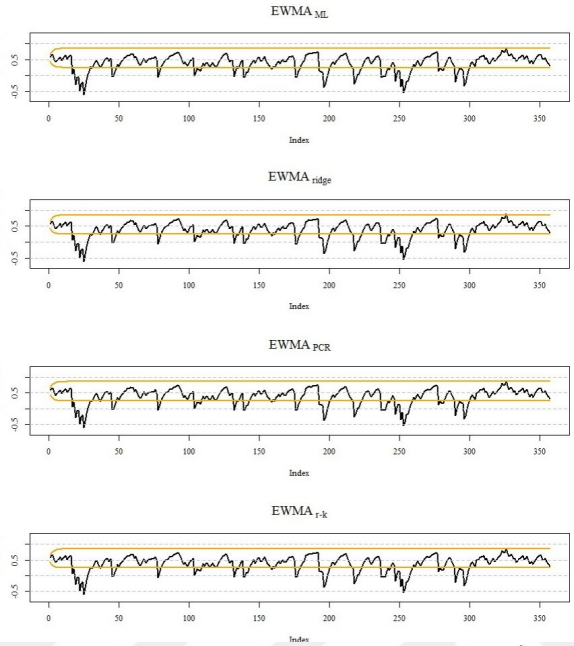


Figure 5.11. Analysis of control set with EWMA charts with $\lambda = 0.2$.

day or a holiday, even the weather condition.

We use the data available from Fanaee-T and Gama (2014) on rides in Washington, DC for 2011-2012. This data set is available in daily and hourly formats. For the application process, we have only considered a third of the hourly data for February 2011. *temp* (x_1), *atemp* (x_2), *hum* (x_3), and *wspeed* (x_4) as predictors, and a daily count of casual users' bike shares as the response variable were included to the model. To eliminate the effect of intercept, we considered data without an intercept term.

The detailed description of predictors included to the model is given below:

- *temp*: Normalized temperature in Celsius. The values are divided to 41 (max).
- *atemp*: Normalized feeling temperature in Celsius. The values are divided to 50 (max).
- *hum*: Normalized humidity. The values are divided to 100 (max).

- *wspeed*: Normalized wind speed. The values are divided to 67 (max).

5.3.1. Data processing

The *"COMPoissonReg"* package is used to estimate the dispersion of the response variable. The estimated dispersion is $\hat{v} = 0.5716$, means that the response is over dispersed. To obtain ML estimator, we used OLS estimator as an initial value and considered $||\hat{\beta}_{est}^{(t)} - \hat{\beta}_{est}^{(t-1)}|| \leq 1 \times 10^{-6}$ as a convergence criterion. After the ML estimator is obtained, we examined the predictors for collinearity. The eigenvalues of the $X'\hat{V}_{ML}X$ matrix where the weight matrix $\hat{V}_{ML}$ is obtained at the final iteration of the ML estimation are $\hat{\psi}_1 = \hat{\psi}_{max} = 44.99537, \hat{\psi}_2 = 2.35618, \hat{\psi}_3 = 0.77508$, and $\hat{\psi}_4 = \hat{\psi}_{min} = 0.00972$. The condition number is calculated as $CN_{ML} = 68.03076$ which is sufficiently large and indicates that there is severe multicollinearity in the data set.

Poisson, Negative Binomial, and COM-Poisson count models are used to find the best-fitting distribution of the response. Log-likelihood, AIC, and BIC values are obtained by using *"MASS"* and *"COMPoissonReg"* packages. The detailed diagnostic analysis in Table 5.17 indicates that COM–Poisson distribution is the best-fitting distribution for response in terms of log-likelihood, AIC, and BIC as compared to Poisson and Negative Binomial distributions.

Table 5.17. Diagnostic analysis of best-fitted distribution for the response of the *BikeShare* data set.

	COM-Poisson	**Negative Binomial**	**Poisson**
Log-likelihood	-498.5213	-499.2390	-645.1237
AIC	1007.0452	1008.4812	1298.2474
BIC	1018.5440	1019.9790	1311.7490

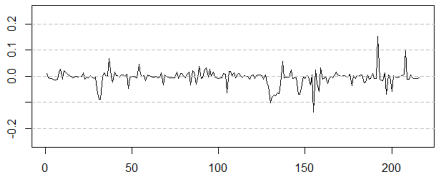
We set the OLS estimator as an initial value, $||\hat{\beta}_{est}^{(t)} - \hat{\beta}_{est}^{(t-1)}|| \leq 1 \times 10^{-6}$ as a convergence criterion, and obtained ridge and Liu estimators. Tuning parameters for ridge estimator are calculated following Eqs. (2.15.a) and (2.15.e), and obtained as $\hat{k}_1 = 18.5225$ and $\hat{k}_5 = 96.5339$. The condition for the Liu tuning parameter given after Eq. (2.17.) is obtained as 1.053782, which is lower than 2. So, we arbitrarily set $\hat{h}_\theta = 0.99$, as stated in Section 2.4. and obtained $\hat{\theta}_{opt} = 0.9991$. Additionally, $\theta = 0.5$, $\theta = 0.85$ are considered for case study.

Estimation results for the model are given in Table 5.18. The application of the Liu and ridge estimation method caused a change in the sign of *atemp* and *windspeed*. Also, Table 5.18 shows that different tuning parameters yield different Liu estimates.

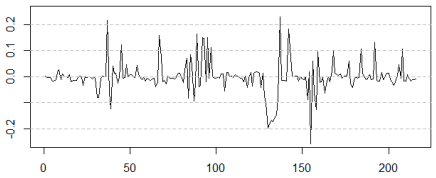
Table 5.18. ML, ridge, and Liu estimation results for COM-Poisson model of the *BikeShare* data set.

	temp	***atemp***	***hum***	***windspeed***
ML	0.535771	-0.06307	-0.08441	-0.11674
Ridge, $\hat{k}_1$	0.005900	0.005579	0.009192	0.005513
Ridge, $\hat{k}_5$	0.000205	0.000205	0.000495	0.000180
Liu, $\hat{\theta}_{opt}$	0.044716	0.035498	-0.00524	0.018801
Liu, $\theta = 0.5$	0.042238	0.035993	-0.00484	0.019482
Liu, $\theta = 0.85$	0.043976	0.035646	-0.00512	0.019004

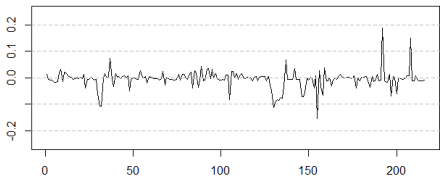
Based on the estimated parameters, we calculated deviance, ridge deviance, and Liu deviance residuals. Graphical presentation of the difference between deviance and ridge deviance, deviance and Liu deviance residuals are given in Fig. 5.12. Fig. 5.12 depicts how different tuning parameter values cause different peaks and different residual values in the observations.



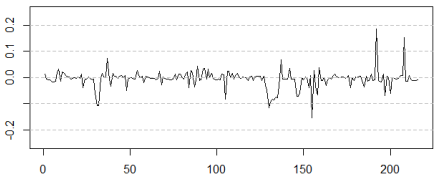
(a) Difference between deviance and ridge deviance residuals for $\hat{k}_1$.



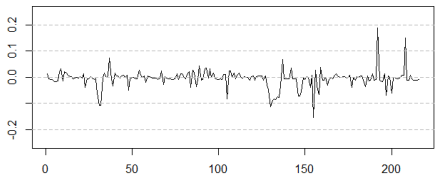
(b) Difference between deviance and ridge deviance residuals for $\hat{k}_5$.



(c) Difference between deviance and Liu deviance residuals for $\hat{\theta}_{opt}$.



(d) Difference between deviance and Liu deviance residuals for $\theta = 0.5$.



(e) Difference between deviance and Liu deviance residuals for $\theta = 0.85$.

Figure 5.12. Difference between residuals obtained from the *BikeShare* data set model.

5.3.2. Monitoring process

Due to the lack of preliminary information regarding the data set, the monitoring process is carried out by obtaining estimators and respective residuals first and then splitting the residuals, as well. We used the first 25% of residuals (historical set) to construct control limits and then measured the performance of control charts by using the other 75% of the residuals (control set).

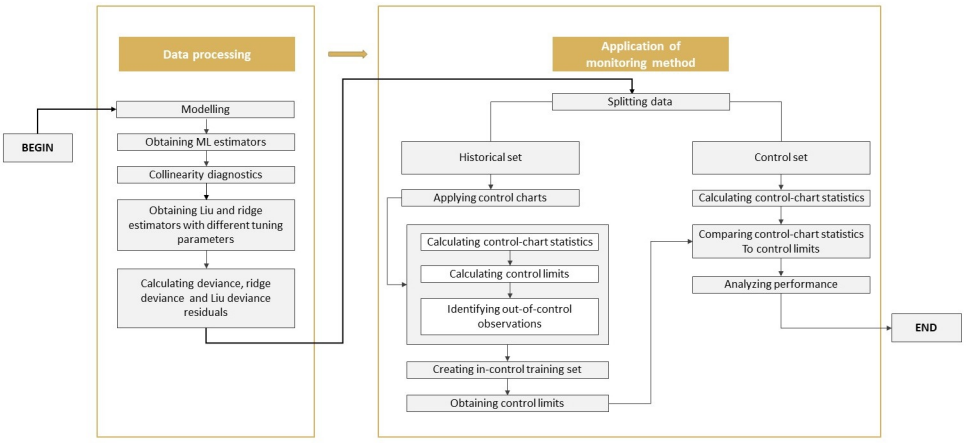


Figure 5.13. Analyzing *BikeShare* data set.

The data set is analyzed according to the flowchart given by Fig. 5.13.

To create in-control historical set, first, we calculated the ML, ridge, and Liu estimators of the training set and then obtained deviance, ridge deviance, and Liu deviance residuals. Later, we constructed Shewhart, CUSUM, and EWMA charts using these 54 residuals. Control chart constants are derived from in-built functions of the *"SPC"* package corresponding $ARL_0 \approx 370$. Control limits for each control chart are constructed using the estimated mean and standard deviation of the corresponding residuals. To obtain these control limits, we set $K = 0.5$ for the CUSUM chart and $\lambda = 0.2$ for the EWMA chart. Then, it is seen that regardless of the estimation method, the Shewhart chart identified 27, the CUSUM chart identified 8, and the EWMA chart identified 4 out-of-control observations, which can be seen in Figs. 5.14 - 5.16. Then, we eliminated 31 unique out-of-control observations detected by all control charts and constructed an in-control data set with remaining residuals.

After eliminating out-of-control observations, we estimated mean and standard deviations of remaining deviance, ridge deviance, and Liu deviance residuals and obtained control limits for Shewhart, CUSUM, and EWMA charts such that

$ARL_0 \approx 370$ by using in-built functions from the *"SPC"* package. Lower and upper control limits (LCL and UCL, respectively) for Shewhart and CUSUM charts, as well as control limits of EWMA chart at convergence, are given in Table 5.19.

Table 5.19. Control limits for residual-based Shewhart, CUSUM, and EWMA charts.

	Shewhart		**CUSUM**		**EWMA**	
	LCL	**UCL**	**LCL**	**UCL**	**LCL (conv.)**	**UCL (conv.)**
deviance	-0.0614	0.8371	-11.8674	11.8674	-1.3567	1.3594
ridge deviance, k_1	-0.0900	0.8439	-11.0673	11.0673	-1.3680	1.3711
ridge deviance , k_5	-0.0295	0.8465	-12.3094	12.3094	-1.3541	1.3911
Liu deviance, $\hat{\theta}_{opt}$	-0.1085	0.8413	-9.9378	9.9378	-1.3727	1.3606
Liu deviance, $\theta = 0.5$	-0.1086	0.8414	-9.9351	9.9351	-1.3728	1.3606
Liu deviance, $\theta = 0.85$	-0.1086	0.8413	-9.9370	9.9370	-1.3728	1.3606

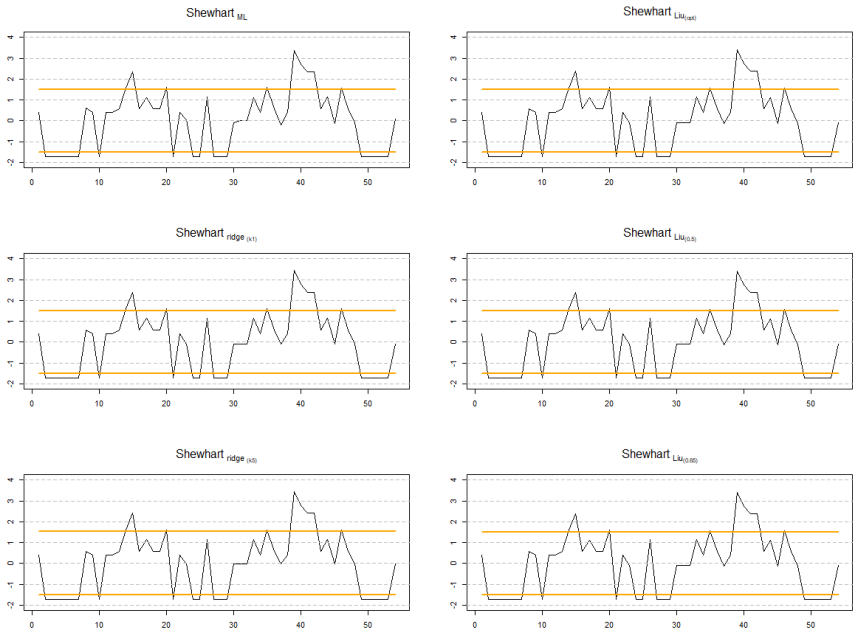


Figure 5.14. Monitoring historical set with Shewhart chart.

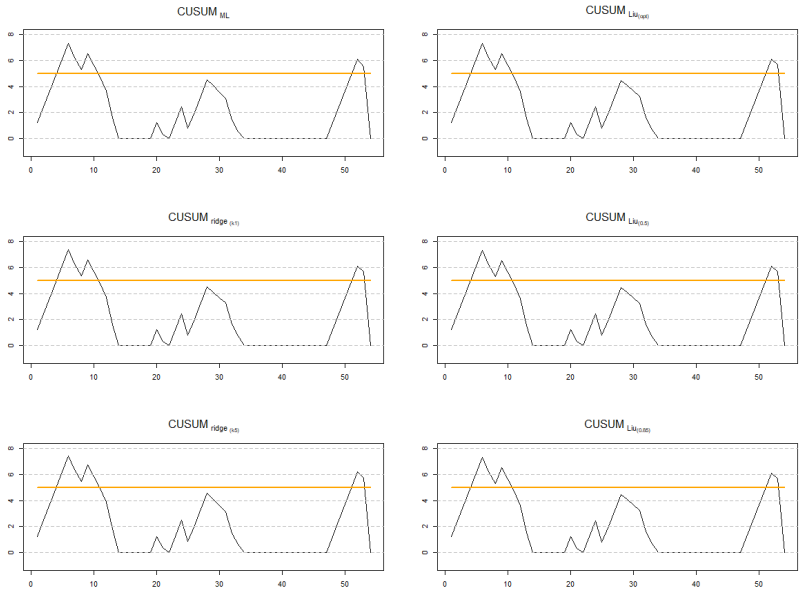


Figure 5.15. Monitoring historical set with CUSUM chart.

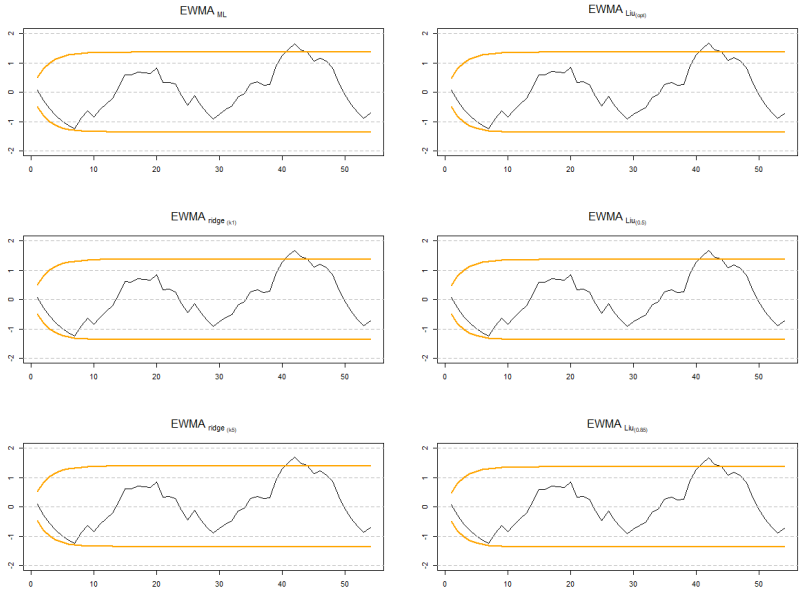


Figure 5.16. Monitoring historical set with EWMA chart.

After we obtained the control limits with an in-control historical set, we applied these control limits to the residuals in control set for comparing the control charts. For this aim, we utilized built-in functions from the *"SPC"* package to calculate ARL_1 of each control chart and performance analysis results are given in Table 5.20.

Table 5.20. Performance analysis of control charts with *BikeShare* data set, ARL_1.

Monitored observations	**Shewhart**	**CUSUM**	**EWMA**
deviance	43.3288	8.8639	16.5684
ridge deviance, k_1	42.1658	9.3312	16.1023
ridge deviance, k_5	41.8575	8.5384	16.1567
Liu deviance, $\hat{\theta}_{opt}$	41.1516	9.6808	15.6933
Liu deviance, $\theta = 0.5$	41.1479	9.6804	15.6919
Liu deviance, $\theta = 0.85$	41.1505	9.6807	15.6929

The results show that among the Shewhart charts, the Shewhart$_{Liu}$ chart is better than Shewhart$_{ML}$ and Shewhart$_{ridge}$ charts. Similarly, EWMA$_{Liu}$ is the best among the EWMA charts. CUSUM$_{ridge(k_5)}$ has the lowest ARL_1 value, it is followed by CUSUM$_{ML}$ and CUSUM$_{Liu}$ charts. The best performed control chart among respective Liu deviance-based control charts belong to the Liu deviance-based control charts with constant tuning parameter of $\theta = 0.5$.

6. CONCLUSIONS

The traditional way to monitor count data in statistical process control is the application of the methods designed for Poisson distribution. However, equidispersion property of the Poisson distribution is a limitation. Although real-life data sets are rarely ideal, the equality of the mean and variance of count data is not always a subject. The possibility of occurrence of the underdispersed or overdispersed state is high. If indications of under- or overdispersion are present in the data set, it is more appropriate to use the COM-Poisson distribution.

In this thesis, we aimed to reduce the negative impact of multicollinearity for count profile monitoring with all three states of dispersion by modifying traditional control charts based on the regression adjustment concept.

We proposed an iterative PCR, ridge, Liu, and *r-k* class estimators for the COM-Poisson model as an alternative to the ML estimator when the predictors are highly inter-correlated. Then, we defined the PCR, ridge, Liu, and *r-k* deviance residuals from the fitted COM-Poisson model with the corresponding estimation method. Later, we established modified Shewhart, CUSUM, and EWMA control charts based on the ridge, Liu, PCR, and *r-k* deviance residuals. Detailed simulation studies considering different combinations of sample size, correlation and dispersion levels, shift types in various shift sizes, and real-life data analysis were conducted to evaluate the performance of the proposed control charts. The performance of the proposed control charts are compared to the respective residual-based control charts in terms of ARL_1 and/or *SDRL*.

According to the results, proposed ridge deviance-based control charts show better performance than deviance-based control charts in case of a large sample size. When the sample size is small, ridge deviance-based control charts lose effi-

ciency over the deviance-based control charts when additive shift or multiplicative shift in the predictors except for intercept is present in the response. Besides, degrees of collinearity, which we considered, do not seriously affect the pattern of each control chart. Analysis of *LPP* data set supports the simulation results. Comparative performance analysis of Liu deviance-based control charts through a simulation study and *BikeShare* data set analysis revealed that the Liu deviance-based control chart's performance is affected by the Liu tuning parameter. Based on the simulation study, Liu's deviance-based control charts are generally well in detecting shifts than deviance-based control charts in terms of having smaller ARL_1 and *SDRL*. The impact caused by a large number of predictors is noticeable when the multiplicative shift occurs in all coefficients. In other cases, few predictors give better results. According to the *SDRL* results, increased dispersion value or the number of predictors results in high *SDRL* for all control charts, regardless of the shift type. Overall, it is noticed that among the Shewhart$_{Liu}$, CUSUM$_{Liu}$, and EWMA$_{Liu}$ control charts, the performance of EWMA$_{Liu}$ is better in having smaller ARL_1 values and CUSUM$_{Liu}$ is more sensitive to the minor variations when compared to the Shewhart$_{ML}$, CUSUM$_{ML}$, and EWMA$_{ML}$.

The *r-k* deviance-based charts primarily outperform the deviance, ridge deviance, and Liu deviance-based control charts, while deviance-based charts show the worst results in most combinations in the case of multicollinearity when principal component-based methods were applied. PCR deviance-based control charts are mostly the second-best control charts. Monitoring the COM-Poisson profile with the Shewhart chart shows that the Shewhart$_{r-k}$ has the best performance compared to other Shewhart charts in terms of ARL_1 and *SDRL* criteria when the number of predictors is large (larger than 2 in our study). Results of the simulation study considering small shifts revealed that the CUSUM charts show better results compared

to the EWMA chart. The performance of the EWMA charts is highly affected by the smoothing parameter value. Both CUSUM$_{r-k}$ and EWMA$_{r-k}$ control charts are more effective in detecting additive shifts than multiplicative shifts in most of the combinations considered in the simulations. Nevertheless, for fixed dispersion value and shift size, the changes in the result values are more plain and consistent in cases with high predictor numbers. The results are generally incompatible when the response is underdispersed. In summary, in the case of multicollinearity, CUSUM$_{r-k}$ and EWMA$_{r-k}$ control charts perform better than alternative CUSUM and EWMA control charts in determining small shifts in the process. Additionally, PCR deviance-based control charts were found to be the second-best option after *r-k* deviance-based control charts. Overall, the best performance indicator varies according to parameters, such as the number of predictors, dispersion level, and shift size. In general, results show that suggested methods based on size reduction lead to structural changes in the residuals.

In conclusion, various methods of COM-Poisson profile monitoring as an alternative to deviance-based control charts under multicollinearity are discussed throughout the thesis. Each of them are proved to be more effective in the case of multicollinearity. while for the best outcome depend on the tuning parameters for biased estimation and the cutoff point for principal component-based approaches.

REFERENCES

Abbas, T., Qian, Z., Ahmad, S., Riaz, M., 2017. Bayesian monitoring of linear profile monitoring using dewma charts. Quality and Reliability Engineering International, 33(8):1783–1812.

Abbasi, A., Özkale, M. R., 2021. The *r-k* class estimator in generalized linear models applicable with sim. and empirical study using a Poisson and gamma responses. Hacettepe Journal of Mathematics and Statistics, 50(2):594–611.

Abdella, G. M., Kim, J., Al-Khalifa, K. N., Hamouda, A. M., 2019. Penalized Conway-Maxwell-Poisson regression for modelling dispersed discrete data: The case study of motor vehicle crash frequency. Safety Science, 120:157–163.

Aguilera, A. M., Escabias, M., Valderrama, M. J., 2006. Using principal components for estimating logistic regression with high-dimensional multicollinear data. Computational Statistics and Data Analysis, 50(8):1905–1924.

Algamal, Z. Y., Asar, Y., 2020. Liu-type estimator for the gamma regression model. Communications in Statistics - Simulation and Computation, 49(8):2035–2048.

Alkhamisi, M. A., Shukur, G., 2007. A monte carlo study of recent ridge parameters. Communications in Statistics—Simulation and Computation, 36(3):535–547.

Amiri, A., Koosha, M., Azhdari, A., 2011. Profile monitoring for Poisson responses. In 2011 IEEE International Conference on Industrial Engineering and Engineering Management. IEEE, pp. 1481–1484.

Amiri, A., Koosha, M., Azhdari, A., Wang, G., 2015. Phase I monitoring of generalized linear model-based regression profiles. Journal of Statistical Computa-

tion and Simulation, 85(14):2839–2859.

Amiri, A., Zou, C., Doroudyan, M. H., 2014. Monitoring correlated profile and multivariate quality characteristics. Quality and Reliability Engineering International, 30(1):133–142.

Asgari, A., Amiri, A., Niaki, S. T. A., 2014. A new link function in GLM-based control charts to improve monitoring of two-stage processes with Poisson response. The International Journal of Advanced Manufacturing Technology, 72(9):1243–1256.

Baye, M. R., Parker, D. F., 1984. Combining ridge and principal component regression: a money demand illustration. Communications in Statistics-Theory and Methods, 13(2):197–205.

Belsley, D. A., Kuh, E., Welsch, R. E., 1980. Regression diagnostics: Identifying influential data and sources of collinearity. John Wiley and Sons.

Boatwright, P., Borle, S., Kadane, J. B., 2003. A model of the joint distribution of purchase quantity and timing. Journal of the American Statistical Association, 98(463):564–572.

Boatwright, P., Borle, S., Kadane, J. B., Minka, T. P., Shmueli, G., 2006. Conjugate analysis of the Conway-Maxwell-Poisson distribution. Bayesian analysis, 1(2):363–374.

Bozdogan, H., 1987. Icomp: A new model-selection criterion. In 1. Conference of the international federation of classification societies. pp. 599–608.

Cano, J., Moguerza, J. M., Psarakis, S., Yannacopoulos, A. N., 2015. Using statistical shape theory for the monitoring of nonlinear profiles. Applied stochastic models in business and industry, 31(2):160–177.

Cao, Q., Zanni-Merk, C., Samet, A., Beuvron, F. B., Reich, C., 2020. Using rule qual-

ity measures for rule base refinement in knowledge-based predictive maintenance systems. Cybernetics and Systems, 51(2):161–176.

Cheng, D. C., Iglarsh, H. J., 1976. Principal component estimators in regression analysis. The Review of Economics and Statistics:229–234.

Conway, R. W., Maxwell, W. L., 1962. A queuing model with state dependent service rates. Journal of Industrial Engineering, 12(2):132–136.

Croarkin, M., Varner, R. N., 1982. Measurement assurance for dimensional measurements on integrated-circuit photomasks. National Bureau of Standards: Technical Note 1164. U.S. Department of Commerce, Washington, DC.

Daoud, J. I., 2017. Multicollinearity and regression analysis. In Journal of Physics: Conference Series, volume 949. IOP Publishing, p. 012009.

Dawoud, I., Kaçıranlar, S., 2017. Evaluation of the predictive performance of the *r-k* and *r-d* class estimators. Communications in Statistics-Theory and Methods, 46(8):4031–4050.

Derakhshani, R., Esmaeeli, H., Amiri, A., 2020. Phase II monitoring of Poisson regression profiles in multi-stage processes. International Journal of Reliability, Quality and Safety Engineering, 27(04):2050 012.

Dobson, A. J., 2002. An introduction to generalized linear models. CRC press, London, 2nd edition.

Fan, S. S., Chang, Y., Aidara, N., 2013. Nonlinear profile monitoring of reflow process data based on the sum of sine functions. Quality and Reliability Engineering International, 29(5):743–758.

Fan, S. S., Jen, C., Lee, T., 2017. Modeling and monitoring the nonlinear profile of heat treatment process data by using an approach based on a hyperbolic tangent function. Quality Engineering, 29(2):226–243.

Fanaee-T, H., Gama, J., 2014. Event labeling combining ensemble detectors and background knowledge. *Prog. Artif. Intell.*, 2(2):113–127.

Farrar, D. E., Glauber, R. R., 1967. Multicollinearity in regression analysis: the problem revisited. The Review of Economic and Statistics:92–107.

Francis, R. A., Geedipally, S. R., Guikema, S. D., Dhavala, S. S., Lord, D., LaRocca, S., 2012. Characterizing the performance of the Conway-Maxwell-Poisson generalized linear model. Risk Analysis: An International Journal, 32(1):167–183.

Frisch, R., 1934. Statistical confluence analysis by means of complete regression systems, volume 5. Universitetets Økonomiske Instituut.

Guevara, R. D., Vargas, J. A., 2015. Process capability analysis for nonlinear profiles using depth functions. Quality and Reliability Engineering International, 31(3):465–487.

Guevara, R. D., Vargas, J. A., 2016. Evaluation of process capability in multivariate nonlinear profiles. Journal of Statistical Computation and Simulation, 86(12):2411–2428.

Guikema, S. D., Goffelt, J. P., 2008. A flexible count data regression model for risk analysis. Risk Analalysis: An International Journal, 28(1):213–223.

Gunst, R., Webster, J., 1975. Regression analysis and problems of multicollinearity. Communications in Statistics-Theory and Methods, 4(3):277–292.

Gupta, R. C., Sim, S. Z., Ong, S., 2014. Analysis of discrete data by Conway-Maxwell-Poisson distribution. AStA Advances in Statistical Analysis, 98(4):327–343.

Gupta, S., Montgomery, D., Woodall, W., 2006. Performance evaluation of two methods for online monitoring of linear calibration profiles. International journal of production research, 44(10):1927–1942.

Haitovsky, Y., 1969. Multicollinearity in regression analysis: Comment. The Review of economics and statistics:486–489.

Hawkins, D. M., 1991. Multivariate quality control based on regression-adjusted variables. Technometrics, 33(1):61–75.

Hawkins, D. M., 1993. Cumulative sum control charting: an underutilized SPC tool. Quality Engineering, 5(3):463–477.

Hoerl, A. E., Kannard, R. W., Baldwin, K. F., 1975. Ridge regression: some simulations. Communications in Statistics-Theory and Methods, 4(2):105–123.

Hoerl, A. E., Kennard, R. W., 1970. Ridge regression: Biased estimation for nonorthogonal problems. Technometrics, 12(1):55–67.

Houshmand, A. A., Javaheri, A., 1998. Multivariate ridge residual charts. Quality Engineering, 10(4):617–624.

Jamal, A., Mahmood, T., Riaz, M., Al-Ahmadi, H. M., 2021. GLM-based flexible monitoring methods: an application to real-time highway safety surveillance. Symmetry, 13(2):362.

Jearkpaporn, D., Montgomery, D. C., Runger, G. C., Borror, C. M., 2003. Process monitoring for correlated gamma-distributed data using generalized-linear-model-based control charts. Quality and Reliability Engineering International, 19(6):477–491.

Jiang, W., 2004. Multivariate control charts for monitoring autocorrelated processes. Journal of Quality Technology, 36(4):367–379.

Jolliffe, I. T., 2002. Principal components in regression analysis. Springer, New York, 2nd edition.

Jowaheer, V., Khan, N. M., 2009. Estimating regression effects in COM-Poisson generalized linear model. International Journal of Computational and Mathematical Sciences, 1(2):59–63.

Kang, L., Albin, S. L., 2000. On-line monitoring when the process yields a linear profile. Journal of quality Technology, 32(4):418–426.

Karaoglan, A. D., Bayhan, G. M., 2014. A regression control chart for autocorrelated processes. International Journal of Industrial and Systems Engineering, 16(2):238–256.

Kendall, M. G., 1957. A course in multivariate analysis: London. Charles Griffin and Co.

Kibria, B. G., 2003. Performance of some new ridge regression estimators. Communications in Statistics-Simulation and Computation, 32(2):419–435.

Kim, J. K., Han, Y. S., Lee, J. S., 2017. Particle swarm optimization–deep belief network–based rare class prediction model for highly class imbalance problem. Concurrency and Computation: Practice and Experience, 29(11):e4128.

Kim, K., Mahmoud, M. A., Woodall, W. H., 2003. On the monitoring of linear profiles. Journal of Quality Technology, 35(3):317–328.

Kinat, S., Amin, M., Mahmood, T., 2020. GLM-based control charts for the inverse gaussian distributed response variable. Quality and Reliability Engineering International, 36(2):765–783.

Kurtoğlu, F., Özkale, M. R., 2016. Liu estimation in generalized linear models: application on gamma distributed response variable. Statistical Papers, 57(4):911–928.

Kwon, J.-H., Kim, E.-J., 2020. Failure prediction model using iterative feature selection for industrial internet of things. Symmetry, 12(3):454.

Lawless, J., 1976. A simulation study of ridge and other regression estimators. Communications in Statistics-Theory and Methods, 5(4):307–323.

Le Cessie, S., Van Houwelingen, J. C., 1992. Ridge estimators in logistic regres-

sion. Journal of the Royal Statistical Society: Series C (Applied Statistics), 41(1):191–201.

Lee, A., Silvapulle, M., 1988. Ridge estimation in logistic regression. Communications in Statistics-Simulation and Computation, 17(4):1231–1257.

Lesaffre, E., Marx, B. D., 1993. Collinearity in generalized linear regression. Communications in Statistics-Theory and Methods, 22(7):1933–1952.

Li, B., Zhang, H., He, J., 2020. Some characterizations and properties of COM-Poisson random variables. Communications in Statistics-Theory and Methods, 49(6):1311–1329.

Liu, K., 1993. A new class of biased estimate in linear regression. Communications in Statistics - Theory and Methods, 22(2):393–402.

Lord, D., Guikema, S. D., Geedipally, S. R., 2008. Application of the Conway–Maxwell–Poisson generalized linear model for analyzing motor vehicle crashes. Accident Analysis and Prevention, 40(3):1123–1134.

Loredo, E. N., Jearkpaporn, D., Borror, C. M., 2002. Model-based control chart for autoregressive and correlated data. Quality and reliability engineering international, 18(6):489–496.

Lucas, J. M., Saccucci, M. S., 1990. Exponentially weighted moving average control schemes: properties and enhancements. Technometrics, 32(1):1–12.

Mackinnon, M. J., Puterman, M. L., 1989. Collinearity in generalized linear models. Communications in statistics-Theory and methods, 18(9):3463–3472.

Mahmood, T., Iqbal, A., Abbasi, S. A., Amin, M., 2022. Efficient GLM-based control charts for Poisson processes. Quality and Reliability Engineering International, 38(1):389–404.

Mahmoud, M. A., Woodall, W. H., 2004. Phase I analysis of linear profiles with calibration applications. Technometrics, 46(4):380–391.

Maleki, M. R., Amiri, A., Castagliola, P., 2018. An overview on recent profile monitoring papers (2008–2018) based on conceptual classification scheme. Computers and Industrial Engineering, 126:705–728.

Mammadova, U., Özkale, M. R., 2021a. Comparison of deviance and ridge deviance residual-based control charts for monitoring Poisson profiles. Communications in Statistics-Simulation and Computation:1–24.

Mammadova, U., Özkale, M. R., 2021b. Profile monitoring for count data using Poisson and Conway-Maxwell-Poisson regression-based control charts under multicollinearity problem. Journal of Computational and Applied Mathematics, 388:113 275.

Mammadova, U., Özkale, M. R., 2022. Conway-Maxwell-Poisson regression-based control charts under iterative Liu estimator for monitoring count data. Applied Stochastic Models in Business and Industry. DOI:10.1002/asmb.2682.

Mandel, B., 1969. The regression control chart. Journal of Quality Technology, 1(1):1–9.

Mansfield, E. R., Helms, B. P., 1982. Detecting multicollinearity. The American Statistician, 36(3a):158–160.

Månsson, K., 2013. Developing a Liu estimator for the negative binomial regression model: method and application. Journal of Statistical Computation and Simulation, 83(9):1773–1780.

Månsson, K., Kibria, B. G., Shukur, G., 2012. On Liu estimators for the logit regression model. Economic Modelling, 29(4):1483–1488.

Mansson, K., Kibria, B. G., Sjolander, P., Shukur, G., 2012. Improved Liu estimators for the Poisson regression model. International Journal of Statistics and Probability, 1(1):2.

Månsson, K., Shukur, G., 2011. A Poisson ridge regression estimator. Economic

Modelling, 28(4):1475–1481.

Marcondes Filho, D., Sant'Anna, A. M. O., 2016. Principal component regression-based control charts for monitoring count data. International Journal of Advanced Manufacturing Technology, 85(5):1565–1574.

Marquardt, D. W., 1970. Generalized inverses, ridge regression, biased linear estimation, and nonlinear estimation. Technometrics, 12(3):591–612.

Marx, B. D., 1992. A continuum of principal component generalized linear regressions. Computational statistics and data analysis, 13(4):385–393.

Marx, B. D., Smith, E. P., 1990. Principal component estimation for generalized linear regression. Biometrika, 77(1):23–31.

Massy, W. F., 1965. Principal components regression in exploratory statistical research. Journal of the American Statistical Association, 60(309):234–256.

McCullagh, P., Nelder, J. A., 1989. Generalized linear models. Routledge, 2nd edition.

McDonald, G. C., Galarneau, D. I., 1975. A monte carlo evaluation of some ridge-type estimators. Journal of the American Statistical Association, 70(350):407–416.

Mestek, O., Pavlík, J., Suchánek, M., 1994. Multivariate control charts: control charts for calibration curves. Fresenius' journal of analytical chemistry, 350(6):344–351.

Mihalovits, M., Kemény, S., 2020. Regression control chart with unknown parameters for detection of out-of-trend results in pharmaceutical on-going stability studies. Journal of Pharmaceutical and Biomedical Analysis, 188:113 375.

Minka, T. P., Shmueli, G., Kadane, J. B., Borle, S., Boatwright, P., 2003. Computing with the COM-Poisson distribution. PA: Department of Statistics, Carnegie Mellon University.

Moldovan, D., Chifu, V., Pop, C., Cioara, T., Anghel, I., Salomie, I., 2018. Chicken swarm optimization and deep learning for manufacturing processes. In 2018 17th RoEduNet conference: networking in education and research (RoEduNet). IEEE, pp. 1–6.

Moldovan, D., Cioara, T., Anghel, I., Salomie, I., 2017. Machine learning for sensor-based manufacturing processes. In 2017 13th IEEE international conference on intelligent computer communication and processing (ICCP). IEEE, pp. 147–154.

Montgomery, D. C., 2020. Introduction to Statistical Quality Control. John Wiley and Sons, New Jersey, 6th edition.

Nadarajah, S., 2009. Useful moment and CDF formulations for the COM-Poisson distribution. Statistical Papers, 50(3):617–622.

Nelder, J. A., Wedderburn, R. W., 1972. Generalized linear models. J. Royal Stat. Soc.: Series A (General), 135(3):370–384.

Özkale, M. R., 2013. Influence measures in affine combination type regression. Journal of Applied Statistics, 40(10):2219–2243.

Özkale, M. R., 2016. Iterative algorithms of biased estimation methods in binary logistic regression. Statistical Papers, 57(4):991–1016.

Özkale, M. R., 2021. The red indicator and corrected VIFs in generalized linear models. Communications in Statistics-Simulation and Computation, 50(12):4144–4170.

Özkale, M. R., Arıcan, E., 2016. A new biased estimator in logistic regression model. Statistics, 50(2):233–253.

Özkale, M. R., Kaçıranlar, S., 2008. Comparisons of the *r-k* class estimator to the ordinary least squares estimator under the Pitman's closeness criterion. Statistical Papers, 49(3):503–512.

Özkale, M. R., Lemeshow, S., Sturdivant, R., 2018. Logistic regression diagnostics in ridge regression. Computational Statistics, 33(2):563–593.

Page, E. S., 1954. Continuous inspection schemes. Biometrika, 41(1/22):100–115.

Park, K., Jung, D., Kim, J.-M., 2020. Control charts based on randomized quantile residuals. Applied Stochastic Models In Business and Industry Abbreviation, 36(4):716–729.

Park, K., Kim, J.-M., Jung, D., 2018. GLM-based stat. control *r*-charts for dispersed count data with multicollinearity between input variables. Qual. Reliab. Eng. Int., 34(6):1103–1109.

Park, T., Davis, C. S., Li, N., 1998. Alternative GEE estimation procedures for discrete longitudinal data. Computational statistics and data analysis, 28(3):243–256.

Paul, R. K., 2006. Multicollinearity: Causes, effects, and remedies. IASRI, New Delhi, 1(1):58–65.

Pierce, D. A., Schafer, D. W., 1986. Residuals in generalized linear models. Journal of the American Statistical Association, 81(396):977–986.

Qasim, M., Amin, M., Amanullah, M., 2018. On the performance of some new Liu parameters for the gamma regression model. Journal of Statistical Computation and Simulation, 88(16):3065–3080.

Qasim, M., Amin, M., Omer, T., 2020a. Performance of some new Liu parameters for the linear regression model. Communications in Statistics-Theory and Methods, 49(17):4178–4196.

Qasim, M., Kibria, B., Månsson, K., Sjölander, P., 2020b. A new Poisson Liu regression estimator: Method and application. Journal of Applied Statistics, 47(12):2258–2271.

Qi, D., Wang, Z., Zi, X., Li, Z., 2016. Phase II monitoring of generalized linear

profiles using weighted likelihood ratio charts. Computers and Industrial Engineering, 94:178–187.

Rao, G. S., Aslam, M., Rasheed, U., Jun, C.-H., 2020. Mixed EWMA-CUSUM chart for COM-Poisson distribution. Journal of Statistics and Management Systems, 23(3):511–527.

Rashid, N., Mokhtar, S., Sabariah, W., Esah, W., 2013. Regression residual control chart for monitoring academic performance of students in higher learning institution. In International Conference on Computing, Mathematics and Statistics: Revolutionizing Solutions Through Expanding Minds.

Riley, J. D., 1955. Solving systems of linear equations with a positive definite, symmetric, but possibly ill-conditioned matrix. Mathematical tables and other aids to computation:96–101.

Roberts, S., 1959. Control chart tests based on geometric moving averages. Technometrics, 42(1):97–101.

Runger, G. C., Wlllemain, T. R., Prabhu, S., 1995. Average run lengths for CUSUM control charts applied to residuals. Communications in Statistics-Theory and Methods, 24(1):273–282.

Saghaei, A., Mehrjoo, M., et al., 2010. Monitoring simple linear profiles using cumulative sum control charts. Amirkabir Journal of Mechanical Engineering, 41(2):73–82.

Sami, F., Amin, M., Butt, M. M., 2022. On the ridge estimation of the Conway-Maxwell-Poisson regression model with multicollinearity: Methods and applications. Concurrency and Computation: Practice and Experience, 34(1):e6477.

Schaefer, R., Roi, L., Wolfe, R., 1984. A ridge logistic estimator. Communications in Statistics-Theory and Methods, 13(1):99–113.

Schroeder, M. A., Lander, J., Levine-Silverman, S., 1990. Diagnosing and dealing with multicollinearity. Western journal of nursing research, 12(2):175–187.

Segerstedt, B., 1992. On ordinary ridge regression in generalized linear models. Communications in Statistics-Theory and Methods, 21(8):2227–2246.

Sellers, K. F., 2012. A generalized statistical control chart for over- or under-dispersed data. Quality and Reliability Engineering International, 28(1):59–65.

Sellers, K. F., Morris, D. S., Balakrishnan, N., 2016. Bivariate Conway-Maxwell-Poisson distribution: formulation, properties, and inference. Journal of Multivariate Analysis, 150:152–168.

Sellers, K. F., Shmueli, G., 2010. A flexible regression model for count data. The Annals of Applied Statistics:943–961.

Shang, Y., Tsung, F., Zou, C., 2011. Profile monitoring with binary data and random predictors. Journal of Quality Technology, 43(3):196–208.

Shewhart, W. A., 1926. Quality control charts. The Bell System Technical Journal, 5(4):593–603.

Shewhart, W. A., 1931. Economic control of quality of manufactured product. Macmillan and Co Ltd, London.

Shmueli, G., Minka, T. P., Kadane, J. B., Borle, S., Boatwright, P., 2005. A useful distribution for fitting discrete data: revival of the Conway-Maxwell-Poisson distribution. Journal of the Royal Statistical Society: Series C (Applied Statistics), 54(1):127–142.

Shu, L., Tsung, F., Tsui, K.-L., 2004. Run-length performance of regression control charts with estimated parameters. Journal of Quality Technology, 36(3):280–292.

Şiray, G. Ü., Sakallıoğlu, S., 2012. Superiority of the *r-k* class estimator over some es-

timators in a linear model. Communications in Statistics-Theory and Methods, 41(15):2819–2832.

Skinner, K. R., Montgomery, D. C., Runger, G. C., 2003. Process monitoring for multiple count data using generalized linear model-based control charts. International Journal of Production Research, 41(6):1167–1180.

Smith, E. P., Marx, B. D., 1990. Ill-conditioned information matrices, generalized linear models and estimation of the effects of acid rain. Environmetrics, 1(1):57–71.

Soleymanian, M. E., Khedmati, M., Mahlooji, H., 2013. Phase II monitoring of binary response profiles. Scientia Iranica, 20(6):2238–2246.

Steiner, S., Jensen, W. A., Grimshaw, S. D., Espen, B., 2016. Nonlinear profile monitoring for oven-temperature data. Journal of Quality Technology, 48(1):84–97.

Stover, F. S., Brill, R. V., 1998. Statistical quality control applied to ion chromatography calibrations. Journal of Chromatography A, 804(1-2):37–43.

Takahashi, Y., Asahara, M., Shudo, K., 2019. A framework for model search across multiple machine learning implementations. In 2019 15th International Conference on eScience (eScience). IEEE, pp. 331–338.

Tripp, R., 1983. Nonstochastic ridge regression and effective rank of the regressors matrix. Ph.D. thesis, Virginia Polytechnic Institute and State University, Blacksburg, VA.

Urgan, N. N., Tez, M., 2008. Liu estimator in logistic regression when the data are collinear. In 20th euro mini conference. pp. 323–327.

Wade, M. R., Woodall, W. H., 1993. A review and analysis of cause-selecting control charts. Journal of quality technology, 25(3):161–169.

Weissfeld, L. A., Sereika, S. M., 1991. A multicollinearity diagnostic for gener-

alized linear models. Communications in Statistics-Theory and Methods, 20(4):1183–1198.

Wichern, D. W., Churchill, G. A., 1978. A comparison of ridge estimators. Technometrics, 20(3):301–311.

Wood, S. N., 2017. Generalized additive models: an introduction with R. Chapman and Hall/CRC press, Florida.

Yeh, A. B., Huwang, L., Li, Y.-M., 2009. Profile monitoring for a binary response. IIE Transactions, 41(11):931–941.

Zaldivar, C., 2018. On the performance of some Poisson ridge regression estimators.

Zeng, L., Zhou, S., 2007. Variability monitoring of multistage manufacturing processes using regression adjustment methods. IIE Transactions, 40(2):109–121.

Zhang, G., 1984. A new type of control charts and a theory of diagnosis with control charts. In World Quality Congress Transactions, volume 3. American Society for Quality Control Milwaukee, WI, pp. 175–185.

Zhang, J., Li, Z., Wang, Z., 2009. Control chart based on likelihood ratio for monitoring linear profiles. Computational statistics and data analysis, 53(4):1440–1448.

APPENDICES

A. Performance of PCR and *r-k* deviance-based control charts

Table A.1. Performance analysis results of the PCR and *r-k* deviance-based Shewhart chart in case of additive shift, $\rho^2 = 0.95$.

p	v	δ	*ARL*				*SDRL*			
			Shewhart$_{ML}$	**Shewhart**$_{ridge}$	**Shewhart**$_{PCR}$	**Shewhart**$_{r-k}$	**Shewhart**$_{ML}$	**Shewhart**$_{ridge}$	**Shewhart**$_{PCR}$	**Shewhart**$_{r-k}$
2	0.75	0.5	45.8740	38.4080	41.5060	38.4080	42.8687	36.8877	39.6328	36.8877
2	0.75	1.5	5.4080	5.0860	5.2660	5.0860	4.7317	4.3403	4.6118	4.3403
2	0.75	2.5	2.0140	1.9720	2.0000	1.8860	1.5255	1.4426	1.4849	1.4425
2	1	0.5	51.4700	47.3060	49.7680	47.3060	46.0780	43.3853	45.6973	43.3853
2	1	1.5	8.9900	8.5460	8.7620	8.5460	8.6538	8.1557	8.4337	8.1557
2	1	2.5	3.5180	3.4360	3.4620	3.4360	3.2772	3.1576	3.1744	3.1576
2	1.5	0.5	65.1260	64.9600	65.7180	64.9600	55.0902	55.0902	55.7826	55.0902
2	1.5	1.5	16.3420	16.0940	16.2720	16.0940	16.3982	15.3612	16.3123	15.3612
2	1.5	2.5	7.2860	7.1840	7.2290	7.1565	2.4087	2.2992	2.3573	2.2992
4	0.75	0.5	50.8960	35.0000	41.2320	33.8740	42.9340	29.1287	36.8110	28.0896
4	0.75	1.5	6.5460	5.0400	5.0440	5.0380	6.3203	4.9198	4.9222	4.9188
4	0.75	2.5	2.1700	1.8920	1.9000	1.8920	1.7004	1.4288	1.4307	1.4288
4	1	0.5	56.6900	42.0460	55.6320	41.4260	48.9483	33.6932	50.7485	33.0688
4	1	1.5	10.1400	8.3080	8.6560	8.2940	10.2106	8.1203	8.7843	8.0957
4	1	2.5	3.7600	3.3840	3.3900	3.3840	3.4300	3.2173	3.2181	3.2173
4	1.5	0.5	58.3040	57.0000	58.4200	56.9080	48.8180	47.6816	49.0468	46.3682
4	1.5	1.5	16.7960	16.7340	16.9700	16.7335	15.7877	15.7040	16.0431	15.7536
4	1.5	2.5	7.6820	7.1880	7.2360	7.1360	2.5652	2.3230	2.3244	2.3230
7	0.75	0.5	35.8260	39.0980	35.8140	29.4920	26.6985	27.4989	26.7981	23.5757
7	0.75	1.5	7.0880	7.9400	7.0580	5.6480	5.7933	6.4446	5.4705	4.6058
7	0.75	2.5	2.6314	2.7140	2.6140	2.2740	1.9728	2.0926	1.8518	1.4619
7	1	0.5	61.5900	68.1240	62.1060	37.8340	47.0798	49.6226	47.2931	32.1020
7	1	1.5	13.2240	15.9620	13.3160	8.7960	11.8670	13.9094	11.7846	7.8648
7	1	2.5	4.9600	5.7060	4.8280	3.6400	3.8582	4.8807	3.7427	3.0306
7	1.5	0.5	88.9040	134.0020	84.3560	46.2260	64.6428	67.4243	62.8199	38.4021
7	1.5	1.5	23.5180	55.2280	21.5500	15.3680	20.8085	48.4964	20.3242	14.0324
7	1.5	2.5	9.9300	20.9460	8.9440	7.3100	9.2461	18.9397	8.9279	6.3137

Table A.2. Performance analysis results of the PCR and *r-k* deviance-based Shewhart chart in case of additive shift, $\rho^2 = 0.99$.

p	v	δ	ARL_1				$SDRL$			
			Shewhart$_{ML}$	**Shewhart**$_{ridge}$	**Shewhart**$_{PCR}$	**Shewhart**$_{r-k}$	**Shewhart**$_{ML}$	**Shewhart**$_{ridge}$	**Shewhart**$_{PCR}$	**Shewhart**$_{r-k}$
2	0.75	0.5	45.4020	37.8940	43.6680	37.8680	42.7222	36.5065	41.7331	36.4450
2	0.75	1.5	5.4740	5.1640	5.3760	5.1320	4.7813	4.4622	4.6712	4.3577
2	0.75	2.5	2.0420	2.0040	2.0080	2.0040	1.5403	1.4409	1.5401	1.4409
2	1	0.5	50.6760	47.4240	50.3060	47.4240	44.9109	43.1731	45.6174	43.1731
2	1	1.5	8.9540	8.5720	8.9380	8.5720	8.5341	7.9913	8.4714	7.9913
2	1	2.5	3.5160	3.4440	3.4840	3.4440	3.2495	3.1398	3.1695	3.1398
2	1.5	0.5	65.8150	65.0180	66.1320	65.0180	54.7236	54.7136	55.2503	54.7136
2	1.5	1.5	16.4360	16.1880	16.4740	16.1880	16.3635	15.3256	16.5217	15.3256
2	1.5	2.5	7.4260	7.3080	7.4120	7.3080	8.1817	7.6628	7.9223	7.6628
4	0.75	0.5	50.9280	36.7480	41.4900	33.8040	42.5299	30.2363	36.3629	27.2879
4	0.75	1.5	6.6980	5.0440	5.0740	5.0380	6.6094	4.9271	4.9739	4.9237
4	0.75	2.5	2.1780	1.9014	1.9020	1.9000	1.7113	1.4343	1.4344	1.4342
4	1	0.5	56.8400	42.9520	56.3920	41.3720	48.6105	34.2522	50.7000	32.6809
4	1	1.5	10.0700	8.3680	8.8400	8.3200	10.1359	8.1601	9.0949	8.1057
4	1	2.5	3.7580	3.4000	3.4060	3.3980	3.4395	3.2078	3.2167	3.2052
4	1.5	0.5	57.9200	57.4580	58.8380	57.4580	48.6304	48.0465	49.2271	48.0465
4	1.5	1.5	16.6780	16.6760	16.9160	16.6760	15.6081	15.6083	15.9586	15.6083
4	1.5	2.5	7.8230	7.2380	7.2620	7.2380	6.7864	6.7862	6.7862	6.7862
7	0.75	0.5	35.9580	38.6180	36.1340	30.0200	26.0350	26.9387	26.1588	23.5314
7	0.75	1.5	7.1160	7.8840	7.0880	5.6240	5.8024	6.4405	5.5616	4.6122
7	0.75	2.5	2.6320	2.7020	2.6060	2.2720	1.8537	2.0794	1.8458	1.4602
7	1	0.5	60.7480	45.1800	60.3220	40.9320	45.9921	36.9346	45.9592	34.6383
7	1	1.5	13.3560	9.6980	13.5460	9.1320	11.8757	8.7602	12.0563	8.2562
7	1	2.5	4.7560	3.7560	4.7220	3.6620	3.9203	3.1788	3.8771	3.0400
7	1.5	0.5	90.2820	45.6080	86.7200	45.6080	65.3262	37.5067	64.0443	37.5067
7	1.5	1.5	24.1120	15.1720	22.2120	15.1720	21.2467	13.8179	20.6526	13.8179
7	1.5	2.5	10.3520	7.3220	9.2500	7.3220	10.1301	6.3289	9.2803	6.3289

Table A.3. Performance analysis results of the PCR and *r-k* deviance-based Shewhart chart in case of multiplicative shift, $\rho^2 = 0.95$.

p	v	δ	ARL_1				$SDRL$			
			Shewhart$_{ML}$	**Shewhart**$_{ridge}$	**Shewhart**$_{PCR}$	**Shewhart**$_{r-k}$	**Shewhart**$_{ML}$	**Shewhart**$_{ridge}$	**Shewhart**$_{PCR}$	**Shewhart**$_{r-k}$
2	0.75	0.5	159.804	141.792	152.648	141.792	92.4863	92.23341	92.48538	92.23341
2	0.75	1.5	142.318	97.65	134.398	97.952	89.81238	79.59636	89.88271	79.60589
2	0.75	2.5	91.208	72.592	88.742	73.546	75.48793	67.12939	74.30047	67.74945
2	1	0.5	151.612	141.518	149.464	141.518	92.44904	91.76974	91.89246	91.76974
2	1	1.5	145.958	104.026	140.238	104.112	92.4552	83.28474	91.71512	83.23416
2	1	2.5	123.342	78.362	120.85	83.178	87.17513	70.04979	86.85884	73.55539
2	1.5	0.5	146.756	146.616	148.028	146.616	92.35978	92.3567	92.41084	92.3567
2	1.5	1.5	124.82	122.638	133.508	122.638	89.22325	88.86892	90.42571	88.86892
2	1.5	2.5	102.428	93.072	99.048	93.072	83.05763	79.05216	81.0549	79.05216
4	0.75	0.5	131.066	110.46	120.354	93.478	77.70545	73.10311	76.21553	64.56498
4	0.75	1.5	52.018	51.166	51.166	49.188	28.75403	27.80598	27.80598	27.8275
4	0.75	2.5	24.372	24.15	23.5	20.324	20.84113	20.5113	19.72877	17.49375
4	1	0.5	150.35	123.532	152.632	110.508	85.49047	80.78403	86.32784	75.47574
4	1	1.5	69.316	68.818	69.656	64.506	39.97534	38.74401	39.2269	36.9025
4	1	2.5	39.75	39.69	39.75	39.626	26.40663	26.32621	26.40663	26.27846
4	1.5	0.5	135.05	124.186	141.432	132.809	84.91542	80.9152	86.63186	83.77353
4	1.5	1.5	98.908	83.614	104.082	93.848	68.1468	59.37907	71.30314	65.34111
4	1.5	2.5	64.73	60.354	62.202	61.068	36.03665	34.58075	35.26884	34.7148
7	0.75	0.5	12.438	11.858	11.742	11.592	13.64481	12.62973	12.54402	12.343
7	0.75	1.5	6.208	6.428	6.046	6.014	2.26855	1.57605	1.95805	1.96284
7	0.75	2.5	4.3478	2.1106	2.0607	1.8184	3.803733	3.111233	3.053258	2.698666
7	1	0.5	44.772	45.474	44.33	39.784	64.2356	65.17903	63.81263	57.69398
7	1	1.5	6.834	6.81	6.818	6.7	1.94525	1.86733	1.98377	1.80139
7	1	2.5	7.4864	5.2492	5.1439	4.1016	4.789736	4.780321	4.732949	4.218354
7	1.5	0.5	136.322	149.776	133.484	49.836	99.76339	99.70919	99.85338	59.89066
7	1.5	1.5	11.31	11.368	11.282	10.818	12.85279	12.83497	12.85677	10.38121
7	1.5	2.5	11.6637	9.4265	8.1809	3.7132	4.755145	4.438007	4.750945	3.770563

Table A.4. Performance analysis results of the PCR and *r-k* deviance-based Shewhart chart in case of multiplicative shift, $\rho^2 = 0.99$.

p	v	δ	ARL_1				$SDRL$			
			Shewhart$_{ML}$	**Shewhart**$_{ridge}$	**Shewhart**$_{PCR}$	**Shewhart**$_{r-k}$	**Shewhart**$_{ML}$	**Shewhart**$_{ridge}$	**Shewhart**$_{PCR}$	**Shewhart**$_{r-k}$
2	0.75	0.5	158.3160	142.3220	158.5520	141.8880	92.5470	92.0166	92.4081	92.0110
2	0.75	1.5	141.8000	110.7880	141.4360	100.3600	90.5304	84.9833	90.1975	80.4963
2	0.75	2.5	91.8380	84.8260	91.6120	74.0540	75.9217	72.7421	75.9166	66.6009
2	1	0.5	148.1660	140.3340	150.4300	140.3340	92.5245	92.0079	92.5702	92.0079
2	1	1.5	139.8860	104.7340	142.8280	105.7540	91.9227	82.0323	91.7209	82.4648
2	1	2.5	122.4440	79.4140	119.9800	89.7340	86.6644	70.7213	78.6929	77.4227
2	1.5	0.5	146.8920	146.7480	149.0080	146.7480	92.4198	92.4153	92.5002	92.4153
2	1.5	1.5	123.4700	121.6440	136.5260	121.6440	88.6880	88.1173	90.9325	88.1173
2	1.5	2.5	101.8880	92.6340	100.8960	92.6340	82.7956	78.3389	80.5672	78.3389
4	0.75	0.5	127.4200	112.7500	116.8120	92.2840	76.4086	72.8774	74.9162	63.3917
4	0.75	1.5	51.7220	50.9900	50.7820	49.0080	27.9442	27.3804	27.4216	27.3314
4	0.75	2.5	26.8580	26.7900	26.4640	22.0940	21.5773	21.4865	21.0878	18.1921
4	1	0.5	147.6920	128.9220	152.7160	104.8440	83.4721	81.8596	83.9296	70.1299
4	1	1.5	66.1420	66.1180	66.3140	60.2360	35.6497	34.6122	34.7068	33.5164
4	1	2.5	41.6072	40.3700	40.4300	40.1060	25.6757	25.6379	25.6734	25.5536
4	1.5	0.5	130.8180	121.0860	138.3660	121.0860	83.7891	79.6903	86.2959	79.6903
4	1.5	1.5	94.5680	77.4580	102.1420	69.2920	64.9866	55.0504	69.2960	47.0485
4	1.5	2.5	59.1972	57.9600	58.3280	52.9440	33.2461	32.5704	33.2383	31.9832
7	0.75	0.5	10.8480	10.5820	10.2840	10.2300	9.0244	8.4791	7.8742	7.8926
7	0.75	1.5	6.3080	6.4680	6.1160	6.0840	2.2178	1.5253	1.9000	1.9061
7	0.75	2.5	4.9646	3.7274	3.6668	3.2232	6.6164	5.9239	5.8384	5.1138
7	1	0.5	39.2620	36.1360	38.7980	35.7020	60.9526	56.7647	60.3322	55.9664
7	1	1.5	6.8520	6.7320	6.8520	6.7000	1.8885	1.7359	1.8885	1.6910
7	1	2.5	4.9129	4.3737	4.8854	4.1487	4.7139	4.4580	4.7039	4.3317
7	1.5	0.5	131.6680	42.7620	127.5440	46.6040	99.7575	55.1865	99.0847	56.5957
7	1.5	1.5	10.0400	9.3480	10.0120	9.9140	7.5491	5.3609	7.5511	7.4687
7	1.5	2.5	8.2715	3.5324	8.1386	3.5308	4.7648	3.7001	4.7639	3.6959

Table A.5. Stage 1 analysis results for residual-based CUSUM and EWMA charts with respective ARL_0 values, in-control mean and in-control standard deviations.

Estimation method	p	v	CUSUM, $K=0.5$				EWMA, $\lambda=0.05$				EWMA, $\lambda=0.1$				EWMA, $\lambda=0.2$			
			h	$\hat{\mu}^0$	$\hat{\sigma}^0$	ARL_0	L	$\hat{\mu}^0$	$\hat{\sigma}^0$	ARL_0	L	$\hat{\mu}^0$	$\hat{\sigma}^0$	ARL_0	L	$\hat{\mu}^0$	$\hat{\sigma}^0$	ARL_0
	4	0.75	4.19	-0.25509	1.03614	376.35	3.44	-0.25522	1.05672	370.50	2.93	-0.26525	1.03623	375.30	2.79	-0.25848	1.03822	361.26
	4	1	4.49	-0.20624	1.05327	382.32	3.51	-0.20728	1.03610	371.51	2.82	-0.20812	1.05520	380.42	2.79	-0.21170	1.05509	380.47
	4	1.5	5.17	-0.18636	1.03368	369.47	3.12	-0.18244	1.06432	366.40	2.85	-0.18644	1.03377	382.99	3.01	-0.18302	1.03309	375.04
	7	0.75	4.23	-0.24113	1.05901	379.59	3.41	-0.23768	1.07826	377.52	2.90	-0.23615	1.05854	375.31	2.77	-0.24172	1.05966	358.72
ML	7	1	4.58	-0.18902	1.07166	375.15	3.42	-0.19500	1.04766	365.31	2.82	-0.19636	1.07197	372.84	2.78	-0.19870	1.06963	358.06
	7	1.5	5.12	-0.17212	1.04774	360.59	3.11	-0.16830	1.11484	373.79	2.81	-0.17708	1.04438	372.37	2.99	-0.17212	1.04774	366.76
	10	0.75	4.37	-0.20930	1.09476	382.65	3.40	-0.20851	1.11097	360.12	2.88	-0.21313	1.09792	369.78	2.73	-0.21106	1.09329	366.01
	10	1	4.76	-0.17234	1.09814	379.64	3.32	-0.17026	1.07622	355.53	2.81	-0.17110	1.09606	379.80	2.73	-0.17110	1.09606	371.09
	10	1.5	5.04	-0.15732	1.06561	378.50	3.06	-0.14945	1.03578	369.49	2.81	-0.15732	1.06561	370.32	2.91	-0.15732	1.06561	382.19
	4	0.75	4.11	-0.25485	1.03677	359.63	3.44	-0.25530	1.05694	370.50	2.92	-0.26484	1.03692	366.66	2.79	-0.25822	1.03887	371.95
	4	1	4.45	-0.20736	1.05722	364.74	3.51	-0.20724	1.03196	371.51	2.81	-0.20736	1.05722	365.10	2.79	-0.21146	1.05614	378.22
	4	1.5	5.15	-0.18274	1.03309	374.32	3.11	-0.18330	1.06638	384.60	2.80	-0.18603	1.03379	361.02	2.99	-0.18606	1.03365	358.52
	7	0.75	4.24	-0.24067	1.06029	378.75	3.35	-0.23863	1.08171	359.83	2.90	-0.23762	1.06197	362.22	2.77	-0.24124	1.06090	365.18
ridge	7	1	4.60	-0.18864	1.07330	378.15	3.37	-0.19041	1.04949	361.46	2.77	-0.19597	1.07366	367.12	2.78	-0.19829	1.07141	364.94
	7	1.5	5.14	-0.17178	1.04858	369.58	3.11	-0.17314	1.04720	370.06	2.87	-0.16849	1.04964	365.92	2.99	-0.17178	1.04858	356.05
	10	0.75	4.35	-0.21325	1.09964	363.48	3.11	-0.17017	1.10765	372.34	2.88	-0.20674	1.09723	364.24	2.79	-0.20540	1.09657	373.63
	10	1	4.68	-0.17064	1.09812	356.50	3.31	-0.20234	1.11173	361.35	2.76	-0.17064	1.09812	367.20	2.78	-0.17344	1.10313	356.71
	10	1.5	4.98	-0.15662	1.06714	361.27	3.11	-0.17012	1.07453	355.53	2.77	-0.16081	1.05900	355.93	2.86	-0.15662	1.06714	356.94
	4	0.75	4.14	-0.26177	1.03964	363.35	3.44	-0.25528	1.05676	370.50	2.92	-0.26492	1.03687	366.66	2.79	-0.25829	1.03883	371.96
	4	1	4.45	-0.20752	1.05652	367.27	3.51	-0.20727	1.03193	371.51	2.80	-0.20752	1.05652	363.59	2.79	-0.21163	1.05543	378.22
	4	1.5	5.11	-0.18318	1.03326	376.88	3.11	-0.18362	1.06618	379.37	2.80	-0.18654	1.03398	356.62	2.99	-0.18663	1.03383	364.58
	7	0.75	4.24	-0.24039	1.06090	378.75	3.35	-0.23860	1.08130	359.83	2.90	-0.23731	1.06263	362.21	2.78	-0.24686	1.06051	367.21
PCR	7	1	4.60	-0.18887	1.07234	378.15	3.37	-0.19049	1.04700	361.46	2.77	-0.19620	1.07271	366.71	2.78	-0.19852	1.07046	364.90
	7	1.5	5.09	-0.17494	1.04775	355.80	3.11	-0.17067	1.10747	381.27	2.90	-0.17002	1.05163	376.09	2.91	-0.17724	1.04456	356.27
	10	0.75	4.35	-0.21229	1.10197	362.40	3.31	-0.20233	1.11109	361.35	2.83	-0.21148	1.10193	364.33	2.78	-0.20448	1.09881	369.41
	10	1	4.71	-0.17088	1.09714	369.91	3.32	-0.17024	1.07400	355.53	2.76	-0.17088	1.09714	367.20	2.77	-0.16974	1.10295	365.69
	10	1.5	5.01	-0.15723	1.06538	375.71	3.08	-0.15841	1.03587	371.73	2.82	-0.15603	1.06904	365.96	2.86	-0.15723	1.06538	364.46
	4	0.75	4.11	-0.25469	1.02753	359.35	3.08	-0.15775	1.03588	379.30	2.92	-0.26467	1.02770	366.66	2.79	-0.25807	1.02963	371.95
	4	1	4.45	-0.20736	1.04773	364.74	3.31	-0.25531	1.05694	370.50	2.80	-0.20736	1.04773	356.10	2.79	-0.21146	1.04665	378.22
	4	1.5	5.14	-0.18617	1.02415	374.72	3.10	-0.20724	1.03195	371.51	2.80	-0.18613	1.02430	358.29	2.98	-0.18668	1.02438	363.49
	7	0.75	4.24	-0.24014	1.05190	378.76	3.11	-0.18332	1.06644	380.52	2.90	-0.23704	1.05364	362.21	2.78	-0.24660	1.05152	367.21
r-k	7	1	4.60	-0.18864	1.06382	378.15	3.35	-0.23864	1.08171	359.83	2.77	-0.19597	1.06418	367.12	2.78	-0.19829	1.06194	364.94
	7	1.5	5.14	-0.17199	1.03883	367.75	3.11	-0.19041	1.04719	361.46	2.87	-0.16868	1.03990	365.92	2.99	-0.17199	1.03883	356.05
	10	0.75	4.35	-0.21205	1.09304	362.40	3.30	-0.17021	1.10787	372.34	2.83	-0.21124	1.09300	364.43	2.78	-0.20424	1.08988	374.34
	10	1	4.68	-0.17063	1.08867	359.20	3.31	-0.20236	1.11173	361.35	2.76	-0.17063	1.08867	367.20	2.78	-0.17343	1.09369	356.71
	10	1.5	4.98	-0.15693	1.05680	364.59	3.11	-0.17012	0.00000	355.53	2.80	-0.15575	1.06052	365.98	2.86	-0.15693	1.05680	364.46

Table A.6. Performance analysis results in terms of ARL_1 of PCR and *r-k* deviance-based CUSUM and EWMA charts in case of additive shift.

p	v	δ	CUSUM, $K=0.5$				EWMA, $\lambda=0.05$				EWMA, $\lambda=0.1$				EWMA, $\lambda=0.2$			
			ML	*ridge*	*PCR*	*r-k*	*ML*	*ridge*	*PCR*	*r-k*	*ML*	*ridge*	*PCR*	*r-k*	*ML*	*ridge*	*PCR*	*r-k*
4	0.75	0.25	23.872	22.992	23.816	22.360	157.584	157.496	157.584	148.528	192.056	190.104	190.104	130.900	199.620	199.172	198.392	192.648
4	1	0.25	25.880	25.892	25.788	25.436	160.940	160.940	160.940	85.752	192.012	191.484	190.268	186.100	196.840	196.184	196.840	187.408
4	1.5	0.25	32.092	31.012	30.784	30.348	171.768	170.104	171.112	199.300	180.856	172.840	173.280	170.716	208.336	204.072	204.388	194.588
7	0.75	0.25	22.588	22.544	22.556	22.228	164.076	163.400	162.392	153.048	151.148	188.768	188.768	117.932	167.208	166.924	167.968	158.072
7	1	0.25	25.924	25.912	25.912	25.604	161.104	157.308	157.308	89.076	190.280	179.428	179.580	171.392	177.392	177.096	177.820	169.568
7	1.5	0.25	31.404	31.680	31.028	31.004	165.156	164.972	164.788	209.160	177.824	192.020	193.444	186.400	210.364	209.820	192.384	205.268
10	0.75	0.25	18.432	18.456	18.504	18.332	78.204	50.332	71.592	69.224	113.636	114.524	102.544	53.536	94.372	93.976	94.580	90.800
10	1	0.25	22.140	21.516	21.604	21.460	90.352	79.248	90.352	79.248	121.680	114.336	115.472	110.264	117.612	117.632	118.332	113.336
10	1.5	0.25	26.992	26.296	26.632	26.064	157.912	193.440	156.760	193.440	139.284	129.268	145.920	134.308	133.176	127.116	128.016	125.288
4	0.75	0.5	24.152	22.792	22.828	22.668	148.688	149.360	148.688	146.664	180.032	178.240	180.012	123.628	189.176	188.136	189.176	185.080
4	1	0.5	26.272	26.104	26.096	25.956	150.884	150.884	150.884	75.268	177.228	176.760	175.684	170.812	168.683	168.498	168.984	160.984
4	1.5	0.5	32.464	32.188	31.236	31.048	166.848	164.092	165.468	190.008	164.072	157.700	158.660	155.284	189.496	183.136	184.352	173.820
7	0.75	0.5	21.404	21.408	21.572	21.336	155.060	150.540	150.376	142.632	140.124	173.144	173.444	110.476	150.792	151.080	151.484	145.676
7	1	0.5	25.284	25.344	25.348	25.136	159.660	155.196	155.196	86.800	172.472	163.172	163.072	152.660	160.440	160.756	160.760	155.156
7	1.5	0.5	30.852	30.660	30.584	30.064	160.632	157.832	160.164	198.944	159.788	175.924	178.956	170.436	194.984	193.216	172.416	188.184
10	0.75	0.5	16.684	16.572	16.640	16.444	70.856	47.344	67.796	63.696	99.068	100.936	91.224	47.200	74.788	82.568	83.772	80.444
10	1	0.5	20.852	19.796	20.144	19.608	85.228	71.452	85.228	71.452	111.676	103.192	104.076	102.104	100.540	107.952	108.704	104.836
10	1.5	0.5	27.832	26.896	27.580	26.064	153.596	186.248	149.028	186.248	124.932	113.412	131.720	120.452	125.384	117.472	118.772	112.840
4	0.75	0.75	23.940	23.100	23.744	22.420	137.964	137.904	137.900	134.784	156.652	155.612	156.624	106.992	174.956	174.268	174.952	172.236
4	1	0.75	26.100	26.016	25.996	25.360	149.244	149.244	149.244	71.956	159.872	158.256	155.500	150.532	148.416	148.552	148.552	144.860
4	1.5	0.75	33.720	33.172	32.916	32.804	161.652	159.136	159.300	176.204	150.852	142.524	143.584	138.780	177.192	168.948	170.868	160.332
7	0.75	0.75	20.748	20.672	20.780	20.492	145.264	139.620	139.620	133.384	128.220	160.476	160.496	101.280	138.352	139.272	138.324	130.344
7	1	0.75	24.000	24.176	24.176	23.528	151.760	148.988	148.988	78.636	159.248	150.196	148.120	141.104	141.892	143.460	143.460	139.472
7	1.5	0.75	29.616	30.012	29.464	28.884	147.124	144.232	145.440	178.460	142.092	157.920	163.180	153.860	180.400	180.060	155.756	173.664
10	0.75	0.75	15.952	15.516	15.712	15.248	60.984	43.624	57.952	56.084	88.116	91.264	84.020	43.012	64.044	75.408	75.484	71.568
10	1	0.75	20.388	19.676	19.716	19.336	79.756	68.936	79.756	68.936	99.004	90.312	91.200	89.984	88.228	93.904	95.736	90.444
10	1.5	0.75	26.608	26.108	26.980	25.824	141.432	169.640	135.620	169.640	113.592	106.436	116.084	110.732	113.860	105.924	106.284	99.288
4	0.75	1	23.560	22.376	22.604	22.124	133.764	133.712	133.700	132.024	142.968	139.536	141.328	96.792	154.684	154.244	154.168	147.860
4	1	1	25.592	25.224	25.228	24.952	141.228	141.228	141.228	63.868	143.864	143.364	141.924	137.124	134.176	134.176	134.176	131.436
4	1.5	1	32.600	32.524	32.340	31.924	143.420	138.792	140.216	159.460	133.680	125.836	126.016	121.860	159.996	154.256	155.704	146.728
7	0.75	1	19.684	19.876	19.872	19.452	135.088	127.744	127.732	121.284	121.092	151.612	152.640	95.512	119.828	119.488	117.784	110.420
7	1	1	23.204	23.280	23.264	22.940	137.912	134.176	134.176	71.560	137.696	127.840	127.564	120.444	123.148	124.820	123.864	120.768
7	1.5	1	28.972	28.908	28.712	28.706	137.796	136.448	136.456	166.308	127.076	139.928	147.848	137.820	163.064	163.076	138.772	156.624
10	0.75	1	16.036	15.888	16.020	15.596	56.288	44.232	53.916	51.664	80.772	84.216	78.156	38.300	60.352	68.604	68.616	67.224
10	1	1	19.632	19.352	19.436	19.028	70.564	62.256	70.564	62.256	87.892	80.720	81.596	78.988	78.708	84.300	85.756	82.296
10	1.5	1	26.076	25.636	26.104	25.336	128.880	153.532	124.140	153.528	101.040	94.120	104.504	98.728	103.088	94.348	94.032	89.428
4	0.75	1.25	21.952	21.240	21.496	20.956	119.364	119.360	118.252	118.064	124.392	123.232	123.548	84.344	139.532	138.860	140.704	135.536
4	1	1.25	24.940	24.768	24.760	24.468	130.152	130.152	130.152	58.724	120.840	120.792	120.436	116.016	122.588	122.588	122.588	118.024
4	1.5	1.25	31.292	31.236	30.544	30.246	131.720	128.084	129.204	146.324	115.576	110.736	110.424	108.724	143.440	137.896	138.608	134.492
7	0.75	1.25	19.240	19.248	19.252	19.140	120.308	116.436	115.512	109.900	101.924	126.352	126.416	80.152	103.240	104.176	102.848	97.284
7	1	1.25	22.192	22.232	22.228	22.152	129.028	126.252	126.252	65.052	122.500	113.684	113.688	106.616	112.112	113.444	113.076	108.104
7	1.5	1.25	27.168	27.412	27.060	27.020	122.284	121.524	121.456	150.372	115.804	130.236	138.892	126.152	152.064	151.320	128.520	145.988
10	0.75	1.25	15.368	15.280	15.352	14.944	51.508	38.400	49.704	47.028	71.452	74.556	69.440	32.604	56.008	62.260	62.400	60.420
10	1	1.25	19.092	18.656	18.880	18.208	67.164	55.460	67.156	55.464	77.456	71.920	73.604	70.872	70.972	76.456	77.508	75.164
10	1.5	1.25	24.148	23.756	24.108	23.672	115.408	139.472	111.484	139.240	88.156	79.864	92.008	84.524	93.564	87.460	86.944	84.048
4	0.75	1.5	20.280	20.004	20.104	19.616	106.892	106.144	104.960	102.772	108.168	106.812	107.352	71.008	120.568	119.992	120.336	112.848
4	1	1.5	22.952	22.880	22.776	22.608	121.888	121.432	121.432	48.728	102.168	101.696	100.168	98.712	110.768	110.104	109.768	107.140
4	1.5	1.5	31.000	31.000	30.696	30.264	119.996	117.504	117.760	131.924	98.600	97.216	96.764	95.820	130.916	126.464	127.812	122.708
7	0.75	1.5	18.708	18.736	18.728	18.644	109.612	102.868	102.860	97.300	86.860	108.360	108.328	68.696	90.744	91.120	88.560	86.196
7	1	1.5	21.776	21.836	21.876	21.696	117.712	114.752	114.684	54.800	105.876	96.340	96.296	91.560	97.504	97.772	97.936	94.392
7	1.5	1.5	26.441	26.208	25.980	25.784	115.968	114.240	114.884	143.560	101.008	115.556	125.700	111.996	136.700	135.564	117.976	132.804
10	0.75	1.5	15.256	15.148	15.404	15.108	49.960	29.912	47.788	42.656	64.416	65.956	60.292	30.596	52.728	58.648	58.668	56.776
10	1	1.5	18.424	17.304	17.672	17.048	59.704	50.024	59.704	50.024	71.804	65.548	66.364	64.236	64.628	69.452	71.992	68.340
10	1.5	1.5	23.728	23.108	23.364	22.700	101.644	122.672	96.212	122.672	82.128	73.668	83.184	76.752	86.136	78.328	78.804	75.444
4	0.75	2	18.532	17.864	18.012	17.428	83.744	83.736	83.456	83.440	78.508	78.212	78.508	55.944	92.796	93.908	94.524	88.956
4	1	2	21.124	20.848	20.840	20.448	105.096	105.080	105.084	35.128	82.380	82.372	80.580	78.860	85.052	83.972	83.968	80.748
4	1.5	2	28.364	28.612	28.292	28.088	95.564	91.928	92.900	91.832	78.248	76.488	76.304	74.992	107.912	104.592	105.304	100.760
7	0.75	2	18.052	18.140	18.200	17.968	79.852	70.764	70.752	68.008	64.780	77.048	77.932	51.344	66.116	66.220	66.116	61.204
7	1	2	19.856	19.924	19.916	19.784	97.640	96.220	96.220	40.776	77.944	73.184	72.828	70.252	72.828	73.308	72.940	68.104
7	1.5	2	24.592	25.084	24.544	24.366	100.152	98.844	98.456	115.608	76.784	90.012	96.388	85.700	117.544	118.656	92.624	107.448
10	0.75	2	13.652	13.608	13.684	13.376	34.092	21.380	31.720	30.032	47.192	48.156	43.588	22.720	42.844	47.204	47.300	46.148
10	1	2	17.636	16.628	16.876	16.356	44.468	37.684	44.192	37.684	56.384	52.308	53.104	51.332	51.484	56.812	57.956	54.616
10	1.5	2	21.668	21.484	21.548	21.224	78.912	95.048	75.556	95.048	62.456	57.076	65.244	61.080	69.208	64.360	64.600	61.308
4	0.75	2.5	17.268	16.704	16.724	16.392	63.180	63.476	63.456	62.480	57.144	56.820	56.928	41.716	66.820	68.568	69.316	64.252
4	1	2.5	20.552	20.300	20.296	19.736	76.064	76.064	76.064	24.764	61.772	61.768	60.828	58.048	69.625	69.327	69.028	65.824
4	1.5	2.5	26.328	26.348	26.100	25.988	76.096	72.460	73.920	78.332	63.676	61.520	61.472	60.120	94.276	91.864	91.620	86.904
7	0.75	2.5	16.848	16.912	16.940	16.616	56.944	51.392	51.912	48.032	46.848	54.088	55.204	34.564	50.760	51.096	50.620	48.400
7	1	2.5	18.756	19.148	19.092	18.716	72.960	68.332	68.332	31.048	56.736	52.364	52.360	50.556	56.088	56.596	55.944	55.500
7	1.5	2.5	23.872	23.944	23.804	23.456	72.168	69.848	70.392	83.652	57.488	68.716	71.048	63.092	90.212	90.856	72.464	83.388
10	0.75	2.5	12.576	12.572	12.788	12.500	28.716	18.564	25.256	24.128	35.296	35.896	32.152	18.536	32.124	35.084	35.152	34.116
10	1	2.5	15.900	15.536	15.716	14.996	34.176	26.428	34.172	26.428	45.120	41.804	41.804	40.100	45.148	48.700	49.216	46.372
10	1.5	2.5	20.968	20.408	20.616	20.188	62.656	74.908	58.916	74.904	50.584	47.684	52.116	49.716	60.980	56.060	56.684	53.844
4	0.75	3	15.980	15.616	15.744	15.444	43.884	42.916	42.900	42.060	40.408	39.884	39.884	27.684	50.808	50.252	50.800	48.476
4	1	3	18.312	18.240	18.232	18.080	58.628	58.628	58.628	20.368	47.440	47.440	46.408	44.768	52.452	52.128	52.124	50.164
4	1.5	3	24.688	24.788	24.516	24.316	63.176	60.528	60.488	64.992	52.516	48.032	48.900	47.384	76.764	73.856	73.836	69.020
7	0.75	3	15.744	15.824	15.940	15.668	39.516	37.536	37.536	34.064	30.440	37.224	37.224	23.912	37.628	37.444	37.192	36.036
7	1	3	17.552	17.752	17.692	17.444	55.376	53.828	53.828	23.852	40.696	37.316	37.304	36.108	42.396	42.224	42.224	39.712
7	1.5	3	22.508	22.472	22.128	22.108	57.236	55.840	55.324	64.668	46.848	52.648	55.488	49.724	72.812	72.568	56.252	68.360
10	0.75	3	11.996	11.844	12.000	11.688	19.068	14.296	17.384	16.568	24.328	24.856	22.652	13.104	24.012	26.592	26.952	25.916
10	1	3	15.008	14.668	14.940	14.088	25.752	21.756	25.744	21.756	31.784	30.816	30.812	29.728	37.436	40.856	40.884	39.560
10	1.5	3	19.052	18.452	18.704	18.180	49.056	59.236	46.592	59.236	42.964	38.132	44.592	41.204	52.380	47.904	48.268	46.608

Table A.7. Performance analysis results in terms of ARL_1 of PCR and *r-k* deviance-based CUSUM and EWMA charts in case of multiplicative shift.

p	v	δ	CUSUM, $K=0.5$				EWMA, $\lambda=0.05$				EWMA, $\lambda=0.1$				EWMA, $\lambda=0.2$			
			ML	*ridge*	*PCR*	*r-k*	*ML*	*ridge*	*PCR*	*r-k*	*ML*	*ridge*	*PCR*	*r-k*	*ML*	*ridge*	*PCR*	*r-k*
4	0.75	0.25	23.688	23.128	23.456	22.748	199.592	198.680	198.880	135.968	212.124	211.360	212.060	206.688	167.248	167.248	167.248	154.028
4	1	0.25	25.184	24.884	24.868	24.656	211.072	208.080	206.840	202.636	212.644	212.888	212.644	205.580	166.720	166.720	166.720	91.008
4	1.5	0.25	33.556	33.180	33.024	32.364	199.488	191.340	191.376	188.924	225.648	220.396	220.908	212.940	186.260	181.628	183.936	216.848
7	0.75	0.25	22.868	22.960	23.048	22.696	165.084	202.204	203.240	129.148	173.016	175.764	176.432	169.160	167.204	166.660	166.660	152.736
7	1	0.25	26.132	27.280	26.996	25.876	197.496	187.144	187.144	179.604	190.980	190.556	190.984	184.016	163.780	161.616	161.616	100.592
7	1.5	0.25	32.840	33.236	32.820	32.628	185.524	204.196	207.076	196.744	221.124	220.952	203.832	217.348	166.868	167.384	166.552	217.040
10	0.75	0.25	17.884	17.936	18.140	17.740	118.932	118.916	114.996	54.112	94.216	101.488	102.200	99.776	78.052	51.064	70.740	68.268
10	1	0.25	21.184	20.572	20.896	20.184	124.892	116.852	117.740	115.424	109.832	119.856	119.112	116.304	92.908	83.332	92.908	83.332
10	1.5	0.25	27.972	27.424	28.172	27.152	147.600	140.376	154.776	145.080	139.160	133.552	133.912	131.064	166.380	204.652	164.460	204.652
4	0.75	0.5	23.744	23.228	23.712	22.792	202.196	200.188	200.000	136.080	208.776	207.468	208.548	202.428	165.860	165.860	165.860	151.944
4	1	0.5	25.020	24.948	24.948	24.732	207.048	204.956	203.212	200.336	207.464	207.708	207.464	201.852	165.724	165.724	165.724	91.008
4	1.5	0.5	33.512	32.976	32.912	32.664	197.960	191.076	191.112	188.580	225.444	220.448	221.300	213.204	186.708	184.296	185.068	218.060
7	0.75	0.5	22.200	22.260	22.356	22.120	158.028	195.328	196.328	122.728	167.724	169.864	171.408	163.912	166.780	164.888	164.888	152.148
7	1	0.5	26.180	26.452	26.424	25.712	199.416	185.796	185.792	177.208	187.732	187.404	187.736	179.684	162.280	160.124	160.124	97.820
7	1.5	0.5	32.216	32.768	31.752	31.084	185.100	203.120	206.000	196.736	220.968	220.820	200.428	216.736	164.316	165.404	164.576	216.072
10	0.75	0.5	17.412	17.320	17.348	17.248	113.056	113.920	110.168	51.400	82.996	89.744	90.416	87.796	71.552	48.052	62.928	61.328
10	1	0.5	20.432	20.252	20.320	20.008	123.348	115.304	115.712	113.992	104.364	113.588	113.608	110.180	86.488	78.584	86.488	78.584
10	1.5	0.5	27.764	27.560	27.704	27.104	139.072	133.508	145.848	137.840	131.908	127.420	127.428	125.480	163.836	200.624	161.816	200.624
4	0.75	0.75	23.740	23.096	24.096	22.660	200.052	199.812	199.800	135.504	207.660	206.592	207.144	201.528	165.832	165.832	165.832	151.936
4	1	0.75	25.008	24.892	24.888	24.664	205.020	203.644	201.164	198.368	205.112	205.548	205.536	197.268	165.244	165.236	165.244	89.004
4	1.5	0.75	32.468	32.268	32.156	31.772	196.020	190.244	191.220	189.756	224.860	219.216	219.912	211.652	185.096	181.772	183.052	216.304
7	0.75	0.75	21.836	21.836	22.124	21.690	156.200	190.232	192.500	122.112	162.812	165.004	165.420	159.052	166.620	164.928	164.928	151.696
7	1	0.75	26.164	26.620	26.620	25.852	197.524	181.392	181.388	176.368	180.476	180.576	180.908	174.356	160.000	158.620	158.620	97.628
7	1.5	0.75	33.336	32.832	32.084	31.748	183.044	199.776	205.592	194.540	218.752	218.580	198.104	214.524	164.072	164.096	163.088	213.468
10	0.75	0.75	16.820	16.696	16.704	16.668	107.832	108.424	103.616	47.068	79.364	87.056	86.436	83.812	66.064	45.184	59.348	55.876
10	1	0.75	19.852	19.012	19.436	18.888	119.512	109.728	109.728	107.996	102.940	111.776	111.036	108.576	83.888	74.200	83.888	74.200
10	1.5	0.75	25.832	25.460	25.544	25.196	137.852	131.320	143.888	136.440	126.868	120.228	120.248	118.696	159.312	196.044	157.880	196.040
4	0.75	1	24.128	23.160	24.196	22.844	197.920	196.792	196.780	135.356	202.148	201.216	201.632	197.184	165.232	165.224	165.224	151.932
4	1	1	25.624	25.532	25.304	24.896	204.592	203.216	200.768	198.328	201.892	202.084	202.316	195.112	165.252	165.244	165.252	90.948
4	1.5	1	32.040	31.552	31.628	31.271	194.872	189.280	190.252	188.396	223.872	217.676	220.324	209.740	183.724	180.420	182.348	216.312
7	0.75	1	22.564	22.512	22.572	22.444	147.672	183.028	184.836	115.020	161.324	161.928	162.648	154.416	166.264	162.624	162.624	148.428
7	1	1	26.004	26.248	26.248	25.752	193.152	177.152	177.140	171.436	178.716	178.720	179.148	172.528	160.264	158.864	158.864	96.316
7	1.5	1	32.584	33.008	31.816	31.232	179.996	195.716	201.224	191.920	214.460	214.288	193.776	210.200	163.776	163.104	162.052	213.360
10	0.75	1	16.072	15.896	15.952	15.816	105.708	106.784	103.004	45.280	71.972	79.508	79.592	76.808	64.764	44.680	60.524	56.468
10	1	1	19.640	19.052	19.300	18.620	114.424	105.480	105.464	103.636	106.920	106.136	105.396	103.488	78.792	66.344	78.792	66.352
10	1.5	1	25.264	24.692	24.812	24.528	132.852	126.728	138.668	131.628	125.224	116.628	116.668	115.096	154.972	190.816	152.700	190.120
4	0.75	1.25	24.000	23.076	24.216	22.684	196.356	195.268	195.456	134.388	202.468	201.840	202.724	197.692	163.132	163.124	163.124	146.644
4	1	1.25	25.496	25.348	25.340	25.036	202.672	202.080	200.752	197.640	197.408	197.600	197.832	191.668	165.248	165.240	165.248	90.676
4	1.5	1.25	31.880	31.604	31.488	31.484	192.080	184.832	185.804	183.944	219.508	214.520	217.164	207.720	182.992	179.680	181.608	214.220
7	0.75	1.25	22.820	22.728	22.844	22.452	146.292	183.172	184.984	115.840	153.964	153.948	154.660	148.176	167.640	160.644	160.644	144.944
7	1	1.25	25.548	25.592	25.592	25.396	189.568	173.544	173.544	167.196	173.480	175.156	175.584	166.256	159.080	157.676	157.676	96.348
7	1.5	1.25	32.872	33.088	31.944	31.156	178.548	194.040	199.420	188.120	213.372	213.200	190.776	208.004	163.628	162.500	161.948	212.484
10	0.75	1.25	14.868	14.696	14.700	14.444	100.432	101.056	96.048	41.948	66.396	73.388	73.936	71.228	62.780	43.160	58.304	56.164
10	1	1.25	19.312	18.900	19.168	18.428	109.256	99.344	99.344	97.756	90.624	97.616	96.876	95.392	71.908	62.508	71.908	62.508
10	1.5	1.25	24.912	24.648	24.836	24.592	130.472	121.640	134.872	128.792	120.656	112.316	113.708	109.704	151.184	184.476	148.172	183.780
4	0.75	1.5	23.948	23.212	24.224	22.784	195.148	194.060	194.248	132.392	202.348	200.836	202.604	197.996	162.832	162.824	162.824	147.804
4	1	1.5	25.560	25.428	25.424	24.920	202.628	202.036	200.712	197.948	196.416	196.608	196.840	190.548	165.236	165.236	165.236	91.028
4	1.5	1.5	32.240	31.880	31.876	31.129	191.744	185.536	185.880	185.240	215.328	209.888	211.828	201.592	182.972	180.444	181.828	214.216
7	0.75	1.5	22.188	22.080	22.208	21.892	140.868	176.836	178.236	112.348	152.212	152.204	152.152	146.284	163.900	160.252	160.252	144.616
7	1	1.5	24.548	25.204	25.216	24.472	185.300	170.932	170.936	166.552	169.996	170.676	171.108	163.552	160.596	159.196	159.196	97.304
7	1.5	1.5	32.476	32.668	31.936	31.856	175.500	190.536	197.212	183.944	208.600	208.592	183.840	201.456	163.500	162.384	161.784	211.132
10	0.75	1.5	14.536	14.392	14.396	14.168	92.836	93.844	89.116	36.556	60.116	68.656	68.912	64.948	58.748	39.692	55.136	51.972
10	1	1.5	19.388	18.988	19.172	18.068	103.980	94.080	94.488	92.424	84.472	90.108	90.548	88.384	67.248	57.868	67.248	57.868
10	1.5	1.5	25.056	24.484	24.696	24.360	124.204	116.048	128.112	124.056	116.244	107.148	108.564	105.092	145.460	180.216	139.000	180.212
4	0.75	2	23.920	23.332	24.024	23.028	189.836	189.132	189.132	130.312	198.544	198.468	198.792	194.356	161.880	160.888	161.880	150.852
4	1	2	25.804	25.584	25.584	25.208	200.376	199.792	198.428	194.328	194.024	194.836	194.448	186.712	164.828	164.828	164.828	89.760
4	1.5	2	31.768	32.228	32.164	31.504	191.040	180.624	184.136	177.600	217.148	211.160	211.176	202.140	182.156	179.808	181.068	211.312
7	0.75	2	20.676	20.676	20.672	20.568	140.712	172.952	173.784	110.772	141.396	141.152	140.560	134.860	158.256	156.732	156.732	141.652
7	1	2	24.504	24.744	24.668	24.248	180.880	166.488	167.324	162.012	163.740	163.736	163.740	160.624	161.432	158.688	158.688	95.192
7	1.5	2	30.400	30.552	29.840	29.072	168.348	192.596	198.644	183.324	200.944	200.940	181.900	197.540	161.512	159.604	161.356	212.064
10	0.75	2	13.768	13.684	13.740	13.468	78.368	80.092	74.916	28.676	50.128	57.652	57.404	55.068	51.976	34.892	48.736	41.408
10	1	2	19.840	18.896	19.112	18.720	89.904	84.368	85.092	82.284	73.756	79.896	79.908	78.268	57.632	47.648	57.632	47.648
10	1.5	2	24.644	24.540	24.620	24.380	119.596	108.968	123.684	117.664	110.900	101.696	103.204	99.144	144.052	175.292	137.916	175.292
4	0.75	2.5	24.928	24.292	24.392	23.540	189.120	187.856	187.676	130.952	197.372	197.648	197.380	191.884	159.496	159.496	159.496	147.128
4	1	2.5	26.392	26.216	26.376	25.708	199.324	197.752	195.788	191.560	190.524	190.104	191.592	183.264	164.820	164.820	164.820	87.044
4	1.5	2.5	32.672	32.468	32.316	31.856	187.188	178.732	180.856	174.272	212.112	208.080	207.376	196.276	181.524	179.832	179.696	179.596
7	0.75	2.5	19.984	19.984	19.984	19.784	132.904	164.596	165.420	105.012	129.428	129.196	128.924	121.576	153.204	151.352	151.352	140.104
7	1	2.5	23.500	23.612	23.612	23.336	173.208	157.752	158.584	155.380	156.416	156.744	156.420	154.088	158.340	154.720	154.720	87.180
7	1.5	2.5	30.712	30.076	30.156	29.856	166.448	185.552	190.928	179.232	195.424	194.524	172.680	189.824	159.572	157.932	159.376	157.164
10	0.75	2.5	12.728	12.712	12.716	12.616	65.400	65.840	61.568	23.028	42.092	46.464	46.144	44.588	42.080	29.292	39.528	33.236
10	1	2.5	18.056	17.484	17.720	17.180	88.388	82.772	82.772	79.868	64.692	69.664	69.680	67.496	50.888	44.308	50.888	44.308
10	1.5	2.5	24.928	24.376	24.644	24.276	111.288	102.772	113.736	108.396	105.336	95.780	97.264	93.484	169.320	161.240	163.908	161.200
4	0.75	3	25.288	24.568	24.780	24.048	189.300	189.060	188.880	127.328	196.688	194.720	195.620	190.644	160.896	160.896	160.896	148.612
4	1	3	25.752	25.600	25.572	25.496	194.800	193.592	193.332	190.500	189.600	188.164	189.656	181.348	163.280	163.272	163.284	85.376
4	1.5	3	32.940	32.332	32.308	32.296	185.108	178.212	179.396	174.468	205.968	200.960	201.244	191.324	177.660	175.680	175.862	175.904
7	0.75	3	20.024	20.124	20.152	19.972	126.960	159.044	159.048	97.208	118.228	118.228	117.044	110.908	149.432	146.276	146.276	136.256
7	1	3	23.540	23.612	23.628	23.444	167.616	151.976	152.800	148.860	146.676	146.672	146.688	141.508	157.240	154.524	154.528	87.068
7	1.5	3	29.920	29.320	29.360	28.924	162.928	177.196	185.188	171.336	186.384	185.480	164.336	180.324	158.252	157.568	158.056	157.164
10	0.75	3	12.288	12.252	12.300	12.192	57.264	57.300	53.316	19.500	35.296	40.028	39.524	37.376	36.312	25.400	35.696	29.812
10	1	3	16.248	15.884	16.176	15.716	81.988	76.500	75.684	72.560	59.376	64.920	64.924	62.944	47.364	41.528	47.364	41.528
10	1.5	3	24.424	23.436	24.204	22.960	99.056	91.456	102.204	95.732	94.036	86.400	87.640	83.416	148.600	147.726	147.640	147.284

Table A.8. Performance analysis results in terms of *SDRL* of PCR and *r-k* deviance-based CUSUM and EWMA charts in case of additive shift.

p	ν	δ	CUSUM, $K=0.5$				EWMA, $\lambda=0.05$				EWMA, $\lambda=0.1$				EWMA, $\lambda=0.2$			
			ML	*ridge*	*PCR*	*r-k*	*ML*	*ridge*	*PCR*	*r-k*	*ML*	*ridge*	*PCR*	*r-k*	*ML*	*ridge*	*PCR*	*r-k*
4	0.75	0.25	18.5333	17.4214	17.3698	16.4535	149.5916	149.1343	149.1343	149.1324	127.4033	128.0968	127.5088	126.5029	170.6420	170.4064	170.6420	166.3885
4	1	0.25	19.8484	19.4662	19.4159	19.4990	140.8532	140.5056	140.6240	140.5843	130.5549	130.7841	130.5549	129.3869	170.1208	170.1208	170.1208	142.1964
4	1.5	0.25	24.9500	24.6198	24.6068	24.4466	145.6712	143.9357	144.3831	142.9936	130.7308	130.3705	129.7072	129.2856	162.7421	162.5640	162.2512	156.8857
7	0.75	0.25	16.6869	16.7103	16.7246	16.5537	149.3127	144.2767	144.2767	144.6975	120.5152	121.1058	122.0082	119.5631	169.4020	168.8587	168.4946	165.3236
7	1	0.25	19.1933	19.1414	19.1414	19.1255	141.6921	140.0789	140.0453	138.3043	131.2955	130.9882	131.6832	128.2750	170.2843	169.5546	169.5546	145.2811
7	1.5	0.25	23.1499	23.5618	22.8170	23.3330	144.6834	144.8009	144.4634	144.2094	128.4524	128.4127	128.2131	128.2573	163.2685	162.8370	162.9694	155.8233
10	0.75	0.25	18.7960	18.2898	18.2843	18.3090	95.7904	96.2212	93.4034	84.6702	75.1720	80.4090	81.0398	78.3973	114.6067	93.5658	109.2094	108.4279
10	1	0.25	21.3545	21.1219	21.1146	21.1341	99.3937	98.0145	98.3950	95.5926	83.2471	86.3684	87.0606	85.0820	136.2776	125.9492	136.2776	125.9492
10	1.5	0.25	23.5578	23.2325	23.1828	22.9012	119.8701	115.5036	123.6875	116.4467	105.0988	102.7300	102.8172	100.5679	150.2574	145.7062	150.2689	145.7062
4	0.75	0.5	18.3055	15.8376	15.8104	15.8108	146.6299	146.2170	146.6370	146.1267	126.0972	126.4250	126.0920	125.4579	166.4451	166.2022	166.4451	167.6669
4	1	0.5	19.2176	19.1066	19.1147	19.1119	138.8140	138.8103	138.5016	137.9935	124.7578	125.0253	125.0253	121.9858	166.9771	166.9771	166.9771	133.0052
4	1.5	0.5	24.3873	24.6761	23.7705	23.9030	142.1236	139.0773	139.6542	138.0820	130.4330	128.0613	127.8804	125.4602	160.7184	160.0701	160.1646	155.1088
7	0.75	0.5	14.2025	14.1974	14.2470	14.1957	142.6252	140.2520	140.5466	139.6649	119.6886	120.0726	120.4907	119.2856	166.1573	164.1412	163.9614	161.4097
7	1	0.5	17.9274	17.9187	17.9187	17.8295	137.2129	134.1444	134.7967	130.6425	125.8620	125.4818	125.4876	123.8069	168.1715	167.4536	167.4536	143.1998
7	1.5	0.5	21.9585	21.6639	21.7391	21.0333	141.3111	141.8473	142.1324	141.1355	130.0168	129.7094	127.8429	129.7859	161.5733	159.9872	160.6005	154.5173
10	0.75	0.5	15.6234	15.5516	15.5672	15.5325	90.8316	91.1963	88.0609	76.9567	69.6089	75.6664	76.5675	74.2482	108.2682	87.1671	106.5312	103.5919
10	1	0.5	19.4056	18.0205	18.4226	17.9966	96.9451	95.1557	95.2788	94.4211	80.9205	83.5923	84.3888	82.5189	132.2763	118.7197	132.2763	118.7197
10	1.5	0.5	26.1263	24.5832	26.1019	23.4117	114.0328	106.6502	117.6927	111.2277	102.9994	99.9382	100.8377	95.5874	147.8164	143.6282	146.7820	143.6282
4	0.75	0.75	18.7583	18.2148	18.5878	17.5621	140.9031	140.4202	140.9060	139.5053	122.9353	123.1216	122.9334	122.1751	161.8962	161.9331	161.8919	167.0645
4	1	0.75	19.5401	19.5263	19.5300	18.8309	132.2431	131.2678	130.8418	130.5178	120.1309	120.1240	120.1240	117.2507	166.2700	166.2700	166.2700	129.8693
4	1.5	0.75	24.2498	24.4148	24.1303	23.8631	138.0891	134.1205	134.9049	132.2946	128.8241	125.9784	126.1201	123.3638	158.7081	158.2197	158.0712	153.2127
7	0.75	0.75	13.7446	13.3147	13.7550	13.3203	136.5141	136.0347	136.0494	132.0336	117.5608	118.5539	117.8226	114.9037	161.5303	159.5017	159.5017	157.7403
7	1	0.75	17.0388	17.5510	17.5510	16.5001	131.6753	128.2859	127.8112	126.4342	120.2534	121.0841	121.0841	119.8963	164.6960	164.2581	164.2581	135.0951
7	1.5	0.75	19.9890	20.5990	20.0761	19.6897	139.8993	139.0390	139.9979	137.9236	129.8291	129.3594	124.2759	128.2112	156.4135	155.1967	155.6166	153.1797
10	0.75	0.75	14.2232	13.2599	13.7860	13.2277	85.4404	87.3048	83.4648	71.4706	62.2805	70.7818	70.9361	68.5980	98.9577	83.3326	96.5779	94.9176
10	1	0.75	19.3092	18.8936	18.8678	18.7643	90.1363	87.4776	87.7420	87.5733	77.2797	80.5111	81.7027	78.2608	125.9245	115.0097	125.9245	115.0097
10	1.5	0.75	23.9710	23.9013	25.6608	23.7474	108.3825	104.0856	109.7793	105.8930	97.0820	93.0351	92.5967	86.1656	142.4110	140.1812	141.2032	140.1812
4	0.75	1	18.1835	17.2451	17.1432	17.0322	134.1979	132.2120	133.3618	129.2367	118.5379	119.3167	119.3608	115.4097	159.2417	159.2895	159.2388	164.9793
4	1	1	19.4610	19.4980	19.5020	19.3589	126.0891	126.0839	125.9495	123.9550	115.5516	115.5516	115.5516	114.0647	161.1465	161.1465	161.1465	119.0087
4	1.5	1	24.2024	24.2259	24.2249	23.8362	131.8738	127.8238	127.6085	124.7474	124.0685	122.6559	123.0773	120.2190	151.8693	150.1708	150.5164	149.0322
7	0.75	1	12.1511	12.0931	12.0586	11.8591	135.6540	135.7146	136.5270	129.2884	109.8290	109.9849	109.0527	105.9942	157.5727	153.8722	153.8773	150.9435
7	1	1	16.4525	16.4145	16.4205	16.3879	126.6143	122.1313	122.0645	120.2390	113.0376	114.2935	113.3325	112.9168	158.9609	158.0538	158.0538	126.0533
7	1.5	1	19.8375	19.1263	19.1136	19.1106	134.2062	132.6690	134.8718	131.6374	125.5320	125.1497	119.1075	124.5202	152.1038	151.4911	151.4913	149.8390
10	0.75	1	15.2274	15.2270	15.2478	15.0196	80.3523	82.5799	80.1240	67.1251	59.9260	65.0897	65.4467	64.9937	93.9665	83.6500	90.8449	89.6592
10	1	1	18.8713	18.7710	18.7339	18.5960	86.2820	84.3306	84.6891	83.7638	73.4766	76.5071	77.6699	75.4802	116.3663	108.0822	116.3663	108.0822
10	1.5	1	23.7518	23.7823	23.7898	23.1751	102.2207	96.6863	104.1363	99.4037	90.7334	85.1565	83.6635	80.3953	138.0108	137.6641	135.5001	137.6656
4	0.75	1.25	16.4831	15.8507	16.3683	15.7963	126.3470	125.7651	125.7772	120.1200	112.5643	111.3929	112.9622	108.9270	151.9192	151.9197	151.2409	162.6445
4	1	1.25	19.7621	19.7078	19.7030	19.6952	114.6274	114.6403	114.6412	112.5980	109.2073	109.2073	109.2073	106.2951	154.3915	154.3915	154.3915	112.1265
4	1.5	1.25	23.3418	23.4352	22.7459	22.7995	120.1956	116.8994	116.3255	115.0693	118.4414	117.3644	117.2567	116.6214	146.4824	144.9830	145.0417	143.3861
7	0.75	1.25	11.5790	11.5760	11.5767	11.5608	122.5872	123.8206	123.8296	116.5886	100.0843	100.0901	98.7867	96.5994	149.6728	147.5610	146.8139	144.4384
7	1	1.25	14.7785	14.7878	14.7918	14.7689	119.2226	114.3264	114.3315	111.6648	107.3858	108.5819	108.0125	105.7792	153.7573	152.8735	152.8735	118.7829
7	1.5	1.25	18.6971	18.7374	18.4805	18.4268	130.4779	127.7107	130.3771	126.0185	122.1778	121.8488	115.8842	121.7730	142.9684	142.3389	142.5282	143.8521
10	0.75	1.25	14.2463	14.2532	14.2360	13.8271	75.2750	77.1127	74.2121	57.6707	58.0337	62.3114	62.2990	61.2300	87.9390	75.9213	86.5386	84.4083
10	1	1.25	18.5671	18.2334	18.6098	17.6485	81.0756	79.2211	80.2455	78.7000	70.0113	73.0102	73.6780	72.6182	111.7448	100.7388	111.7449	100.7395
10	1.5	1.25	21.3343	21.3339	21.2909	21.2357	92.8099	85.1688	95.9322	88.4068	85.4507	80.6815	79.1263	77.4562	130.8515	131.4111	128.2511	131.1722
4	0.75	1.5	14.8002	14.6891	14.7382	14.3983	116.8830	115.2169	116.0398	106.5943	105.6965	107.3140	107.4831	103.1883	142.9119	143.0211	142.0755	155.1636
4	1	1.5	16.8172	16.7869	16.7864	16.7867	101.6092	101.3447	100.1872	98.9247	100.1124	100.0739	100.1124	98.7462	149.4250	148.8985	148.8985	97.8439
4	1.5	1.5	23.0054	22.9805	22.8843	22.7801	106.8132	105.7065	104.7725	104.0723	113.5196	112.2066	112.8711	112.0658	137.9985	137.4835	136.7583	134.3250
7	0.75	1.5	11.2408	11.2347	11.2385	11.2042	112.3840	115.2006	114.9680	106.2255	93.5581	93.1564	90.7358	89.9400	141.5398	137.1481	137.1443	134.5739
7	1	1.5	14.8917	14.9245	14.9092	14.8082	110.1882	104.8174	104.8197	102.4881	99.5754	100.3343	99.5993	98.0087	147.4825	146.4091	146.3574	107.6070
7	1.5	1.5	18.3721	18.3314	18.1260	18.1392	123.4668	118.1265	123.2078	117.8251	120.5946	119.9059	113.1091	119.4256	138.6026	136.4134	137.3942	139.7764
10	0.75	1.5	14.5577	14.3955	15.0510	14.3943	70.6032	71.0531	68.1526	55.5707	55.8515	60.0822	60.1216	59.4347	83.8730	61.6683	81.8413	78.2765
10	1	1.5	17.7080	15.9746	16.6916	15.9404	76.7290	72.5140	73.2114	71.7767	66.5342	68.6837	70.8270	68.4816	102.4284	91.1487	102.4284	91.1487
10	1.5	1.5	21.1895	20.7757	20.8711	20.4479	89.7866	80.9965	89.9780	82.6999	82.5242	74.8151	74.8180	73.1728	120.1665	122.7505	116.0303	122.7505
4	0.75	2	12.6123	12.3149	12.3490	11.7638	94.0172	93.2842	94.0670	87.9552	89.0370	89.7477	89.6252	87.9470	123.0257	123.0171	123.0288	142.8372
4	1	2	15.2049	15.1604	15.1641	14.8063	88.5555	88.5325	86.7958	86.4259	77.9455	78.7989	78.8015	76.6842	136.0249	136.0195	136.0192	75.7873
4	1.5	2	20.9401	20.7919	20.7545	20.7092	91.3942	88.6192	88.6398	88.2277	102.5154	100.0941	101.1536	97.7219	119.5599	116.8894	116.9583	115.4479
7	0.75	2	11.8274	11.1528	11.2091	11.1119	92.4048	92.3444	92.8064	86.3814	72.0989	72.0488	72.0989	67.0209	116.2158	107.2421	107.2170	106.3794
7	1	2	13.0759	13.0339	13.0392	13.0312	87.2884	86.6137	85.9642	84.6763	79.3640	80.4703	79.5126	74.8291	131.7523	130.8590	130.8590	85.4998
7	1.5	2	17.9740	17.2449	16.9629	17.1640	108.6999	104.6449	108.2276	103.2339	112.8861	113.2900	94.3105	106.2970	125.4657	124.5804	124.3501	126.1216
10	0.75	2	12.5296	12.4631	12.5338	12.4601	57.9523	58.3274	55.3823	42.5248	50.0546	53.8303	53.9211	53.3588	63.8883	47.8770	60.2831	59.5104
10	1	2	15.8785	15.0747	15.2552	15.0065	63.7308	61.7388	62.6834	60.7659	53.7180	55.8836	56.9781	55.0953	80.0384	71.5612	80.0523	71.5612
10	1.5	2	19.0454	19.0654	19.0430	19.0297	72.3064	68.3536	76.0602	70.4281	70.5605	66.3805	65.9420	63.6319	101.0604	105.2786	99.4764	105.2786
4	0.75	2.5	11.6598	11.3876	11.3687	11.3411	71.4094	71.3279	71.4143	69.1021	65.1390	68.0392	68.4626	61.8774	102.1237	103.7260	103.7304	120.8451
4	1	2.5	15.4739	15.2958	15.2945	14.5795	71.7447	71.7457	71.5097	66.8303	68.6421	70.1486	69.4171	67.0159	110.2563	110.2563	110.2563	53.1587
4	1.5	2.5	18.8618	18.6750	18.6892	18.6561	78.4731	76.4732	76.4262	74.4050	89.9113	89.1005	88.9497	85.0853	100.4306	96.4079	98.0450	95.2775
7	0.75	2.5	9.9776	9.9428	9.9551	9.8844	68.6816	67.9902	68.9603	61.4098	57.8066	58.0150	57.7148	55.1661	91.6966	84.8203	85.3141	83.1697
7	1	2.5	12.0367	12.2464	12.2808	12.0364	70.9712	66.5130	66.5157	65.5432	63.9121	64.4857	63.4997	63.0676	107.7036	102.7805	102.7805	69.3397
7	1.5	2.5	17.2577	17.3198	17.2875	16.7906	90.4859	88.0429	90.1531	82.8265	94.2752	94.4814	77.6514	88.7322	104.0166	101.8151	102.2188	106.7479
10	0.75	2.5	10.1838	10.1847	10.5864	10.1742	46.6624	47.9738	42.2369	36.4665	37.7706	40.8966	40.8668	39.5904	55.5429	41.6065	51.8758	51.3789
10	1	2.5	14.4892	14.2070	14.4539	13.5261	55.4823	52.2279	52.2279	49.6335	50.8697	52.8365	53.9505	50.8300	66.7425	50.0923	66.7398	50.0923
10	1.5	2.5	18.7789	18.5673	18.5131	18.5932	61.0466	59.1495	63.0678	60.2760	63.6258	58.6687	58.6224	57.4411	88.4203	91.7016	84.2274	91.6996
4	0.75	3	11.7062	10.8706	11.0532	10.5617	49.2629	48.4123	48.4123	44.8651	47.4307	47.0733	47.0636	45.8452	77.9723	75.6230	77.9938	97.9140
4	1	3	12.7068	12.7437	12.7461	12.6759	57.4907	57.4907	54.8290	50.9148	51.7601	51.5407	51.5392	48.1995	92.2378	92.2378	92.2378	45.6400
4	1.5	3	18.0983	18.1133	18.0636	18.0343	67.3908	60.0282	62.8054	59.7975	74.3067	72.0878	72.4148	68.1251	86.8030	83.7071	83.4185	84.4338
7	0.75	3	9.2542	9.2293	9.4372	9.2241	45.4538	47.2969	47.2870	43.0804	39.7326	40.0860	39.7677	39.3929	70.3661	68.5913	68.5913	66.3068
7	1	3	10.8885	11.0257	11.0426	10.6684	52.5577	48.7951	48.7974	47.2937	48.0598	48.0860	48.0860	44.5372	89.1903	87.7315	87.7315	53.9039
7	1.5	3	16.2818	16.1923	15.4517	16.1047	75.8288	72.8018	75.4469	69.5737	81.8058	81.8157	61.5286	75.6730	89.2776	88.1129	87.4854	88.9781
10	0.75	3	9.0055	8.9722	9.0173	8.6613	31.6369	32.0123	29.2483	24.6626	26.2105	29.4725	29.7681	28.8201	38.2472	34.1064	36.3096	36.1019
10	1	3	13.8488	13.5717	13.8389	12.4173	41.6339	40.7921	40.7878	38.7880	44.5260	45.4458	45.4618	45.3490	51.9053	44.8767	51.8888	44.8767
10	1.5	3	16.5868	16.4738	16.6369	16.2859	55.0370	49.6582	58.0880	52.2934	56.5909	52.5409	52.9725	52.0924	73.8184	77.9188	71.6974	77.9188

Table A.9. Performance analysis results in terms of *SDRL* of PCR and *r-k* deviance-based CUSUM and EWMA charts in case of multiplicative shift.

p	ν	δ	CUSUM, $K=0.5$				EWMA, $\lambda=0.05$				EWMA, $\lambda=0.1$				EWMA, $\lambda=0.2$			
			ML	*ridge*	*PCR*	*r-k*	*ML*	*ridge*	*PCR*	*r-k*	*ML*	*ridge*	*PCR*	*r-k*	*ML*	*ridge*	*PCR*	*r-k*
4	0.75	0.25	17.6736	17.2966	17.8919	17.1976	150.3529	150.2109	150.1220	155.5543	128.6099	129.1385	128.7730	129.3042	172.1568	172.1568	172.1568	166.7558
4	1	0.25	20.2553	20.0363	20.0209	20.0218	142.6041	141.9547	142.2013	141.3255	131.7208	131.9184	131.7208	132.0811	171.0524	171.0524	171.0524	147.1205
4	1.5	0.25	25.6398	25.3944	25.2412	25.0144	146.1528	144.9848	145.1550	144.3803	129.9073	130.0650	129.9798	131.4462	164.4071	163.9065	164.1672	156.4856
7	0.75	0.25	16.8422	16.9321	16.9304	16.6764	154.9043	146.2349	146.5884	151.9150	124.3410	124.8986	125.5873	123.7121	170.7963	170.3429	170.3429	165.0079
7	1	0.25	19.9037	21.9357	21.9539	19.7391	142.2299	141.6646	141.6646	140.2673	132.4771	132.1361	132.4784	131.4006	170.9705	170.4418	170.4418	153.5434
7	1.5	0.25	26.5813	27.3404	26.5095	26.7004	146.5592	146.5582	146.5211	146.5189	127.5648	127.5431	130.2876	128.1726	165.2070	165.8711	165.4744	156.4482
10	0.75	0.25	16.6951	16.7050	16.9784	16.7395	96.2741	96.2807	96.3126	86.7991	81.0815	84.0033	84.4726	83.7861	114.1205	93.0431	109.5721	108.4111
10	1	0.25	18.4846	17.7968	18.2910	17.5178	99.0524	97.9167	97.9096	97.1773	84.8816	87.0815	86.9519	85.7983	138.7788	130.3641	138.7788	130.3641
10	1.5	0.25	24.7267	24.4567	25.1063	24.4481	121.3303	119.4049	125.3023	119.7702	103.7879	103.2889	103.0208	102.3230	153.3790	147.2033	153.0220	147.2033
4	0.75	0.5	17.8829	17.5986	18.1209	17.4360	150.1207	149.9101	149.7437	155.5372	128.1821	128.3726	128.3053	128.5648	172.0814	172.0814	172.0814	166.1012
4	1	0.5	20.2650	20.2047	20.2047	20.0731	142.3876	141.5549	141.9634	141.0615	131.4980	131.7056	131.4980	131.3210	170.7135	170.7135	170.7135	147.1225
4	1.5	0.5	25.6173	25.3236	25.2809	25.2693	146.8788	145.6329	145.8024	145.0796	130.5675	130.7257	130.3938	131.8724	164.7882	164.5895	164.1946	156.2417
7	0.75	0.5	15.8115	15.7271	15.8483	15.7328	152.4045	146.5898	146.9712	148.1919	124.4302	124.6425	125.5447	123.4562	170.4598	169.7279	169.7279	165.0677
7	1	0.5	20.3175	20.4197	20.4378	20.1290	142.4137	141.2255	141.2274	139.4948	132.1170	131.8745	132.1184	131.0367	170.2599	169.7124	169.7124	151.1523
7	1.5	0.5	25.0641	25.8814	25.1725	25.1707	146.9127	146.7121	146.3623	146.2938	128.1077	128.0814	130.9868	128.4455	164.4672	165.1723	164.7665	156.3817
10	0.75	0.5	16.1308	16.0876	16.0863	16.0849	96.2439	96.3855	96.1009	84.6253	76.0394	80.5295	81.2695	79.6109	108.0929	89.2324	101.3146	100.3808
10	1	0.5	18.1901	18.1984	18.1816	17.8777	99.1224	97.2201	97.4779	97.3198	83.5760	85.1603	85.0250	84.3775	133.7930	126.0183	133.7930	126.0183
10	1.5	0.5	26.4672	26.3508	26.3640	26.1565	117.2935	115.4266	120.4987	116.8564	100.0901	100.2747	99.3657	99.0514	151.7941	146.2701	151.3747	146.2701
4	0.75	0.75	17.9882	17.4726	18.1822	17.3417	149.8479	149.8973	149.5409	155.4092	128.0940	128.1386	128.2458	128.6592	172.0898	172.0898	172.0898	166.1037
4	1	0.75	20.2890	20.2162	20.2177	20.0876	141.5080	141.1040	141.3369	140.4368	130.9942	131.3836	130.8076	130.5439	170.4125	170.4154	170.4125	145.2649
4	1.5	0.75	24.8013	24.6975	24.9292	24.5426	146.9248	145.7519	145.9712	145.4475	130.2795	130.6534	130.1906	131.4936	164.5450	164.0231	163.9851	156.3824
7	0.75	0.75	15.3041	15.3136	15.6411	15.5296	150.5990	144.7204	145.2268	146.3039	123.8390	123.9749	123.9062	122.4587	170.3128	169.7288	169.7288	165.2772
7	1	0.75	19.9668	20.0696	20.0696	19.7370	142.0518	140.4369	140.4387	139.2502	130.4786	130.5965	130.8602	129.1408	169.6923	169.5484	169.5484	151.1850
7	1.5	0.75	27.4095	27.1695	26.2777	27.1393	142.8421	145.4259	145.9978	145.6946	127.2638	127.2388	129.7430	127.5317	164.8066	165.1869	164.5946	156.6697
10	0.75	0.75	16.5640	16.5623	16.5627	16.5619	95.3615	95.6472	94.6017	80.5103	75.1176	79.3168	79.2032	77.4216	103.3181	87.6541	98.2136	95.9982
10	1	0.75	17.7030	16.6663	17.4118	16.5418	97.9514	94.5246	94.5246	94.2448	84.2064	85.5378	85.3343	85.1441	132.2348	122.2442	132.2348	122.2442
10	1.5	0.75	23.3147	23.0189	22.9297	22.9132	117.3705	115.1955	120.8004	117.1159	97.9399	96.0094	95.9805	95.3579	151.0384	146.3032	150.8665	146.3027
4	0.75	1	18.1272	17.6483	18.2911	17.5264	149.3845	149.1856	148.8214	155.2360	128.2039	128.6043	128.3331	128.6821	171.7149	171.7180	171.7180	166.1082
4	1	1	21.0314	21.0531	20.5950	20.3693	141.9957	141.5889	141.8300	140.8568	130.5395	130.7221	130.3629	130.0695	170.4035	170.4064	170.4035	147.0452
4	1.5	1	24.3227	24.2113	24.6622	24.3133	146.8263	145.4854	145.7151	145.3255	129.8766	129.8820	130.2450	131.2680	163.8843	163.3523	163.6437	156.3761
7	0.75	1	15.9963	16.0495	16.0583	15.9381	147.5642	142.9414	143.8748	142.0342	123.7962	123.3593	123.6880	121.3518	170.0237	169.2930	169.2930	164.1734
7	1	1	19.1583	19.2893	19.2130	19.1411	141.4329	139.2178	139.2239	137.5163	130.2549	130.3182	130.7045	128.7739	169.8584	169.7057	169.7057	150.3226
7	1.5	1	27.2191	27.7470	26.4527	27.0876	145.8584	145.6333	145.7416	145.6467	128.9332	128.9027	129.9414	128.6549	165.0649	164.8071	164.2308	155.8911
10	0.75	1	15.3370	15.2778	15.3331	15.3330	94.0835	94.1849	93.9229	78.5389	72.6418	75.6212	75.5469	75.1210	102.2553	86.2562	98.6841	96.2687
10	1	1	17.8904	17.5357	17.8408	16.7730	96.3024	93.5616	93.5476	93.2453	82.6305	85.0956	84.8413	84.2471	126.4450	113.1652	126.4450	113.1688
10	1.5	1	22.2246	21.8142	21.9043	21.8106	114.4665	112.1324	117.9428	114.3731	95.0210	92.1179	92.1062	91.3776	148.8874	144.5594	148.1772	144.2096
4	0.75	1.25	17.8662	17.4100	18.0898	17.2911	149.5898	149.3507	149.1653	155.3398	128.5034	129.1505	128.7106	129.1478	171.2213	171.2243	171.2243	164.1736
4	1	1.25	20.9020	20.5098	20.5139	20.3229	142.1379	141.9928	142.0117	140.9856	130.4529	130.6423	130.2909	130.1027	170.4052	170.4080	170.4052	146.6224
4	1.5	1.25	24.3045	24.0085	24.4337	24.4252	146.3272	145.1248	145.3852	144.9334	130.5338	130.3413	130.7713	131.5345	163.8860	163.3406	163.6409	157.0234
7	0.75	1.25	16.5359	16.4627	16.5270	15.9465	146.9067	142.6290	143.5624	142.1169	121.5087	121.4966	121.8805	119.8412	170.1033	168.7167	168.7167	162.7763
7	1	1.25	18.3345	18.3941	18.3941	18.3398	141.7174	139.3009	139.3009	137.7766	128.4261	129.4047	129.8055	126.4135	169.0136	168.8782	168.8782	150.3711
7	1.5	1.25	25.9936	26.3383	24.9602	26.1941	146.7137	146.6179	146.5163	146.3262	130.6723	130.6406	130.5756	130.5609	165.3838	164.7654	164.5214	156.1845
10	0.75	1.25	12.9389	12.9394	12.9355	12.9316	91.7456	92.3360	90.9602	74.4255	69.0553	72.0875	72.7153	71.0707	99.4869	84.7046	96.3346	95.4857
10	1	1.25	17.6193	17.4018	17.7273	16.6235	92.4230	89.9930	89.9930	90.0187	79.5132	80.7689	80.4216	79.9680	117.5072	108.4242	117.5072	108.4242
10	1.5	1.25	21.5897	21.5748	21.5976	21.5361	113.0129	108.5528	115.2078	112.2284	94.1563	91.6939	92.0757	90.2810	145.8877	142.1490	144.9814	141.7617
4	0.75	1.5	17.6073	17.2429	17.7769	17.0719	149.7312	149.4834	149.2997	154.1561	128.6044	129.2061	128.8116	129.5996	171.2729	171.2759	171.2759	164.5784
4	1	1.5	20.7492	20.7347	20.7368	20.4658	142.0511	141.9057	141.9271	141.1653	130.2358	130.4270	130.0768	130.2751	170.4095	170.4095	170.4095	147.1492
4	1.5	1.5	23.8630	24.2756	24.6229	23.9832	146.5392	145.4541	145.9091	145.2493	130.4832	130.0753	130.7119	130.7274	163.8594	163.6892	163.6478	157.0321
7	0.75	1.5	14.5169	14.5201	14.5181	14.4572	145.0598	141.8488	142.4462	139.8746	120.5729	120.5676	120.4105	118.8415	168.5724	168.3247	168.3247	162.4185
7	1	1.5	17.2375	18.9133	18.9183	17.2749	140.9438	138.4296	138.4253	136.8823	127.1427	127.5854	128.0062	125.5658	169.4056	169.2779	169.2779	150.2833
7	1.5	1.5	25.9410	25.9410	25.0349	25.0288	146.5789	146.1949	146.2621	145.8028	129.5904	129.5869	128.8489	128.9022	165.1893	164.5654	164.3429	155.5586
10	0.75	1.5	12.9341	12.9499	12.9596	12.9218	88.9978	89.5276	87.0228	67.2732	66.2356	70.4809	70.8641	68.5132	95.2397	80.3267	92.1163	90.5514
10	1	1.5	18.0912	17.8577	18.1482	16.3946	90.7124	87.6147	88.0003	87.5103	76.3074	77.1782	77.6499	76.6628	111.6482	103.2768	111.6482	103.2768
10	1.5	1.5	22.3290	21.5465	21.5792	21.5491	110.3701	106.6589	112.8839	111.1798	90.3843	86.8587	87.0237	85.3768	144.3489	142.2002	142.3393	142.1992
4	0.75	2	17.6585	17.4406	17.4051	17.3664	148.8955	148.1254	148.1254	152.8130	129.2099	129.6607	129.4321	129.8572	170.5803	170.2049	170.5803	166.0830
4	1	2	21.2966	21.3656	21.3656	21.2108	141.3388	141.1775	141.2195	140.5214	130.4026	130.9659	130.2517	129.7742	170.6771	170.6771	170.6771	146.7188
4	1.5	2	23.5106	24.3184	24.1726	23.6800	147.2393	144.5494	145.7705	144.0210	129.9882	129.9616	130.3328	130.8366	163.7685	163.5273	163.3592	156.4063
7	0.75	2	12.6165	12.5601	12.5597	12.0606	144.6856	141.3555	141.7873	139.0866	116.4890	116.5458	115.2612	114.2665	167.3059	166.4914	166.4914	160.7895
7	1	2	17.5638	17.5339	17.5619	17.4192	138.8954	136.3880	136.8651	135.3529	124.8668	124.8655	124.8648	124.0786	169.1544	168.8044	168.8044	148.2188
7	1.5	2	22.4426	22.5318	22.1827	22.2758	141.5849	146.3193	146.6359	145.7218	129.1440	129.1410	129.7333	129.0463	164.5008	163.7392	164.3397	155.5511
10	0.75	2	11.2934	11.2987	11.3113	11.2866	83.3631	84.2077	82.2009	58.0902	58.8211	64.3855	64.3263	62.2802	90.6664	74.9088	87.1908	81.6610
10	1	2	20.8410	19.7383	19.9028	19.7217	86.1359	84.0597	84.4048	83.0738	72.0817	74.4946	74.4853	73.6915	103.1049	89.3149	103.1049	89.3149
10	1.5	2	21.9311	21.8873	21.8984	21.8317	106.8072	99.5875	110.3803	105.9992	87.1459	83.1611	83.4599	82.2664	142.1869	140.6807	140.6740	140.6807
4	0.75	2.5	19.1876	18.9133	18.8932	17.4143	149.1579	148.2811	148.1109	153.3222	128.4262	128.7408	128.4438	127.7776	170.0770	170.0770	170.0770	165.1224
4	1	2.5	22.2020	22.0560	22.1334	21.9187	141.0420	140.5816	140.6251	140.5199	130.2920	130.4299	130.4962	129.4116	170.6823	170.6823	170.6823	145.0363
4	1.5	2.5	24.5773	24.2041	24.4981	24.3337	146.1287	143.8245	144.5398	142.4982	129.4653	129.5626	129.6490	130.0032	163.8123	163.1746	163.0464	156.5723
7	0.75	2.5	11.2896	11.3431	11.3431	11.2195	139.7286	138.4103	138.8975	133.6574	111.7945	111.8386	110.9825	109.0332	165.3877	164.7284	164.7284	160.1004
7	1	2.5	15.3087	15.3717	15.3717	15.0605	138.9135	135.8571	136.3847	136.1183	124.5862	124.9925	124.5818	123.8214	168.2044	167.3831	167.3831	142.3499
7	1.5	2.5	23.7482	22.6127	23.3635	22.6552	140.3788	144.4848	145.1484	143.8481	127.5704	127.8452	127.2599	126.8278	163.3566	162.8242	163.2298	155.1120
10	0.75	2.5	10.2546	10.2617	10.2620	10.2539	76.3537	77.0482	74.2709	51.4010	51.7920	55.5908	55.4891	53.9088	82.1426	69.0126	79.6507	74.1881
10	1	2.5	19.1423	18.2774	18.7959	17.7676	86.0813	83.5540	83.5540	82.7562	69.0337	71.2777	71.2670	69.9505	93.4229	86.1109	93.4229	86.1109
10	1.5	2.5	22.7467	22.7609	22.6984	22.7118	102.1418	97.8586	103.5457	101.4176	82.7366	78.6893	78.4686	77.6728	132.5099	132.8848	131.9531	131.8183
4	0.75	3	19.4794	17.9094	19.7039	17.5316	148.8790	148.2235	148.0543	150.2679	128.5669	128.2556	128.0266	127.6258	170.1970	170.1970	170.1970	166.1621
4	1	3	21.8205	21.8934	21.9101	21.8807	139.8023	139.6775	139.8467	139.7692	130.5036	130.3720	130.4606	128.9191	169.9517	169.9547	169.9502	143.2618
4	1.5	3	23.7392	23.6926	24.0619	23.6768	145.5643	143.7293	144.1984	142.3321	129.8618	129.0982	129.3380	129.1574	163.7185	163.0399	162.9083	157.1003
7	0.75	3	11.4034	11.4629	11.4720	11.3155	136.4560	137.0695	137.0661	127.2079	105.8064	105.8064	105.6539	103.5325	163.7897	162.1084	162.1084	158.0039
7	1	3	16.2381	16.2810	16.3078	16.2563	138.3255	133.8012	134.3712	133.6885	122.6790	122.6792	122.6705	120.9339	167.5929	167.1932	167.1967	141.3554
7	1.5	3	22.3050	21.3378	21.8946	21.2549	139.1987	142.3999	143.0607	141.3433	127.6235	127.8392	125.1217	125.5766	162.2624	162.3018	162.1331	154.8933
10	0.75	3	10.5114	10.5212	10.5346	10.4965	71.0238	70.6666	68.0586	45.7383	44.2667	49.9585	49.5686	47.1139	76.0362	63.4014	74.9421	69.4728
10	1	3	15.8067	15.1698	15.8177	14.9003	84.1577	82.1580	81.8611	80.1253	64.9276	68.3179	68.3206	66.7012	90.0773	81.9266	90.0773	81.9266
10	1.5	3	23.3511	22.9991	23.1695	22.3383	94.7661	89.9670	97.1426	91.3972	77.8024	75.1789	75.3191	73.8445	126.2742	128.9034	124.9285	124.9085

B. Performance of Liu deviance-based control charts

Table B.10. Performance analysis results of Liu deviance-based Shewhart chart in terms of ARL_1.

Shift type	Shift size	p	v	ML	Ridge ($\hat{k}_1$)	Ridge ($\hat{k}_2$)	Liu ($\hat{\theta}_{opt}$)	Liu ($\theta = 0.5$)	Liu ($\theta = 0.85$)
Additive	0.5	2	0.5	147.0600	4.8600	4.8600	4.8600	4.8600	4.8600
	0.5	2	1	162.8900	38.6300	38.6300	38.6300	38.6300	38.6300
	0.5	2	1.5	154.5500	50.1900	50.1900	50.1900	50.1900	50.1900
	0.5	4	0.5	105.9900	65.1600	75.3000	84.1900	86.5200	86.5200
	0.5	4	1	179.0800	119.2400	119.2400	119.2400	119.2400	119.2400
	0.5	4	1.5	205.1000	139.8700	139.8700	139.8700	139.8700	139.8700
	1.5	2	0.5	119.8400	4.4800	4.3500	4.4800	4.4800	4.4800
	1.5	2	1	144.5000	31.9700	31.9700	31.9700	31.9700	31.9700
	1.5	2	1.5	143.7700	42.5300	42.5300	42.5300	42.5300	42.5300
	1.5	4	0.5	85.8000	50.8200	55.1000	69.4900	69.7400	69.7400
	1.5	4	1	176.1500	107.0300	107.0300	107.0300	107.0300	107.0300
	1.5	4	1.5	199.3700	128.1900	128.1900	128.1900	128.1900	128.1900
	2.5	2	0.5	94.6900	3.3200	3.0800	3.3200	3.3200	3.3200
	2.5	2	1	129.6700	27.4300	27.4300	27.4300	27.4300	27.4300
	2.5	2	1.5	136.5100	39.6200	39.6200	39.6200	39.6200	39.6200
	2.5	4	0.5	69.2700	40.3600	46.4500	54.7200	55.3800	55.3800
	2.5	4	1	165.5000	93.5600	93.5600	93.5600	93.5600	93.5600
	2.5	4	1.5	192.8000	112.9300	112.9300	112.9300	112.9300	112.9300
Multiplicative (all regressors)	0.5	2	0.5	22.6600	2.6200	2.6200	2.6200	2.6200	2.6200
	0.5	2	1	110.6000	22.3800	22.3800	22.3800	22.3800	22.3800
	0.5	2	1.5	141.4000	39.0300	39.0300	39.0300	39.0300	39.0300
	0.5	4	0.5	9.3300	8.6800	8.6800	8.8900	8.9800	8.9800
	0.5	4	1	49.7000	34.2700	34.2700	34.2700	34.2700	34.2700
	0.5	4	1.5	120.4600	57.8400	57.8400	57.8400	57.8400	57.8400
	1.5	2	0.5	8.9500	1.8900	1.8800	1.8900	1.8900	1.8900
	1.5	2	1	74.0100	11.3600	11.3600	11.3600	11.3600	11.3600
	1.5	2	1.5	128.1700	23.8700	23.8700	23.8700	23.8700	23.8700
	1.5	4	0.5	6.4100	4.8800	4.6000	5.6200	5.6200	5.6200
	1.5	4	1	35.6900	21.0800	21.0800	21.0800	21.0800	21.0800
	1.5	4	1.5	94.1900	43.4200	43.4200	43.4200	43.4200	43.4200
	2.5	2	0.5	3.2900	1.5700	1.5700	1.5700	1.5700	1.5700
	2.5	2	1	50.3200	7.1800	7.1800	7.1800	7.1800	7.1800
	2.5	2	1.5	108.9100	16.4500	16.4500	16.4500	16.4500	16.4500
	2.5	4	0.5	3.2100	2.0100	2.0200	2.1300	2.3400	2.3400
	2.5	4	1	20.2600	11.7800	11.7800	11.7800	11.7800	11.7800
	2.5	4	1.5	65.2900	27.8500	27.8500	27.8500	27.8500	27.8500
Multiplicative (intercept)	0.5	2	0.5	105.7700	4.1500	3.8900	4.1500	4.1500	4.1500
	0.5	2	1	141.6200	32.3400	32.3400	32.3400	32.3400	32.3400
	0.5	2	1.5	145.1400	43.4400	43.4400	43.4400	43.4400	43.4400
	0.5	4	0.5	57.9000	40.1800	44.5400	48.5200	48.5600	48.5600
	0.5	4	1	161.9300	93.0200	93.0200	93.0200	93.0200	93.0200
	0.5	4	1.5	195.7400	114.9200	114.9200	114.9200	114.9200	114.9200
	1.5	2	0.5	28.6700	2.1600	2.1400	2.1600	2.1600	2.1600
	1.5	2	1	93.1400	16.6800	16.6800	16.6800	16.6800	16.6800
	1.5	2	1.5	124.3900	31.0000	31.0000	31.0000	31.0000	31.0000
	1.5	4	0.5	12.4700	9.3900	9.3700	10.6000	10.7800	10.7800
	1.5	4	1	90.4800	50.2400	50.2400	50.2400	50.2400	50.2400
	1.5	4	1.5	171.8700	73.1700	73.1700	73.1700	73.1700	73.1700
	2.5	2	0.5	6.4900	1.5100	1.5100	1.5100	1.5100	1.5100
	2.5	2	1	57.8600	8.1800	8.1800	8.1800	8.1800	8.1800
	2.5	2	1.5	106.5100	17.7400	17.7400	17.7400	17.7400	17.7400
	2.5	4	0.5	4.8800	3.5900	3.5100	4.2200	4.4800	4.4800
	2.5	4	1	48.8900	25.7400	25.7400	25.7400	25.7400	25.7400
	2.5	4	1.5	119.2400	44.9700	44.9700	44.9700	44.9700	44.9700

Table B.11. Performance analysis results of Liu deviance-based Shewhart chart in terms of *SDRL*.

Shift type	Shift size	p	ν	ML	Ridge ($\hat{k}_1$)	Ridge ($\hat{k}_2$)	Liu ($\hat{\theta}_{opt}$)	Liu ($\theta = 0.5$)	Liu ($\theta = 0.85$)
Additive	0.5	2	0.5	90.97749	4.3073	4.3073	4.3073	4.3073	4.3073
	0.5	2	1	89.23362	40.49363	40.49363	40.49363	40.49363	40.49363
	0.5	2	1.5	89.23643	46.90534	46.90534	46.90534	46.90534	46.90534
	0.5	4	0.5	69.92282	43.87165	51.79706	53.83079	53.44782	53.44782
	0.5	4	1	85.48002	84.16932	84.16932	84.16932	84.16932	84.16932
	0.5	4	1.5	75.63325	90.93887	90.93887	90.93887	90.93887	90.93887
	1.5	2	0.5	86.45223	4.08417	4.06533	4.08417	4.08417	4.08417
	1.5	2	1	91.46728	33.61403	33.61403	33.61403	33.61403	33.61403
	1.5	2	1.5	88.76437	41.40613	41.40613	41.40613	41.40613	41.40613
	1.5	4	0.5	55.98815	31.37365	36.01053	48.76488	48.58765	48.58765
	1.5	4	1	86.70455	80.77089	80.77089	80.77089	80.77089	80.77089
	1.5	4	1.5	77.8495	90.78224	90.78224	90.78224	90.78224	90.78224
	2.5	2	0.5	74.76989	2.84753	2.60646	2.84753	2.84753	2.84753
	2.5	2	1	87.24993	29.00185	29.00185	29.00185	29.00185	29.00185
	2.5	2	1.5	89.12682	39.82025	39.82025	39.82025	39.82025	39.82025
	2.5	4	0.5	48.68463	28.02471	29.46346	38.83214	39.03238	39.03238
	2.5	4	1	90.34221	76.17922	76.17922	76.17922	76.17922	76.17922
	2.5	4	1.5	80.82184	84.83047	84.83047	84.83047	84.83047	84.83047
Multiplicative (all regressors)	0.5	2	0.5	19.89559	2.52058	2.52058	2.52058	2.52058	2.52058
	0.5	2	1	81.88768	20.81935	20.81935	20.81935	20.81935	20.81935
	0.5	2	1.5	89.45915	40.26775	40.26775	40.26775	40.26775	40.26775
	0.5	4	0.5	2.68819	3.0567	3.0567	3.23558	3.13392	3.13392
	0.5	4	1	33.13854	27.10588	27.10588	27.10588	27.10588	27.10588
	0.5	4	1.5	82.40069	49.80269	49.80269	49.80269	49.80269	49.80269
	1.5	2	0.5	7.93715	0.47576	0.48435	0.47576	0.47576	0.47576
	1.5	2	1	62.75171	10.50106	10.50106	10.50106	10.50106	10.50106
	1.5	2	1.5	89.29512	22.02869	22.02869	22.02869	22.02869	22.02869
	1.5	4	0.5	4.31264	4.30058	4.26259	4.40044	4.40044	4.40044
	1.5	4	1	27.55269	17.68445	17.68445	17.68445	17.68445	17.68445
	1.5	4	1.5	69.66904	39.44384	39.44384	39.44384	39.44384	39.44384
	2.5	2	0.5	3.34977	0.49508	0.49508	0.49508	0.49508	0.49508
	2.5	2	1	50.70685	6.37492	6.37492	6.37492	6.37492	6.37492
	2.5	2	1.5	85.05406	16.93005	16.93005	16.93005	16.93005	16.93005
	2.5	4	0.5	3.73098	2.61649	2.6723	2.78247	3.00834	3.00834
	2.5	4	1	17.1805	8.99603	8.99603	8.99603	8.99603	8.99603
	2.5	4	1.5	56.76561	25.15489	25.15489	25.15489	25.15489	25.15489
Multiplicative (intercept)	0.5	2	0.5	80.87162	3.97871	3.65126	3.97871	3.97871	3.97871
	0.5	2	1	90.56189	33.61638	33.61638	33.61638	33.61638	33.61638
	0.5	2	1.5	89.40801	41.70163	41.70163	41.70163	41.70163	41.70163
	0.5	4	0.5	38.14723	27.00983	30.46024	31.13057	31.13315	31.13315
	0.5	4	1	89.19838	74.66113	74.66113	74.66113	74.66113	74.66113
	0.5	4	1.5	79.77725	85.85033	85.85033	85.85033	85.85033	85.85033
	1.5	2	0.5	25.20282	1.6311	1.5433	1.6311	1.6311	1.6311
	1.5	2	1	76.85949	16.33349	16.33349	16.33349	16.33349	16.33349
	1.5	2	1.5	89.10087	33.66329	33.66329	33.66329	33.66329	33.66329
	1.5	4	0.5	9.1773	5.70421	5.69875	7.00183	7.20103	7.20103
	1.5	4	1	73.43049	43.80973	43.80973	43.80973	43.80973	43.80973
	1.5	4	1.5	88.4207	63.36742	63.36742	63.36742	63.36742	63.36742
	2.5	2	0.5	6.49682	0.5019	0.5019	0.5019	0.5019	0.5019
	2.5	2	1	51.88119	7.34928	7.34928	7.34928	7.34928	7.34928
	2.5	2	1.5	84.15886	16.74946	16.74946	16.74946	16.74946	16.74946
	2.5	4	0.5	4.25046	3.83216	3.78038	4.07227	4.19023	4.19023
	2.5	4	1	41.74869	24.47156	24.47156	24.47156	24.47156	24.47156
	2.5	4	1.5	84.16932	39.21164	39.21164	39.21164	39.21164	39.21164

Table B.12. Performance analysis results of Liu deviance-based CUSUM chart in terms of ARL_1.

Shift type	Shift size	p	v	ML	Ridge ($\hat{k}_1$)	Ridge ($\hat{k}_2$)	Liu ($\hat{\theta}_{opt}$)	Liu ($\theta = 0.5$)	Liu ($\theta = 0.85$)
Additive	0.5	2	0.5	5.3600	5.1900	5.1300	5.2300	5.1900	5.1900
	0.5	2	1	12.0400	11.6700	11.4400	11.6700	11.7000	11.7000
	0.5	2	1.5	14.9700	14.8500	14.8400	14.9100	14.8900	14.8900
	0.5	4	0.5	17.5800	17.2500	17.0300	18.0300	17.2700	17.2700
	0.5	4	1	23.9300	23.2800	23.2600	23.9100	23.2800	23.2800
	0.5	4	1.5	25.3000	25.1300	25.1000	25.1800	25.1300	25.1300
	1.5	2	0.5	4.9900	4.7700	4.7000	4.8900	4.8100	4.8100
	1.5	2	1	11.2400	10.7800	10.7000	10.7700	10.8200	10.8200
	1.5	2	1.5	14.1500	13.9200	13.9100	14.1400	14.0700	14.0700
	1.5	4	0.5	15.2700	14.9700	14.8000	15.5300	15.0400	15.0400
	1.5	4	1	21.7500	21.2100	21.1700	21.7500	21.2200	21.2200
	1.5	4	1.5	23.5300	22.7000	22.6400	23.5500	23.4000	23.4000
	2.5	2	0.5	4.5900	4.4500	4.3800	4.4700	4.4300	4.4300
	2.5	2	1	10.6600	10.2600	10.1000	10.3100	10.3300	10.3300
	2.5	2	1.5	13.6800	13.3500	13.3400	13.6200	13.4300	13.4300
	2.5	4	0.5	13.2700	13.0700	12.7600	13.4500	13.0500	13.0500
	2.5	4	1	20.7100	20.3200	20.3300	20.5700	20.4300	20.4300
	2.5	4	1.5	22.2400	21.6900	21.6300	22.2300	21.5800	21.5800
Multiplicative (all regressors)	0.5	2	0.5	3.8500	3.5800	3.4600	3.5900	3.6200	3.6200
	0.5	2	1	10.1800	9.8700	9.7200	9.9000	9.9400	9.9400
	0.5	2	1.5	13.2900	12.8700	12.9400	13.0400	12.9500	12.9500
	0.5	4	0.5	10.1700	10.0200	9.8700	10.1700	9.9800	9.9800
	0.5	4	1	18.0300	17.5500	17.5100	17.9600	17.6000	17.6000
	0.5	4	1.5	21.1400	20.1900	20.5400	20.7400	20.6400	20.6400
	1.5	2	0.5	2.5900	2.4000	2.3100	2.4200	2.4000	2.4000
	1.5	2	1	8.3800	8.1800	7.9900	8.1500	8.1900	8.1900
	1.5	2	1.5	11.5500	11.4200	11.3900	11.4800	11.4600	11.4600
	1.5	4	0.5	9.0900	9.0700	9.0200	9.0900	9.0400	9.0400
	1.5	4	1	14.4600	13.9700	13.8400	14.2500	14.0300	14.0300
	1.5	4	1.5	17.3200	16.6000	16.4800	16.9100	16.7000	16.7000
	2.5	2	0.5	1.7100	1.5200	1.4400	1.5200	1.5200	1.5200
	2.5	2	1	7.5000	7.3400	7.2200	7.3200	7.3500	7.3500
	2.5	2	1.5	10.4400	10.2100	10.1500	10.3800	10.3700	10.3700
	2.5	4	0.5	8.8100	8.8100	8.8300	8.8200	8.8200	8.8200
	2.5	4	1	12.3000	12.2100	12.1400	12.2600	12.2500	12.2500
	2.5	4	1.5	15.2200	14.8800	14.8700	14.9200	14.8800	14.8800
Multiplicative (intercept)	0.5	2	0.5	4.9400	4.7200	4.6700	4.7800	4.7200	4.7200
	0.5	2	1	11.4900	10.9100	10.8000	10.9100	10.9200	10.9200
	0.5	2	1.5	14.1600	13.8800	13.9000	14.1000	14.0700	14.0700
	0.5	4	0.5	14.8400	14.7700	14.4600	15.1100	14.7700	14.7700
	0.5	4	1	21.7400	20.9900	20.8500	20.8400	21.3800	21.3800
	0.5	4	1.5	24.7900	23.8300	23.8000	24.7100	23.9400	23.9400
	1.5	2	0.5	3.5100	3.3500	3.2900	3.4300	3.3800	3.3800
	1.5	2	1	9.2900	8.9900	8.9200	9.0000	9.0000	9.0000
	1.5	2	1.5	12.5400	12.4500	12.3700	12.5200	12.4600	12.4600
	1.5	4	0.5	9.9200	9.8700	9.8300	9.9900	9.8700	9.8700
	1.5	4	1	16.8600	16.5400	16.4100	16.8600	16.6800	16.6800
	1.5	4	1.5	18.1500	17.9200	18.0000	18.1000	18.0400	18.0400
	2.5	2	0.5	2.4500	2.3100	2.1800	2.3200	2.3300	2.3300
	2.5	2	1	7.6800	7.5000	7.3800	7.5000	7.5000	7.5000
	2.5	2	1.5	10.6900	10.4200	10.5200	10.6200	10.4500	10.4500
	2.5	4	0.5	8.7000	8.7100	8.6500	8.7800	8.7000	8.7000
	2.5	4	1	13.2400	13.0800	13.0500	13.1800	13.1100	13.1100
	2.5	4	1.5	15.7000	15.5600	15.5200	15.6700	15.5800	15.5800

Table B.13. Performance analysis results of Liu deviance-based CUSUM chart in terms of *SDRL*.

Shift type	Shift size	p	ν	ML	Ridge ($\hat{k}_1$)	Ridge ($\hat{k}_2$)	Liu ($\hat{\theta}_{opt}$)	Liu ($\theta = 0.5$)	Liu ($\theta = 0.85$)
Additive	0.5	2	0.5	2.65734	2.6538	2.68922	2.68039	2.6538	2.6538
	0.5	2	1	7.03882	6.80377	6.52033	6.80377	6.78889	6.78889
	0.5	2	1.5	8.92174	8.93857	8.92885	8.94635	8.9533	8.9533
	0.5	4	0.5	7.73686	7.69189	7.51458	7.86269	7.66016	7.66016
	0.5	4	1	13.85128	13.72199	13.72423	13.99225	13.72199	13.72199
	0.5	4	1.5	17.76273	17.77507	17.75359	17.76442	17.77507	17.77507
	1.5	2	0.5	2.50273	2.45516	2.48811	2.49824	2.42441	2.42441
	1.5	2	1	6.17651	6.20712	6.19855	6.24381	6.21757	6.21757
	1.5	2	1.5	8.8724	8.72928	8.72642	8.89971	8.80546	8.80546
	1.5	4	0.5	6.20416	6.23072	6.0901	6.3401	6.23138	6.23138
	1.5	4	1	11.8429	11.56974	11.53584	11.9082	11.57686	11.57686
	1.5	4	1.5	14.48844	13.61441	13.63642	14.59821	14.48395	14.48395
	2.5	2	0.5	2.33192	2.3184	2.29503	2.32275	2.30059	2.30059
	2.5	2	1	5.7885	5.78431	5.57505	5.7941	5.79965	5.79965
	2.5	2	1.5	8.32425	8.05892	8.05003	8.37159	8.24765	8.24765
	2.5	4	0.5	5.15459	4.95692	4.72053	5.21968	4.95359	4.95359
	2.5	4	1	10.98485	10.93613	10.94542	11.15892	11.10015	11.10015
	2.5	4	1.5	13.26443	12.82304	12.75304	13.77462	12.9252	12.9252
Multiplicative (all regressors)	0.5	2	0.5	2.4323	2.44827	2.40482	2.44359	2.42925	2.42925
	0.5	2	1	5.58431	5.5484	5.44802	5.57875	5.5419	5.5419
	0.5	2	1.5	8.21533	8.32748	8.20932	8.32631	8.32341	8.32341
	0.5	4	0.5	2.18911	1.77438	1.76967	2.18911	1.78244	1.78244
	0.5	4	1	9.32987	8.98731	8.97917	9.34706	8.94262	8.94262
	0.5	4	1.5	11.95597	11.6223	11.79964	11.79707	11.82039	11.82039
	1.5	2	0.5	1.811	1.75017	1.67819	1.80827	1.75017	1.75017
	1.5	2	1	4.34087	4.39755	4.30532	4.41433	4.39809	4.39809
	1.5	2	1.5	6.47602	6.4702	6.40531	6.50576	6.49504	6.49504
	1.5	4	0.5	0.52223	0.48879	0.42592	0.52223	0.46613	0.46613
	1.5	4	1	6.4773	6.07922	6.07937	6.38048	6.14126	6.14126
	1.5	4	1.5	9.39645	9.31186	8.77417	9.39895	9.2985	9.2985
	2.5	2	0.5	0.9127	0.7328	0.70382	0.7328	0.7328	0.7328
	2.5	2	1	3.95147	3.95126	3.93895	3.95335	3.95921	3.95921
	2.5	2	1.5	5.5019	5.29468	5.19879	5.50577	5.50388	5.50388
	2.5	4	0.5	0.3911	0.3911	0.30894	0.35257	0.35257	0.35257
	2.5	4	1	5.0972	5.10702	5.0721	5.10843	5.11218	5.11218
	2.5	4	1.5	7.65931	7.60834	7.60636	7.64686	7.60834	7.60834
Multiplicative (intercept)	0.5	2	0.5	2.54147	2.44877	2.42874	2.4704	2.41521	2.41521
	0.5	2	1	6.50403	6.46652	6.50446	6.49329	6.49247	6.49247
	0.5	2	1.5	8.81031	8.6673	8.65544	8.82146	8.83092	8.83092
	0.5	4	0.5	6.02968	6.04351	5.90886	6.30288	6.03168	6.03168
	0.5	4	1	11.89488	11.24675	11.28555	12.0888	11.65396	11.65396
	0.5	4	1.5	16.42044	15.81607	15.77903	16.5171	15.88888	15.88888
	1.5	2	0.5	2.06661	1.98313	1.94217	2.07174	2.00515	2.00515
	1.5	2	1	4.96047	4.83963	4.74771	4.86573	4.86573	4.86573
	1.5	2	1.5	7.33318	7.27743	7.18186	7.33083	7.27872	7.27872
	1.5	4	0.5	2.00499	1.9921	2.00129	2.07064	1.9921	1.9921
	1.5	4	1	8.6159	8.32289	8.31901	8.6159	8.59564	8.59564
	1.5	4	1.5	9.50617	9.4626	9.47108	9.54692	9.4842	9.4842
	2.5	2	0.5	1.37279	1.33248	1.2204	1.33372	1.32721	1.32721
	2.5	2	1	3.62556	3.69249	3.63731	3.69249	3.69249	3.69249
	2.5	2	1.5	5.81865	5.58303	5.67771	5.81662	5.58281	5.58281
	2.5	4	0.5	0.95054	0.94739	0.81549	0.89951	0.95054	0.95054
	2.5	4	1	5.84072	5.78752	5.76825	5.85827	5.79072	5.79072
	2.5	4	1.5	8.74819	8.66737	8.61516	8.77501	8.68917	8.68917

Table B.14. Performance analysis results of Liu deviance-based EWMA chart in terms of ARL_1.

Shift type	Shift size	p	v	ML	Ridge ($\hat{k}_1$)	Ridge ($\hat{k}_2$)	Liu ($\hat{\theta}_{opt}$)	Liu ($\theta = 0.5$)	Liu ($\theta = 0.85$)
Additive	0.5	2	0.5	2.4400	2.3600	2.2700	2.4400	2.3600	2.3900
	0.5	2	1	12.3500	11.3000	11.4700	11.8300	11.6000	11.6100
	0.5	2	1.5	19.3200	16.1400	15.9800	16.4800	16.2200	16.2200
	0.5	4	0.5	19.0900	13.6700	14.9800	19.3300	16.3100	16.3100
	0.5	4	1	85.3700	69.7100	66.7100	72.2900	72.1300	72.2900
	0.5	4	1.5	96.4400	60.0600	74.5200	86.9200	78.2200	79.6800
	1.5	2	0.5	2.1700	2.1600	2.1400	2.1600	2.1600	2.1600
	1.5	2	1	10.6000	8.9300	9.0800	9.6900	9.4100	9.6200
	1.5	2	1.5	16.0500	12.3700	11.9200	12.6000	12.4300	12.5000
	1.5	4	0.5	10.4500	7.4900	8.3500	10.9400	8.7400	8.8200
	1.5	4	1	64.1700	43.5900	42.1600	46.4300	45.6200	46.4300
	1.5	4	1.5	70.1900	42.8100	57.6100	63.7400	58.4500	59.5900
	2.5	2	0.5	1.8800	1.8700	1.7900	1.8700	1.8700	1.8700
	2.5	2	1	9.2000	7.4200	7.6000	8.3200	8.0000	8.1000
	2.5	2	1.5	14.0900	10.4600	10.4400	10.6300	10.6100	10.6100
	2.5	4	0.5	6.2900	5.0700	5.2100	5.4200	5.4200	5.7100
	2.5	4	1	39.7500	30.1000	29.7900	33.7700	33.4700	33.7700
	2.5	4	1.5	50.9400	38.6400	41.6700	45.5600	41.8700	41.8700
Multiplicative (all regressors)	0.5	2	0.5	1.8500	1.8300	1.8200	1.8400	1.8300	1.8300
	0.5	2	1	10.0400	7.9600	8.2200	8.8800	8.3800	8.4200
	0.5	2	1.5	13.7300	11.5100	11.5000	11.8600	11.5700	11.5700
	0.5	4	0.5	2.8900	2.5500	2.4700	2.9100	2.8800	2.8800
	0.5	4	1	20.8500	17.5600	16.9800	18.6400	18.4900	18.6400
	0.5	4	1.5	45.6900	33.9900	40.0800	40.6900	40.1400	40.1400
	1.5	2	0.5	1.5100	1.5100	1.5100	1.5100	1.5100	1.5100
	1.5	2	1	6.1800	4.7500	5.0600	5.6900	5.6300	5.6500
	1.5	2	1.5	8.9900	7.2400	7.2000	7.3000	7.2400	7.2400
	1.5	4	0.5	1.3300	1.1900	1.1300	1.3300	1.2500	1.2500
	1.5	4	1	8.8600	7.8000	7.7300	7.8800	7.8800	7.8800
	1.5	4	1.5	18.1400	16.0800	16.6100	16.8500	16.6800	16.6800
	2.5	2	0.5	1.3300	1.3300	1.3300	1.3400	1.3300	1.3300
	2.5	2	1	3.7800	3.2000	3.2500	3.4500	3.4500	3.4500
	2.5	2	1.5	6.8500	5.2600	5.1900	5.3000	5.2500	5.2600
	2.5	4	0.5	1.0000	0.9900	0.9900	0.9900	0.9900	0.9900
	2.5	4	1	4.7000	4.6800	4.6300	4.6800	4.6800	4.6800
	2.5	4	1.5	9.6600	8.4100	8.9600	9.5600	9.3700	9.3700
Multiplicative (intercept)	0.5	2	0.5	2.1500	2.1400	2.1200	2.1400	2.1400	2.1400
	0.5	2	1	11.1500	9.4700	9.6000	10.4000	10.1900	10.2800
	0.5	2	1.5	16.3300	12.2700	12.2400	13.0200	12.7500	12.7600
	0.5	4	0.5	8.4900	6.4400	6.5200	8.5000	7.0200	7.0200
	0.5	4	1	53.7500	42.3800	38.8900	42.6700	42.6000	42.6700
	0.5	4	1.5	65.0400	44.4200	51.7800	57.9400	54.1000	54.1300
	1.5	2	0.5	1.5200	1.5100	1.5100	1.5200	1.5100	1.5100
	1.5	2	1	6.9800	5.2700	5.7000	6.2900	6.0700	6.2200
	1.5	2	1.5	10.0300	7.3700	7.3700	7.3900	7.3700	7.3700
	1.5	4	0.5	2.6700	2.2800	2.2800	2.6700	2.4800	2.5700
	1.5	4	1	16.6800	14.7700	14.7200	15.4900	14.9600	15.4900
	1.5	4	1.5	30.1300	22.2300	25.0900	27.4700	25.2900	25.6600
	2.5	2	0.5	1.2700	1.2500	1.2500	1.2700	1.2500	1.2500
	2.5	2	1	3.9600	3.2400	3.4100	3.6400	3.6300	3.6300
	2.5	2	1.5	7.1500	5.4200	5.3900	5.5000	5.4100	5.4200
	2.5	4	0.5	1.1000	1.0700	1.0400	1.0700	1.0700	1.0700
	2.5	4	1	7.4400	6.1700	6.1600	6.4400	6.3900	6.4400
	2.5	4	1.5	12.7100	10.9300	11.3900	12.0600	11.7800	11.8700

Table B.15. Performance analysis results of Liu deviance-based EWMA chart in terms of *SDRL*.

Shift type	Shift size	p	v	ML	Ridge ($\hat{k}_1$)	Ridge ($\hat{k}_2$)	Liu ($\hat{\theta}_{opt}$)	Liu ($\theta = 0.5$)	Liu ($\theta = 0.85$)
Additive	0.5	2	0.5	2.31813	2.13669	2.05164	2.31813	2.13669	2.19466
	0.5	2	1	12.23690	12.17895	12.13110	12.20436	12.18735	12.20222
	0.5	2	1.5	18.88492	18.81080	18.87175	18.91351	18.84778	18.84778
	0.5	4	0.5	19.26085	12.89651	15.62484	20.61916	16.82463	16.82463
	0.5	4	1	75.41921	67.62985	67.16530	69.34489	69.23400	69.34489
	0.5	4	1.5	86.44652	65.29415	75.02324	81.86674	78.01942	78.40520
	1.5	2	0.5	1.99324	1.98136	1.96763	1.98136	1.98136	1.98136
	1.5	2	1	9.67350	8.65552	8.61896	8.87472	8.83219	8.91575
	1.5	2	1.5	16.35653	15.96001	15.12932	16.01582	16.00588	16.00101
	1.5	4	0.5	10.04909	7.53382	9.11733	10.85843	9.51158	9.48693
	1.5	4	1	64.27863	45.97880	44.02898	47.63648	47.58744	47.63648
	1.5	4	1.5	71.39635	42.79903	63.70927	68.02561	63.74133	66.10268
	2.5	2	0.5	1.34388	1.33163	1.02695	1.33163	1.33163	1.33163
	2.5	2	1	8.15194	6.42758	6.45365	7.26597	7.18513	7.16904
	2.5	2	1.5	14.31200	13.50522	13.49926	13.60566	13.59925	13.59925
	2.5	4	0.5	5.94758	5.41591	5.70997	5.95297	5.72917	5.83065
	2.5	4	1	42.96353	33.47918	33.41761	37.13129	37.09796	37.13129
	2.5	4	1.5	50.85078	41.70070	42.52588	47.39973	42.48655	42.48655
Multiplicative (all regressors)	0.5	2	0.5	0.93292	0.89629	0.87723	0.92593	0.89629	0.89629
	0.5	2	1	9.90569	6.83317	7.09477	7.53692	7.08449	7.07449
	0.5	2	1.5	13.63343	13.00595	12.99899	13.16766	13.02090	13.02090
	0.5	4	0.5	3.52738	3.24538	3.15703	3.56233	3.50536	3.50536
	0.5	4	1	25.24970	21.52198	21.12613	23.00933	23.01766	23.00933
	0.5	4	1.5	53.85645	37.75971	48.34176	48.34706	48.40924	48.40924
	1.5	2	0.5	0.50190	0.50190	0.50190	0.50190	0.50190	0.50190
	1.5	2	1	5.22766	4.14034	4.19642	4.83892	4.81207	4.79850
	1.5	2	1.5	7.75081	7.55206	7.55634	7.58434	7.55206	7.55206
	1.5	4	0.5	1.41538	0.89191	0.74245	1.41538	1.12110	1.12110
	1.5	4	1	10.92121	9.07932	9.02115	9.18064	9.18064	9.18064
	1.5	4	1.5	24.78266	21.40002	22.07850	22.15068	22.11628	22.11628
	2.5	2	0.5	0.47727	0.47727	0.47727	0.48050	0.47727	0.47727
	2.5	2	1	3.28995	2.74727	2.78495	2.92199	2.92199	2.92199
	2.5	2	1.5	6.07215	5.78641	5.62627	5.82274	5.76841	5.78641
	2.5	4	0.5	0.10050	0.10050	0.10050	0.10050	0.10050	0.10050
	2.5	4	1	5.63579	5.62033	5.48993	5.62033	5.62033	5.62033
	2.5	4	1.5	11.80893	9.81604	10.68890	11.63489	11.55052	11.55052
Multiplicative (intercept)	0.5	2	0.5	1.97969	1.96763	1.95359	1.96763	1.96763	1.96763
	0.5	2	1	11.26996	9.27600	9.22558	10.27417	10.21928	10.18473
	0.5	2	1.5	16.48832	15.17572	15.14451	16.30348	16.04030	16.04896
	0.5	4	0.5	8.23518	6.51587	6.65323	8.25241	7.57829	7.57829
	0.5	4	1	55.14124	48.95493	42.40067	48.98240	48.95697	48.98240
	0.5	4	1.5	66.48775	45.98528	54.85667	60.50339	56.58934	56.58005
	1.5	2	0.5	0.68977	0.67527	0.67527	0.68977	0.67527	0.67527
	1.5	2	1	5.90637	4.62652	5.15097	5.35345	5.28696	5.26839
	1.5	2	1.5	9.25891	7.97345	7.97345	7.99530	7.97345	7.97345
	1.5	4	0.5	3.20221	2.83727	2.83727	3.20221	3.00806	3.07033
	1.5	4	1	22.21296	17.85867	17.83292	20.60033	17.86279	20.60033
	1.5	4	1.5	33.21026	25.34749	31.02933	32.27191	30.98527	31.04331
	2.5	2	0.5	0.45267	0.44230	0.44230	0.45267	0.44230	0.44230
	2.5	2	1	3.69500	3.03321	3.18229	3.31302	3.28571	3.28571
	2.5	2	1.5	6.01453	6.02434	5.99868	6.09821	6.00733	6.02434
	2.5	4	0.5	0.47140	0.27393	0.22010	0.27393	0.27393	0.27393
	2.5	4	1	9.24537	6.42195	6.41356	6.71181	6.70405	6.71181
	2.5	4	1.5	13.77124	11.46594	12.27439	13.21823	13.14247	13.13936